Invisible to arbuscular mycorrhizal fungi:

Positional cloning and characterisation of a novel arbuscular mycorrhizal mutant in *Zea mays*

Bethan Frances Manley

Darwin College, Cambridge

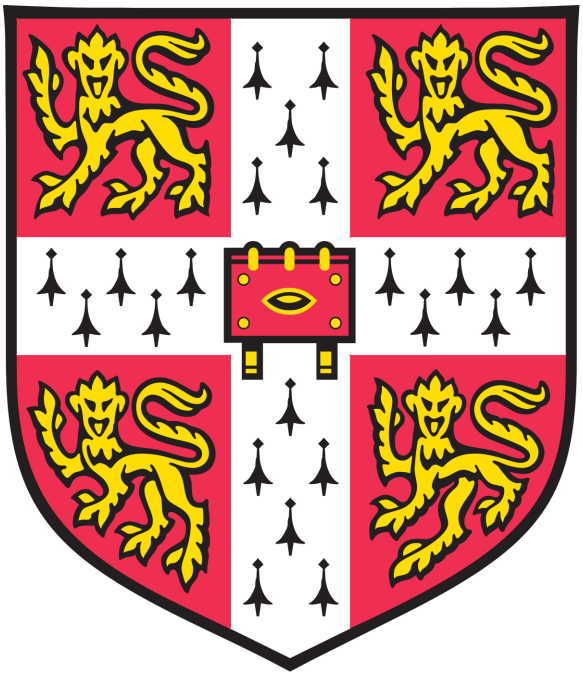

Thesis submitted to the University of Cambridge for the degree of Doctor of Philosophy

Submitted: June 2020

Preface

This thesis consists of my own work and any collaborations have been declared within the text. It is not substantially the same as previous works by myself or others and does not exceed the prescribed word limit for the Biology degree committee.

Abstract

***Invisible to arbuscular mycorrhizal fungi:* Positional cloning and characterisation of a novel arbuscular mycorrhizal mutant in *Zea mays* – Bethan Frances Manley**

Arbuscular mycorrhizal fungi from the *Glomeromycotina* form a beneficial symbiotic relationship with the root systems of a majority of plant species, enabling plants to profit from increased phosphate uptake efficiency. Further understanding of this interaction may prove vital in meeting the challenge of an increasing demand for phosphate supply in agriculture. Establishment of this symbiotic interaction relies on molecular crosstalk between the fungus and the plant roots in the rhizosphere, even before physical contact has occurred. A forward genetics screen has identified *invisible to arbuscular mycorrhizal fungi* (*ina*), a *Zea mays* mutant phenotype that displays a complete block in colonisation when inoculated with the arbuscular mycorrhizal fungus *Rhizophagus irregularis*. Extensive phenotyping has established that this maize mutant lacks the ability to signal to its symbiotic partner during the pre-symbiotic stage, abolishing the ability to initiate their beneficial relationship. To identify the impact of the removal of this signal, a transcriptomics analysis of *Rhizophagus irregularis* has found distinct transcriptomic signatures when spores are exposed to WT and mutant plant exudates. Positional cloning methods have identified a deleted region in the *ina* genome containing three candidate genes that may be responsible for this phenotype. Although further research is required to confirm the gene behind the *ina* phenotype, it was discovered that among these three candidate genes is the ortholog of a gene with a known role in the arbuscular mycorrhizal symbiosis, *STR2*.

Acknowledgements

I owe an enormous debt of gratitude to Uta Paszkowski, for welcoming me into her wonderful lab group, her constant support and unerring scientific knowledge, and for lending me *ina*. I have received so much advice and experimental help from the Paszkowski lab, and their influence can be found throughout this work. Thank you also to the attendees of the Endosymbiosis meetings, who provided invaluable discussion.

This research wouldn't be possible without the help and expertise of Bailin Li, Jennifer Jaqueth, April Leonard, and Shawn Thatcher at Corteva, and I thank them for their company and scientific support during my time in the Midwest.

The Plant Sciences Department is a fantastic community. Thank you to Greg Habrych and Sebastien Müller for their computational support, and for the departmental and greenhouse staff that make research possible. I'd also like to give special thanks to Annie and her positivity and coffee, a key factor in my productivity.

I am hugely thankful for the support of my friends, including those in the Plant Sciences Department. The Paszkowski lab is a truly exceptional group of people, and I want to thank them for making my years in the lab so enjoyable. Outside of the lab, I am very grateful for my wonderful friends from Trelawney Road, Bristol. I am especially thankful for my friends from Darwin College, and particularly Callum, Charlie, and Magda, who navigated this PhD experience with me, and without whom my time at Cambridge would be far less colourful.

Thank you to my family for being with me through my many phases and interests, and for always providing me with emotional and intellectual support.

Lastly, a thank you to the remarkable Iain, for your calming effect, patience, and for sharing these Cambridge years with me.

Table of Contents

CHAPTER 1

Introduction

1.1 An introduction to the Arbuscular Mycorrhizal symbiosis

The growth, development, and evolutionary history of terrestrial plants is intricately tied to their interactions with a diverse microbial community. Plants provide an ecological niche for bacteria, protists, fungi, and archaea, and their interactions with these organisms include parasitism, pathogenicity, and symbiosis (1). Nowhere is this tight linkage between plants and their microbial communities more apparent than in the rhizosphere, where plant-microbe interactions may open up new avenues for plant acquisition of soil-borne nutrients (2). The rhizosphere microbiome includes an enormous number of fungal species (3), including the Arbuscular Mycorrhizal (AM) fungi from the subphylum Glomeromycotina that have an ancient alliance with terrestrial plants (4).

Although the plant kingdom has diversified and adapted to a plethora of available niches on land, their early embryophyte ancestors that first colonised the terrestrial environment were likely only able to do so through associations with symbiotic fungi (5). Fossil evidence in the Rhynie Chert from the Devonian reveals that AM fungi are incredibly ancient organisms (6), and there is increasing evidence that fungi transitioned to a life on land before plants (7) and subsequently facilitated the movement of plants to a terrestrial existence (8). Indeed, plant genes known for their involvement in hosting AM fungi have been identified in the common ancestor of embryophytes (9), and AM fungi currently colonise extant liverworts from early plant lineages (10).

The association between plants and AM fungi was likely required due to the maladaptation of early plant lineages for the uptake of required nutrients from the soil (11). Despite the development of root systems that have evolved for the efficient acquisition of nutrients from the soil, modern terrestrial plants still associate with AM fungi, and this mutualistic relationship centres on the exchange of nutrients between symbiotic partners (12). AM fungi form extensive hyphal networks in the soil that extend beyond the boundaries of a plant root system and hence are highly efficient at taking up soil-borne nutrients such as phosphate (Pi) and nitrogen (N) to provide for their plant partner. In return, plants provide

photosynthetically-derived carbon to AM fungi (13). In an established symbiotic system, the fungal extraradical hyphae radiate out from colonised roots and form an in interconnected network between different plant individuals of a variety of species and life stages (14). This creates a dynamic system whereby fungal hyphae originating from different germinated spores fuse to create a foraging web for exchange of nutrients and fungal genetic information (15-17).

The AM symbiosis has a major impact on plant nutrition and growth, and 80% of all terrestrial plant species engage in this beneficial relationship (12). AM fungi supply significant amounts of P to plants by foraging beyond the nutrient depletion zone created by plant root systems (18), and, in industrial agriculture, may reduce the leaching of nutrients from the soil (19). Due to the substantial proportion of photosynthates that plants provide to AM fungi, it is likely that this symbiosis is an important component of the global carbon cycle (20, 21). Understanding more about the AM symbiosis could prove to be hugely beneficial for developments in sustainable agriculture and in understanding grassland and forest ecologies (22).

1.2 The pre-symbiotic stage of the AM symbiosis

AM fungi are endosymbionts, and hence colonise and form structures inside the cortical cells of plant roots. Before a working symbiosis has been established, the AM fungi exist as dormant spores in the soil (12). Although AM fungal spores have the capability of germinating in the absence of a plant host, they are unable to complete their life cycle without a symbiotic relationship with a suitable plant host (23). In order for the symbiotic relationship to commence, the two organisms exchange signals to alert one another to their presence, and to set in motion a suite of genetic and physiological changes that commit each individual to a symbiotic existence (24, 25).

1.2.1 Plant-derived signals and their effects on AM fungi

It has long been known that compounds produced by plant roots are capable of inducing the germination and branching of AM fungal spores. A primary morphological response displayed by AM fungi upon recognition of signals from a potential host plant is the induction of hyphal

growth and branching that facilitates physical contact between fungus and plant (26-28). There is also evidence of increased fungal metabolic activity (29), potentially fuelled by the consumption of storage lipids (30, 31), and extensive changes in gene expression associated with the transition from dormancy to a symbiotic stage of the AM fungal life cycle (32, 33). A number of compounds are known to induce these morphological and genetic changes in AM fungi before physical contact has occurred, and it is likely that these different compounds act together to produce a synergistic effect on the fungal symbiont, causing a number of responses required to begin the symbiotic phase of this life cycle. Indeed, evidence from fractionation of plant root exudates suggests that a number of different compounds are responsible for inciting a response in AM fungi (34).

1.2.1.1 Strigolactones

Strigolactones (SLs) are a class of plant hormone that regulate shoot branching (35), and were initially identified due to their exudation from roots that influences germination of *Striga lutea,* a parasitic weed (36, 37). It was later identified that SLs are a potent activator of fungal germination and hyphal branching, and that this was associated with increased respiration rate in AM fungi (29, 38, 39).

SL biosynthesis relies on the action of the protein DWARF27 (D27), which modifies carotenes, before their cleavage by CAROTENOID CLEAVAGE DIOXYGENASE 7 (CCD7) and further modification by CAROTENOID CLEAVAGE DIOXYGENASE 8 (CCD8) into carlactone, a precursor of SLs (40). Cytochrome P450 monooxygenases MORE AXILLARY GROWTH 1 and 1-like (MAX1 and MAX1-like) further process carlactone into the different forms of SLs (41, 42). Carlactone is also capable of inducing hyphal branching in AM fungal spores in both its synthetic and naturally-occurring forms (43).

SL levels are increased under low phosphate growth conditions, likely intensifying the signal for a symbiotic fungal partner to aid phosphate uptake for the plant (35). This exudation of SLs appears to be widespread among AM hosts, and although SLs are present in the root exudates of non-host *Arabidopsis thaliana,* they are produced at much lower concentrations than the concentrations produced by AM host plants (44). Despite the known importance of SLs in inducing germination and hyphal branching of AM fungi, mutants of the SL biosynthetic pathway, including *CCD7* and *CCD8*, have been studied in multiple plant species, and do not

show abolished AM colonisation, though the colonisation level is reduced compared to plants with a working SL biosynthetic pathway (45-47).

A transporter responsible for exuding SLs from roots has been identified in *Petunia hybrida*, and mutants of this gene, ABC transporter *PDR1*, display reduced AM colonisation to a level comparable to that of mutants of SL biosynthesis (48).

1.2.1.2 Chitinaceous compounds

The discovery of NO PERCEPTION 1 (NOPE1), a Major Facilitator Transporter, shed light on a novel plant-derived molecule required during the pre-symbiosis. NOPE1 is hypothesised to transport an N-acetylglucosamine (GlcNAc)-related compound, and in mutants of *NOPE1,* there is a severely compromised ability of AM fungi to colonise roots. When *R. irregularis* spores were provided with root exudates produced by WT and *nope1* mutant plants, a distinct fungal transcriptomic response was seen to the different genotypes. Spores treated with *nope1* exudates responded with a reduced number of induced transcripts compared to spores treated with WT exudates (33). GlcNAc can act as a signal to induce hyphal growth and morphological changes in filamentous fungi including *Candida albicans* (49-51), and can also be utilised as a sugar substrate by fungi (52), therefore it is highly possible that the GlcNAc-related compound found to be hugely important for *R. irregularis* colonisation of plant roots could plausibly act as either signal or nourishment substrate for the fungus during the pre-symbiotic stage (33).

1.2.1.3 Flavonoids

Flavonoids are another compound known to induce hyphal elongation in AM fungi, leading to the proposition that these compounds were one of the plant-derived signals that lead to activation of AM fungi (53-55). Additionally, flavonoids show differential accumulation in *Medicago sativa* roots according to symbiotic status (56) and have been implicated in increasing the number of points of entry through which the fungus penetrates roots (57). However, despite their effect on hyphal growth, flavonoids were found to be dispensable for pre-symbiotic interactions, as maize mutants deficient in the biosynthesis of flavonoids displayed WT levels of AM colonisation (58).

1.2.1.4 Fatty acids

Fatty acids are receiving increasing attention as a stimulator of AM fungal spores with a potential role in pre-symbiotic interactions. An initial report found that 2-hydroxy fatty acids (FAs) of varying chain length were capable of stimulating growth and branching of the AM species *Gigaspora gigantea*. This response to 2-hydroxy FAs was not observed in *R. irregularis,* perhaps due to the inherent difficulties of studying hyphal growth patterns in this species, as *R. irregularis* spores are much smaller and more difficult to observe than the larger *G. gigantea* spores (59). Recent work has stimulated hyphal branching, higher metabolic status, and secondary spore formation in a number of AM fungal species, including *R. irregularis*, through the addition of a number of distinct FAs, adding weight to the hypothesis that FAs play a role in pre-symbiotic interactions (60).

1.2.2 Symbiotic fungal signals and plant perception

AM fungi contribute to the pre-symbiotic molecular dialogue with their own signalling compounds released into the soil to prime their plant hosts for existence as a symbiont. The fungi release a swathe of molecules upon germination in an analogous fashion to the production of root exudates by plants, and these AM fungal-produced compounds are collectively termed Germinated Spore Exudates (GSE). The active components of GSE were identified as lipochitooligosaccharides (LCOs) and the short-chain chitooligosaccharides (COs) chitotetraose (CO_4) and chitopentaose (CO_5), and are collectively termed Mycorrhizal factors or 'Myc' factors (61, 62). When *R. irregularis* spores were incubated with the synthetic SL, GR24, the spores produced an altered GSE composition with increased short-chain CO concentrations, and was more potent in inducing a plant response (61).

As well as chitinaceous molecules, a secreted protein, SL-INDUCED PUTATIVE SECRETED PROTEIN 1 (SIS1) (1.5.2), was identified that, when knocked down by host-induced gene silencing (HIGS), resulted in reduced colonisation, suggesting the positive regulation of colonisation by this protein. As the name suggests, SIS1 production is increased by treatment of fungal spores with SLs (63).

1.2.2.1 Plant perception of chitinaceous molecules

Plants encounter an array of microorganisms, and are equipped with the ability to recognise microbe-derived molecules called Microbe-Associated Molecular Patterns (MAMPs), an important ability for recognising potential microbial pathogens that may cause harm, or when recognising a potential symbiotic partner (64). MAMPs are conserved molecular features common to groups of microorganisms, and the compounds that enable plants to recognise fungi are largely derived from the fungal cell wall that is composed of β-(1,3) glucan and chitin assembled into complex, fibrous structures (65, 66). Although the exact composure of the fungal cell wall varies by species, chitin oligosaccharides formed from polymers of *N*-acetylglucosamine (GlcNAc) are a ubiquitous component (66), and hence chitinaceous molecules such as those found in GSE are recognised as MAMPs by plants (67). Plants identify MAMPs through membrane receptors that recognise ligands and form protein complexes to transduce recognition of a microbial component through to cellular signalling pathways (68). Although the ability to host AM fungi is a widespread condition within the angiosperms, a subsection of these form an additional symbiotic relationship with N-fixing rhizobial bacteria, a phenomenon referred to as the root nodule symbiosis (69). Like AM fungi, rhizobia engage in pre-symbiotic communications with their legume hosts, and produce chitinaceous signals, LCOs, termed Nodulation (Nod) factors, that act as signals to their potential plant host (70). Nod factors and AM-produced Myc factors are both recognised by Receptor-Like Kinases (RLKs). One known RLK with a role in plant perception of AM fungi is SYMBIOSIS RECEPTOR KINASE (SYMRK) (71), which activates a calcium-signalling response in the plant host, leading to a suite of molecular and gene expression changes (61, 72). Known components of this calcium spiking response include cation channels localised to the nuclear envelope that counter the flux of Ca^{2+} (73, 74), a calcium- and calmodulin-dependent serine/threonine protein kinase (CCaMK) required for translating the calcium signal to cellular responses (75), and its phosphorylation target, CYCLOPS, that transduces the signal to activate symbiosis-related responses (76, 77). The methods by which AM fungi and N-fixing rhizobia then physically contact their host and proceed to a symbiotic stage differ (78, 79), but this conservation of the recognition of chemically-related chitinaceous molecules and initial signalling mechanisms has led to the naming of this pathway as the Common Symbiosis Signalling Pathway (CSSP) (80).

Plant Lysin Motif (LysM)-RLKs such as rice CHITIN ELICITOR RECEPTOR KINASE 1 (CERK1), homolog of the legume NOD FACTOR RECEPTOR 1 (NFR1), recognise MAMPs during immune responses (67, 81). CERK1 plays an additional role in the recognition of chitinaceous molecules produced by fungi during the AM symbiosis (81, 82), and is required for the calcium spiking response that occurs following plant perception of chitin (83). Mutants of *CERK1* display reduced colonisation by AM fungi, highlighting the role of this receptor in the plant perception of pre-symbiotic signals (81, 82). *CERK1* is known to form a receptor complex with CHITIN ELICITOR BINDING PROTEIN (CEBiP) during its role in immunity signalling and the recognition of pathogenic MAMPs (81, 84). However, mutants of *CEBiP* do not display a mycorrhizal phenotype, suggesting a role of *CERK1* in a pathway unique to AM symbiosis signalling, one that does not require all components of immunity signalling (82).

1.2.2.2 Plant perception through D14L

SLs are a hugely important plant-derived signal during the pre-symbiosis (1.3.1.1), and understanding plant SL signalling is also important when considering plant perception and preparation for a symbiotic encounter. SL signalling in plants involves F-box protein-mediated proteolysis, a mechanism that is commonly seen in plant hormone signalling transduction (85). The F-box proteins MORE AXILLARY GROWTH 2 (MAX2) and DWARF 3 (D3) in *A. thaliana* and *Oryza sativa*, respectively, are responsible for the transduction of SL signals (35). Another essential component of SL signalling transduction is the α/β-hydrolase DWARF14 (D14), which acts as both a receptor and an enzyme (86), and interacts with MAX2 in *A. thaliana* (87) and D3 in *O. sativa* (88). SLs are a class of butenolide, as are karrikins, molecules found in smoke that causes a germination response in fire-chasing plants. The *A. thaliana* karrikin-sensing α/β-hydrolase KARRIKIN INSENSITIVE 2 (KAI2), and its rice homolog DWARF14LIKE (D14L), act with MAX2/D3 to transduce karrikin signalling, thus MAX2/D3 is a shared component of both strigolactone and karrikin sensing in plants (89, 90).

A seminal discovery in AM pre-symbiotic communications was the identification that *D14L* is essential for colonisation of rice by AM fungi, first noted when a mutant of *D14L* was analysed that displayed a complete block in its ability to host *R. irregularis* (91). Despite the fact that D14L binds karrikin and transduces karrikin signalling, it is not karrikin but another, unknown, ligand that binds D14L during AM symbiosis signalling, likely another butenolide, though

whether this is endogenously produced *in planta* or a fungal-derived signal is unknown (91-93).

1.3 Physical contact and the formation of internal fungal structures

Once mutual recognition has occurred, and the AM fungal spores have recognised the presence of a host plant, there is an increase in hyphal growth in the direction of the plant roots. This growth through the soil increases the chances of the fungal hyphae meeting the host root and enabling physical contact. The degree of hyphal branching depends on the proximity of a germinating AM fungal spore to a suitable host root system, with higher-order branching taking place as the fungus nears a root (26, 94). The initiation of more extensive branching only in the close proximity of the host root may be particularly important for AM fungal species with smaller spores, such as *R. irregularis,* due to their reduced capacity for storage of energy reserves compared to species that produce larger spores, such as *Gigaspora* species (12).

Once physical contact between the plant and fungus occurs, the fungal hypha swells into a bulbous penetration structure, the hyphopodium, and this structure enables entry into the root epidermal cells (95). While hyphopodium formation occurs, root epidermal cells undergo extensive structural changes. Architectural changes in the distribution of plant endoplasmic reticulum and cytoskeleton in these epidermal cells result in the formation of the pre-penetration apparatus (PPA) (78, 96). The PPA acts as a tunnel through the cell, and, following penetration into the plant cell, the fungus is guided through this tunnel into the inner root where it spreads intercellularly until it colonises the cortical cells. Here, it is encased in a plant membrane compartment that separates it from the plant cytosol, termed the periarbuscular membrane (PAM).

There are two key developmental strategies adopted by AM fungi during their movement through the root cortical cells, *Paris*-type, where fungal spread is exclusively intracellular and arbuscule coils are formed, and *Arum*-type, where hyphae move intercellularly before penetrating cortical cells to form neat lines of arbuscules (97). The well-studied lab AM fungus, *R. irregularis* undergoes an *Arum*-type development upon colonisation of a majority of studied hosts (12), though *R. irregularis* growth has been observed to follow *Paris*-type morphology in other host species such as *Brachypodium distachyon* (98).

1.3.1 The formation and lifespan of arbuscules

The PAM is continuous with the plant cell membrane, and changes its dynamics with the growth of the fungus (99). Fungal development inside cortical cells starts as a thick hyphal branch and later undergoes dichotomous branching to create finer and finer branches to form an arbuscule, the core symbiotic structure responsible for nutrient exchange between partners (78). The PAM is a highly specialised structure that involves *de novo* membrane synthesis during arbuscule formation and branching (99, 100), and it contains its own unique membrane proteins required for symbiotic nutrient exchange (101, 102). Between the plant and fungal cell walls is the periarbuscular space (PAS), the area where nutrients are deposited by one symbiotic partner and taken up by another (103).

A fully established AM symbiosis is dynamic and involves recurring formation and senescence of arbuscules, so that a root system at a later stage during the symbiosis hosts both young and degrading arbuscules at the same time. Each individual arbuscule is short-lived and following the extensive fine branching and activity for 2-3 days, they start to collapse (104, 105). This process of senescence is tightly regulated by the plant through symbiosis-specific regulators of arbuscule degeneration such as a MYC-like transcription factor (MYB1), and is associated with a unique transcriptional program including the induction of genes encoding secreted hydrolases (106).

1.3.2 Spore and vesicle formation

At later stages in the symbiosis, the fungus produces vesicles, lipid storage bodies, where it likely deposits the carbon obtained from its plant host (12, 107). Lipids are also stored during the late stages of the symbiosis in the fungal spores (108). AM fungi are coenocytic and produce multinucleate spores that germinate in response to the presence of a host and restart the initial stages of the symbiosis. A number of the many nuclei within these spores are donated from parental hyphae into developing spores, and more arise from mitotic divisions within the spore itself (109).

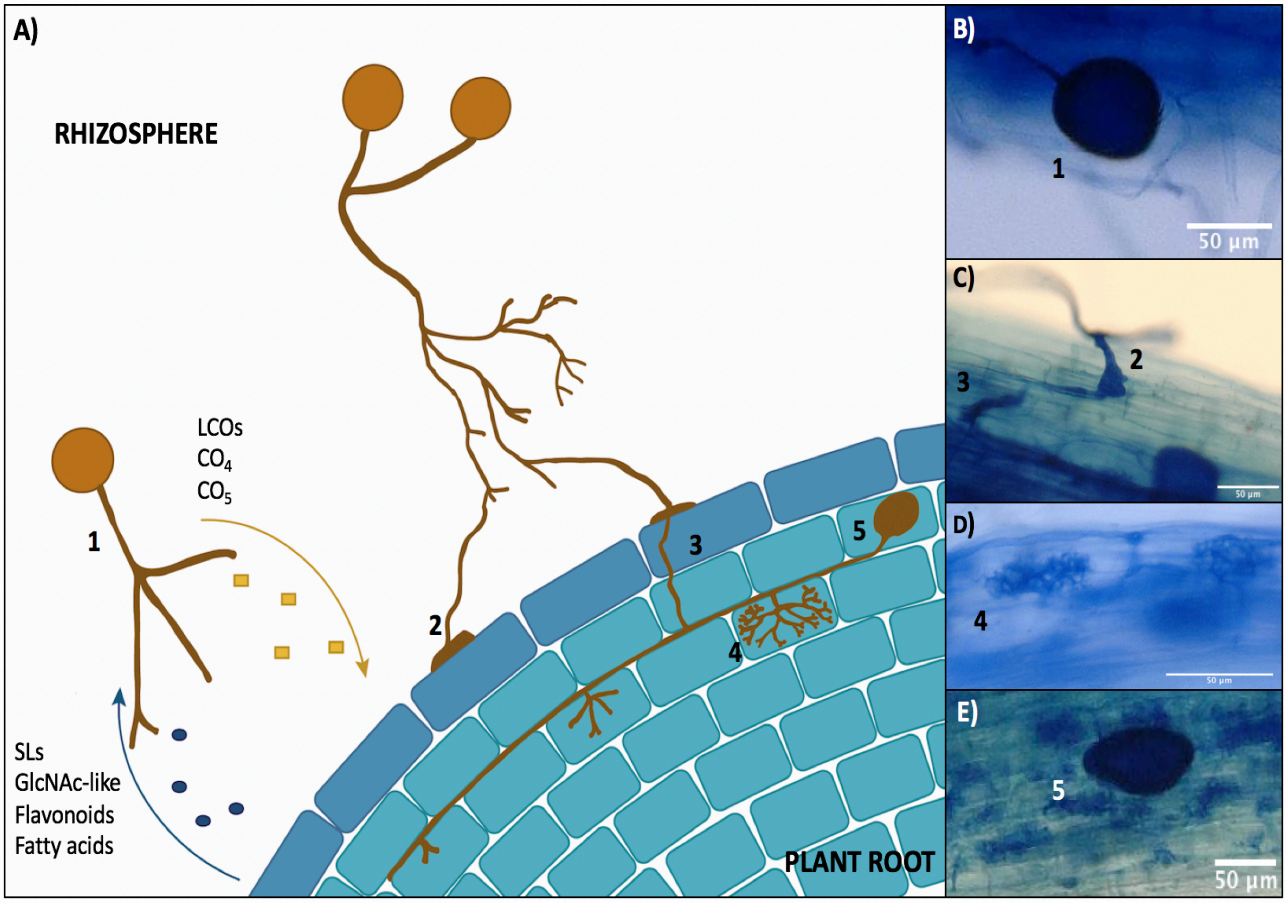

Figure 1.1: AM fungal colonisation of host roots. A) Colonisation proceeds through a series of defined steps: **1.** Pre-symbiotic communication between plant and fungus involving the exchange of signaling compounds. **2.** Physical contact between symbionts results in the formation of a fungal penetration structure, the hyphopodium. **3.** The fungus moves through the outer cortex. **4.** Arbuscules are formed in the inner cortical cells. **5.** Lipid storage vesicles are formed, as are secondary fungal spores. **B)** Trypan Blue image of a *R. irregularis* spore. **C)** Image of *R. irregularis* forming a hyphopodium, penetrating the maize root epidermis and passing through the outer cortex, stained with Trypan Blue. **D)** Arbuscule formation in maize inner cortical cells visualised by Trypan Blue staining. **E)** Trypan Blue staining of a *R. irregularis* vesicle.

1.4 Nutrient exchange between plants and AM fungi

The central purpose of the AM symbiosis is the cross-kingdom trade of nutrients. Plants provide a service to AM fungi that they provide for a majority of the world's heterotrophic organisms; they fix carbon for use in organic processes. AM fungi are auxotrophs, and, as opposed to numerous other auxotrophs that obtain carbon from living or dead plant matter,

they barter for plant-derived carbon by providing their own service to plants, the increased uptake of minerals (12).

1.4.1 Nutrient delivery from AM fungi to plant hosts

AM fungi are able to provide soil nutrients to plants by extending their hyphal network beyond the reach of the root system of the plant, allowing the collection of minerals such as phosphate from areas that have not been depleted by direct uptake from plant roots (110). This has recently been studied in maize, where phosphate uptake was positively correlated with the size of extraradical hyphal network in the soil during a working symbiosis (111). AM fungi take up phosphate from the soil in the form of inorganic phosphate (Pi), and this uptake occurs via high-affinity symporters facilitated by the action of H^+-ATPases and Na^+-ATPases that counter the influx of Pi anions (112, 113). The fungus converts Pi to chains of polyphosphate (polyP) for translocation from extraradical hyphae to intraradical hyphae (114-116). It is likely that polyP is then hydrolysed to Pi for transport to the plant at the arbuscule interface (117, 118).

The mechanism by which the fungus unloads its phosphate to the PAS for uptake by the plant is unknown (119). Considerably more is known about how the plant subsequently acquires this fungal-derived phosphate from the PAS. Phosphate is transported from the PAS into the arbuscule-containing cortical cells by phosphate transporters from the phosphate transporter (PHT) family, specifically, by transporters from the subfamily PHT1, whose members also facilitate direct uptake of phosphate from the soil (120). PHT1 family members required for phosphate uptake at the arbuscule are induced under mycorrhizal colonisation conditions when they can be seen to localise to the PAM, and have been identified in a number of plant species (101, 105, 121-123).

Though phosphate uptake is the most well-studied benefit provided to plants by their partnership with AM fungi, the symbiosis also provides N to plants. N is taken up from the soil by AM fungi and assimilated into amino acids for transport to the intraradical hyphae and internal fungal structures, where it is subsequently converted and predicted to be transferred to host plants as ammonium (124, 125). Plant ammonium transporters have been identified that localise to the PAM and are transcriptionally induced under mycorrhizal colonisation conditions (126, 127).

The arbuscule may function not only as a site of nutrient transfer, but as a hub where the efficacy of the symbiosis is monitored. Nutrient uptake from the arbuscule could act as a measure of the benefit provided by the hosted fungus. This has been proposed in studies of phosphate transport due to the observation that arbuscules collapse prematurely in mutants of the mycorrhizal-specific phosphate transporters in *M. truncatula, MtPT4*, and rice, *OsPT11* (122, 123). The early collapse of the arbuscule in these cases may prevent the continued proliferation of a fungus that the plant perceives to be of little benefit (122). In rice, this nutrient sensing has been proposed as the purpose of an additional rice phosphate transporter, *OsPT13.* Mutants of *OsPT13* display reduced colonisation and stunted arbuscules, yet these plants do not show a reduced transfer of Pi to plants, leading to the hypothesis that *OsPT13* plays a role in monitoring Pi levels in arbusculated cells and dictating arbuscule development based on this sensing (123). Plant monitoring of nutrient exchange also involves N transfer by the fungus, according to observations that premature degeneration of arbuscules in *Mtpt4* individuals no longer occurs under N deprivation conditions, suggesting that the transport of N to the host plant is a sufficient signal to ensure a normal arbuscule lifespan despite a lack of phosphate uptake from the fungus (128, 129). Mutants of an ammonium transporter required for this prolonged lifespan of *Mtpt4* displayed no reduction in symbiotic uptake of N, suggesting that this ammonium transporter fulfils a signalling purpose (128).

1.4.2 Carbon delivery to the fungal symbiont

AM fungi are obligate biotrophs and hence are unable to complete their life cycle without a host to nourish them with carbon (12). Estimates place the percentage of photosynthetic carbon provided from a plant to symbiotic AM fungi at 4-20%, and thus there is a significant flow of carbon from plant to fungus (130). The primary form of carbon provided to the fungus is a question that has received particular attention in recent years.

1.4.2.1 Carbohydrates

Intraradical hyphae of AM fungi are capable of direct carbohydrate uptake in the form of hexoses such as glucose, though substantial uptake has not been observed in extraradical

hyphae (131-133). Transmembrane transporters of carbohydrates have been identified in AM fungal species including *R. irregularis. RiMST2* is likely expressed *in planta* and has a high affinity for glucose, and knockdown of *RiMST2* expression causes reduced colonisation and abnormal arbuscule formation (134). Additional monosaccharide transporters *RiMST5* and *RiMST6* have also been identified (135).

Roots colonised by AM fungi act as carbon sinks, where sugars are directed from their site of production in leaves to roots (136). AM colonisation induces cell-specific induction of invertases near fungal structures (137), likely cleaving sucrose for use by the fungus as monosaccharides (134). The hypothesis that carbohydrates may be transported to AM fungi within plant tissue is supported by the finding that the promoters of SUGARS WILL EVENTUALLY BE EXPORTED TRANSPORTERs (SWEETs), potential exporters of monosaccharides and disaccharides, are induced in root tissue colonised by AM fungi (138).

Sugars taken up by intraradical hyphae within the plant are likely incorporated into glycogen, before their exportation to extraradical hyphae (132, 139). Despite this known uptake and transport of carbohydrates, however, carbon is stored in AM fungi predominantly in lipid-form (140).

1.4.2.2 Lipids

It has been known for some time that lipids play an important role in the life cycle of AM fungi. FAs exist in AM fungi predominantly in the form of 16:0 and 16:1ω5 FAs, palmitic acid and palmitvaccenic acid, respectively (141, 142), and these fungi store lipids as triacylglycerol (TAG) (140, 143).

The *de novo* production of FAs is carried out by a number of reactions conserved across kingdoms, and this essential metabolic process is reliant upon the enzyme, or set of enzymes, fatty acid synthase (FAS) (144). Animals and some fungi possess a FAS encoded by a single protein (145, 146), whereas other fungi produce FAS encoded by two subunits (147). When known features of FAS from animal and fungal species were analysed against the *R. irregularis* genome, no multidomain FAS-encoding sequences could be found (143). Data from the genome sequencing of AM fungi has clarified that these organisms lack genes encoding the machinery to synthesise 16:0 FAs *de novo* (148, 149). However, research into lipid biosynthetic pathways of AM fungi discovered that *R. irregularis* and *G. rosea* possess the

ability to elongate and desaturate 16-carbon FAs, and that transcripts involved in elongation and desaturation were induced in intraradical hyphae upon colonisation of host roots. Although AM fungi do not produce their own FAs *de novo*, they clearly have a source of FAs that they are capable of processing and catabolising for their needs (143, 150).

Therefore, lipids are a more important carbon source for AM fungi than previously thought. The hosts of AM fungi possess biochemical machinery to specifically biosynthesise lipids for their fungal guests. FA synthesis by FAS uses acetyl-CoA as a starting unit from which a fatty acyl chain is synthesised, with malonyl-ACP as a donor of carbon units (151). *DISORGANISED ARBUSCULES* (*DIS*), encoding a β-keto-acyl ACP synthase 1 (KAS1) enzyme, is hypothesised to produce FAs for the specific purpose of providing to AM fungi (152, 153). *DIS* falls into the group of KAS1 condensing enzymes that release a molecule of CO_2 from malonyl-ACP to extend a fatty acyl chain during successive rounds of elongation. Arbuscules formed within *dis* mutants are stunted, and overall AM colonisation is reduced compared to WT plants. *DIS* is induced in colonised tissue, probably to increase the production of specific lipids to provide for the AM fungal symbiont (153).

An additional lipid biosynthesis gene involved in producing lipids for AM fungi was first identified due to its conservation in AM hosts. This gene encodes an acyl-acyl carrier protein (ACP) thioesterase (*Fat*) (154), a FA biosynthetic enzyme that acts in the plastid to terminate the fatty acyl chain elongation and release free FAs (155). *M. truncatula* and *L. japonicus* plants defective in this acyl-ACP thioesterase, named *FatM* (*Fat* required for AM symbiosis), were distinguishable from WT due to their reduced AM colonisation level and the formation of stunted arbuscules (154, 156, 157). Plants contain three classes of thioesterases, *FatA*s*, FatB*s*,* and *FatC*s*. FatB* thioesterases have a substrate preference for hydrolysing 16:0-ACPs (158), and *FatM* displays the highest similarity to *FatB* enzymes (157). *FatB* is even able to complement the AM phenotype of the *fatm* mutant, to a similar extent to complementing with the *FatM* gene itself, restoring WT arbuscules and high colonisation (156). It was concluded that *FatM* likely has similar FA specificities to *FatB*, and that the mycorrhizal-specific function of this enzyme is due to its specific expression that is known to be induced in colonised cells containing arbuscules where it likely produces lipids for the fungus (156).

A previously-reported gene, *REDUCED ARBUSCULAR MYCORRHIZATION 2* (*RAM2*) (159), was recently found to act downstream of *DIS* and *FatM* (153). Mutants of *RAM2* were identified due to severely low AM colonisation, and, in rare patches of colonised tissue, the observation

of stunted arbuscules. *RAM2* has been shown to be required for the accumulation of plant-derived lipids in AM fungi (160). *RAM2* is specifically induced in arbuscule-containing cells and encodes a glycerol-3-phosphate acyl transferase (GPAT) (161, 162). GPATs are involved in the biosynthesis of membrane and storage lipids (163). *RAM2* is a member of a GPAT family that produces 16:0 β-monoacylglycerols (β-MAGs) (161), which serve as precursors for cutin biosynthesis (164). Levels of these β-MAGs were lower in *ram2* and *dis* mutants, and thus *DIS* probably provides FA precursor substrates for *RAM2* to produce 16:0 β-MAGs (153). A parallel analysis on the mutant phenotypes and lipid profiles of *RAM2* and *FatM* have led to the hypothesis that *FatM* provides 16:0 FAs that may serve as substrates for *RAM2* to convert to 16:0 βMAGs to provide to the symbiotic fungus (156).

Additional hypothesised players in this pathway to provide lipids for AM fungi are *STUNTED ARBUSCULE 1* (*STR1*), and *STUNTED ARBUSCULE 2* (*STR2*). These are half-sized ATP-binding cassette (ABC) transporters that have been studied in *M. truncatula* and in rice. In both organisms, mutants of *STR1* and *STR2* support severely reduced colonisation and host small, stunted arbuscules (165, 166). Half-size ABC transporters are known to transport suberins, compounds partially composed of FAs, and lipids, in *A. thaliana* (167). Mutant phenotypes of *FatM, RAM2,* and the *STR* transporters have been compared in one analysis, revealing their similarity. A current hypothesis is that the half-sized transporters *STR1* and *STR2* together export 16:0 βMAGs from the plant across the PAM into the PAS for the fungus to take up as a carbon source (156).

The GRAS-transcription factor *REDUCED ARBUSCULAR MYCORRHIZATION 1* (*RAM1*) has a role in producing lipids for the cross-kingdom transfer of lipids due to its regulation of *RAM2, DIS* and *STR* (153, 159, 168-170). *RAM1* is highly expressed in colonised tissue, where it regulates the expression of *RAM2* and *STR.* Mutants of *RAM1* also display severely low colonisation, and in these individuals the induction of genes required for fungal lipid provisioning, *RAM2, DIS,* and *STR* by AM colonisation is reduced or abolished (153, 159, 168, 170). An additional GRAS-transcription factor, REQUIRED FOR ARBUSCULE DEVELOPMENT (RAD1), whose expression is regulated by RAM1, is also known to exert control over the expression of *STR* genes, and *rad1* mutants display stunted arbuscules and reduced *STR* and *STR2* expression (168, 171, 172).

In addition to the genetic evidence highlighted above, lipid profiling experiments utilising heavy carbon isotopes have provided some evidence for the transfer of lipids from plants to

AM fungi (153, 170). The understanding of cross-kingdom lipid transfer in the AM symbiosis is still in its infancy, though increasing evidence is mounting for a hugely important lipid export pathway in plants that functions solely to provide a carbon source for AM fungi. Though 16:0 β-MAGs are a good candidate, it is yet unknown exactly which form of lipids are transported to AM fungi (153). The requirement for genes in this lipid export pathway for fungal development (153, 156) and the use of TAGs as the main carbon store in AM fungi highlights that lipids are an essential nutritive source for this fungal symbiont (140).

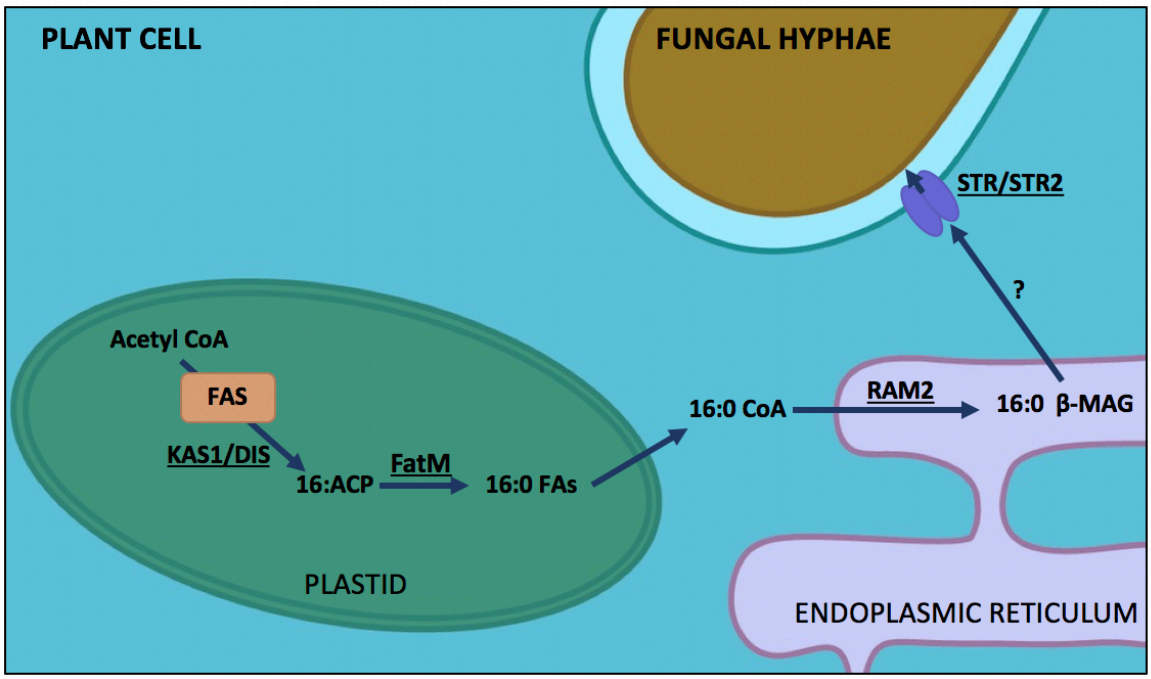

Figure 1.2: Schematic representation of fatty acid (FA) production and delivery to AM fungal symbionts. Lipids are synthesised by fatty acid synthase (FAS) in the plant plastid, where KASI/DIS and FatM are active in tissue colonised by AM fungi. These enzymes produce 16:0 fatty acids (FAs) which are further processed by RAM2, another mycorrhizal-induced enzyme that produces 16:0 β-MAGs, which are a candidate for the form of lipid that is then transported to the fungus. The complex formed by the two half-sized ABC transporters STR/STR2 is predicted to transport these lipids to the fungus, though this has yet to be confirmed.

1.5 Fungal genetics and genomics

A large body of information exists on AM fungal morphology and interactions within plants, and now an increasing resource of research focusing on the molecular workings of the fungal symbionts themselves is available due to advances in sequencing technology. Unravelling the

molecular pathways of these fungi is essential in understanding the full picture of the symbiosis, and may reveal novel findings, such as the initial observation that AM fungi do not possess the required molecular machinery to produce FAs (149).

Research into AM fungal genetics has brought a strong focus onto the sexual reproduction of these fungi. It is yet unclear whether AM fungi are heterokaryotic (173), supporting populations of genetically different nuclei, or homokaryotic, where the numerous nuclei are highly genetically similar (174, 175). These spores are often described as asexual, and evidence based upon analyses of recombination rate have concluded that AM fungi are ancient asexual organisms and produce spores clonally (176). Recent evidence, however, suggests that, not only do AM fungi show signs of infrequent recombination (177, 178), a number of species contain conserved meiotic genes and therefore are likely to be able to undergo conventional meiosis (179). It may be that, although the predominantly clonal life history of these fungi contributes to their ecological success, these organisms are indeed capable of gene exchange and sexual reproduction, though the environmental conditions that could trigger this rare sexual stage is unknown (175).

1.5.1 Available AM fungal genome sequencing data

The most well-studied AM fungal species is *R. irregularis*, and one strain of *R. irregularis,* DAOM197198, was the first of the AM fungi to have its whole genome sequenced, revealing a large genome of roughly 154Mb with a high TE content (149). This is a sizable genome relative to other fungi such as those from the *Ascomycota* and *Basidiomycota* with average genome sizes of roughly 37Mb and 47Mb, respectively (180). *R. irregularis* has continued to be a focus for AM fungal genomics (181). A further five isolates of *R. irregularis* have now been sequenced and were concluded to be highly genetically divergent between coding regions of different isolates, leading to the hypothesis that such genotypic differences may be one of the factors that enable AM fungi to associate with such a wide range of different plant hosts (182).

To date, sequencing data is also available on AM fungal species *R. clarus* (183), *R. diaphanus, R. cerebriforme* (184)*, Diversispora epigaea* (185), and *Gigaspora rosea* (184). It has become clear through studies of these diverse AM species that AM fungi encode a large repertoire of protein kinases, and lack genes required for a number of processes, including the production

of FAs *de novo* and the degradation of plant cell walls (183-185). The significance of the loss of these metabolic pathways in AM fungal ecology is striking when AM fungal genomes and gene repertoires are compared to those of related fungi from the Mucoromycotina and Mortierellamycotina, as the expansion and contraction of gene families along the evolutionary trajectory toward a symbiotic life cycle is visible (184, 185).

1.5.2 Transcriptome and secretome datasets of AM fungi

Understanding of the gene repertoire of AM fungi has been advanced through transcriptomics analyses. Transcriptomic datasets are available for spores, extraradical hyphae, and colonised roots in *R. irregularis* (149, 186), *G. rosea* (148), and *G. margarita* (187). Additional datasets have analysed *R. irregularis* transcripts that are differentially expressed in response to different phosphate levels (188).

In agreement with genomics data, AM fungal transcriptomes reveal conserved features that appear to be important for a symbiotic lifestyle, including the enrichment of transcripts associated with signal transduction, transport, and secreted proteins, and a lack of core metabolic pathway-encoding genes, such as the lack of FAS-encoding candidates and thiamine synthesis (148, 187, 189).

Plant-colonising fungi are entering a defended territory upon colonisation, and are recognised by the plant immune system. These fungi use secreted proteins, effectors, in a number of ways such as suppressing the host immune response, manipulating the host cell physiology, or shielding the fungus itself (190). Searching for secreted proteins of AM fungi became possible with the availability of transcriptome datasets, and secreted proteins have been identified and characterised by searching for the signatures such as small size and the presence of signal peptides (191-193). Laser microdissection enabling analysis of specific stages of fungal symbiotic growth such as extraradical hyphae, interradical hyphae, and arbuscules, has shown that a different subset of secreted proteins may be important in each stage of the symbiosis (194).

The first AM fungal secreted protein to be studied was SECRETED PROTEIN 7 (SP7), which was focused on due to its homology to repeat-containing proteins from *Plasmodium* that are expressed during host invasion. It was demonstrated that SP7 is localised to the nucleus and can cross the plant membrane, and overexpression of the gene encoding SP7 causes

enhanced mycorrhizal colonisation of transformed 'hairy root' cultures (195). Recent evidence supports a possible role of SP7 at the root epidermis, as extraradical hyphae close to host roots expressed SP7 at higher levels than hyphae further away in the soil (196).

The *R. irregularis* putative secreted protein SL-INDUCED PUTATIVE SECRETED PROTEIN 1 (SIS1) was selected for further study due to its high expression in SL-treated spores and in colonised host plant tissue compared to non-treated control spores. SIS1 function was validated by HIGS knockdown of expression, which resulted in reduced colonisation levels and the presence of stunted arbuscules compared to control root colonisation, where SIS1 expression and arbuscule morphology was WT. The presence of the putative secreted protein SIS1 may have a positive regulatory effect on the colonisation of host plants (63).

Further studies characterised the additional secreted proteins RiSLM, a chitin-binding putatively-secreted LysM protein in *R. irregularis* that is induced in mycorrhizal roots (197), and *R. irregularis* CRINKLER EFFECTOR 1 (RiCRN1) that was demonstrated to be important for the WT progression of the symbiosis and arbuscule development (198).

The secretomes of *R. clarus* (193), *R. proliferus* (192), and *G. rosea* (191) have also been studied. AM fungi likely produce a core set of conserved secreted proteins, though there is a clear difference in effector repertoire in more distantly-related species (191-193). Research into AM fungal secretomes has revealed the likely importance of secreted proteins in the different life cycle stages and host interactions AM fungi undergo. The secreted proteins described here are some of the more well-studied genes encoded by AM fungal genomes, due to their frequency in the transcriptome and the potential interesting effects they may have on host plants (174, 196).

1.5.3 Functional characterisation of AM fungal genes

Expression analyses are useful initial steps toward understanding gene function in AM fungi, as the spatial and temporal regulation of fungal genes may act as clues to when and where they function (199). For example, *R. irregularis* phosphate and ammonium transporters were observed to be induced in extraradical hyphae during colonisation, leading to hypotheses that these transporters are involved in uptake of their respective nutrients for transfer to the host plant (200-202).

Functional characterisation needs to be carried out to develop an understanding on the biological relevance of genes revealed during transcriptomics analyses of AM fungi. Reverse genetics methods that mutate genes of interest and study mutant phenotypes are key methods for understanding gene function, which requires mutagenesis of the genome or genetic transformation of the organism in question (203). Particle bombardment allowing for transformation of *G. rosea* has previously been carried out (204, 205), and this has also been attempted with *R. irregularis,* though stability of transformation was not achieved (206). Transformation of AM fungi has thus far proven challenging and is currently not an available tool for developing an understanding of AM fungal genetics, largely due to the multinucleate state of these fungi (205). Despite this core difficulty, several AM fungal genes are known and possible functions postulated, and alternative methods are being used to enhance understanding of AM fungal gene function.

RNA interference (RNAi) can be used as a tool for reverse genetics analyses. Due to a lack of transformation protocol for AM fungi, this method has been used in the transformation of host plants with constructs that target fungal genes. A transformed host is relied upon to produce small RNAs that are transferred to the fungal partner in colonised tissue, causing the fungal RNA silencing machinery to reduce expression of the gene of interest. This enables knockdown and understanding of *R. irregularis* gene function in colonised tissue, but its use is limited to those stages of the AM fungal life cycle where the fungus is in direct contact with the host plant, and may not be applied to pre-symbiotic stages (63, 198). Expression of fungal monosaccharide transporter *MST2* (1.4.2.1) has been reduced using RNAi, enabling analysis of its knockdown phenotype and the identification that it is required for WT levels of colonisation and arbuscule development (134). Additionally, expression of *R. irregularis* 14-3-3-encoding genes was reduced using RNAi in host plants. 14-3-3 proteins bind and regulate diverse signalling proteins such as kinases, phosphatases, and transmembrane receptors. RNAi-mediated knockdown of these genes impaired arbuscule formation and resulted in the reduced expression of plant phosphate transporter *MtPT4*, suggesting an essential role for this gene in associations with host plants (207).

A number of AM fungal genes have been functionally characterised by taking advantage of the established transformation systems of *Saccharomyces cerevisiae* (yeast). In the case of the *R. irregularis* ammonium transporters *AMT1* and *AMT2,* functionality was studied by expressing these transporters in a triple knockout of yeast with impaired ammonium uptake.

AMT1 and *AMT2* expression in this yeast mutant restored growth, demonstrating roles in ammonium uptake (201, 202). This same method was applied to studying genes potentially involved in AM fungal nitrogen assimilation and transfer (208).

In addition to complementation of yeast mutants, AM fungal genes can be studied through their expression in transformable fungi. This method was used when a *R. irregularis* gene was identified with sequence homology to the STE12 transcription factors (TFs) which are necessary for early host infection in hemibiotrophic pathogenic fungi including *Magnaporthe* and *Colletotrichum* species (209). Fungal pathogens of plants display a wide array of life cycle strategies, with some obtaining organic sustenance from the living host, the biotrophs, and others, the nectrotrophs, killing hosts to live off their organic compounds. Hemibiotrophic pathogens display life cycles that begin with a biotrophic stage causing no harm to the plant, as AM fungi do, followed by a nectrotrophic stage that kills the plant host (210). Expression of *RiST12* in a mutant of the hemibiotrophic fungus *Colletotrichum lindemuthianum* impaired in penetration of plant hosts restored the ability of this fungus to infect its host (211). The function of *R. irregularis* transmembrane protein PREFERENTIALLY EXPRESSED IN PLANTA (PEIP1) was also studied through its expression in a transformable fungal species. As its name suggests, *PEIP1* is expressed in colonised plant tissue. *PEIP1* was expressed in *Oidiodendron maius*, a fungus that intracellularly colonises the root cells of ericaceous shrubs. Expression of *PEIP1* in *O. maius* enabled a higher colonisation rate of the roots of its host, *Vaccinium myrtillus*, compared to WT colonisation levels for this system, implicating a role of *PEIP1* in endosymbiosis establishment (212).

Validation of the predicted fungal gene complement can be aided by proteomics analyses, and several proteomics datasets have been produced using AM fungi (213, 214). A proteomic profiling of the extraradical hyphae of *R. irregularis* was unable to assign a function to 53.6% of the total identified proteins, with the majority of these unassigned, hypothetical proteins (85.8%), being specific to the Glomeromycotina. This work demonstrates the difficulties that may be incurred when studying molecular regulation of the AM symbiosis, and the drawbacks in attempting to infer meaning from sequencing datasets of AM fungi that are currently poorly understood (215). Although these mechanisms exist to study AM fungal gene function, due to the likely high percentage of unique protein-encoding genes and lack of transformation pipeline to study them in AM fungal species themselves, there is currently a limited understanding of the AM fungal gene repertoire and its functions.

1.6 Maize as a model plant to study the genetics of the AM symbiosis

The AM symbiosis, and particularly its genetic regulation, has been studied extensively in model legume species that also engage in the root nodule symbiosis such as *L. japonicus* (74, 152, 157) and *M. truncatula* (101, 159). Rice has been used as a monocotyledonous model to study the genetics behind the AM symbiosis including identification of mycorrhizal-specific phosphate transporters *OsPT11* and *OsPT13* (121, 123), half-sized ABC transporters *OsSTR* and *OsSTR2* (165), receptor *D14L* (91), and PAM-localised receptor-like kinase *OsARK1* (216). Developing an understanding of how the symbiosis works in rice is hugely important, as it is difficult to extrapolate findings from such a small subsection of the angiosperm population, the species that host nitrogen-fixing rhizobia, without also studying additional model species (79).

Zea mays (maize) is a monocotyledonous plant that is an essential crop species. Maize is the second most highly produced crop in the world, though it is the crop with the most widespread distribution, grown in seventy countries, and is a hugely important dietary staple in developing nations (217). In developing nations, a vast majority of maize produced is by small-scale farming methods that do not supply a huge quantity of nutrient fertiliser (217), and this system could be one of the key beneficiaries of the AM symbiosis (218, 219). As such, studying the AM symbiosis in maize is important for translational research. Maize has a sequenced reference genome with gene model annotation (220, 221), and a number of inbred lines have been sequenced (222-224). In addition, transformation using clustered regularly interspaced short palindromic repeats (CRISPR)-CRISPR associated protein 9 (Cas9) genome editing is possible in maize, making this a viable system to study the genetics behind the AM symbiosis (225, 226).

Although maize is not one of the core model species used to study the AM symbiosis, it was a forward genetics screen in maize that enabled the identification of *NOPE1*, the transporter of a GlcNAc-related compound that is required for AM colonisation (1.2.1.2), and that has a conserved function in other AM-host species (33). In addition to *NOPE1,* the phosphate transporter *ZmPT6*, the ortholog of key PAM-localised phosphate transporters *MtPT4* and rice *OsPT11* (1.4.1) has been studied in maize, and this transporter is also induced under mycorrhizal conditions (111, 227-229). Additional research into the AM symbiosis in maize

has found that maize inbred lines display large differences in the extent to which they benefit from hosting AM fungi and that the extent of extraradical hyphae formed outside the root is a better indicator of the benefits received from the symbiosis than the percentage of root colonised by internal fungal structures (111, 230). Additional studies aiming to understand maize as a host for AM fungi have been largely based on ecological and field-level research (231-233).

Aside from these examples, the genetic components and their mutant phenotypes and functions discussed in this introduction have not been studied in maize, and it may not be safe to assume a similar regulation of the AM symbiosis to that identified in rice, particularly due to the life history of maize as an ancient tetraploid (234, 235).

1.6.1 Carrying out a forward genetics screen in maize

One of the methods by which to conduct a forward genetics screen in maize is through the transposable element systems that exist in this species, such as the *Mutator (Mu)* elements (236, 237). Plants of the *Robertson's Mu* strain contain a large number of copies of *Mu* elements with a high rate of transposition leading to a high mutation frequency, making this system highly effective in generating lines where the *Mu* element has interrupted a potential gene of interest (238). The *Mu* lines contain an active transposon, the *MuDR* autonomous element, that excises and inserts nonautonomous *Mu* elements into unlinked areas of the genome, often in gene-rich regions (239).

This *Mu* system was utilised in a screen aiming to identify novel plant genes involved in the AM symbiosis. The *Mu*-mutagenised lines were examined for perturbations in the interaction between maize and *R. irregularis* by screening for changes in the accumulation of the yellow chromophore, mycorradicin (240). Maize root systems that have formed a functional symbiosis with AM fungi accumulate mycorradicin, causing the roots to appear visibly yellow (241). In comparison, non-colonised roots are pale white in colour. Mycorradicin is an apocarotenoid formed upon oxidative cleavage of a carotenoid precursor, and accumulates late during the symbiotic relationship, when the arbuscules within cortical cells begin to degrade (242). This chromophore accumulation is a phenomenon unique to the Poaceae, and it is exclusively observed in roots that are colonised by an AM fungus. Attempts to encourage the accumulation of this chromophore using an increase in nutrient levels or hormone

treatment has proved unsuccessful (243). Mycorradicin accumulation is therefore a specific and useful tool in carrying out a high-throughput screen of mutagenised maize lines for alterations to root colonisation properties by *R. irregularis.* As such, a number of mutant phenotypes were identified based on mycorradicin accumulation in 1,250 *Mu*-mutagenised maize lines. Seven lines were observed where mycorradicin phenotype was stable and heritable, and of these, one displayed increased yellow accumulation, four displayed patchy or reduced accumulation, and two were identified due to an absence of mycorradicin accumulation (240). A result of this forward genetics screen was the discovery of the Major Facilitator Transporter *NOPE1* (1.2.1.2), identified due to a lack of accumulation of this yellow pigment in mutant roots, caused by a strongly reduced colonisation level (33). The identification of this component of the symbiosis highlights the potential of this forward genetics screen in monocotyledonous plants, and further important components of the AM symbiosis may yet be discoverable through the additional mycorradicin phenotypes observed during the screen (33, 240).

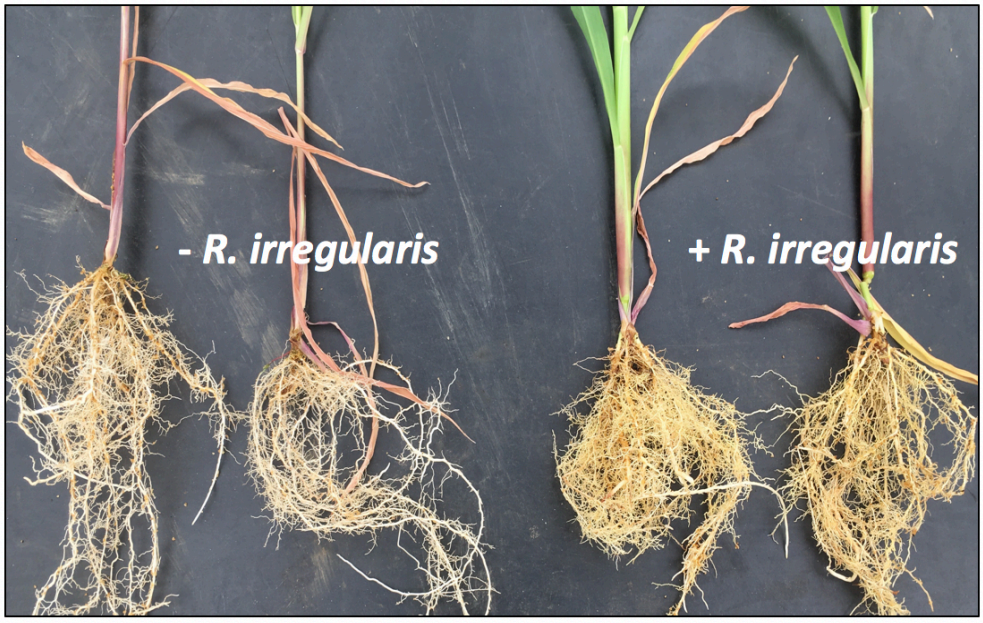

Figure 1.3: Accumulation of the yellow pigment mycorradicin in the root systems of colonised and non-colonised *Z. mays* plants. Maize plants were grown for 6 weeks in the presence or absence of *R. irregularis* inoculum. The two individuals not provided with inoculum (- *R. irregularis*) have pale white root systems, while two individuals grown with fungal inoculum (+ *R. irregularis*) display an accumulation of mycorradicin, causing the root systems to appear visibly yellow.

1.7 Research objectives

Identifying novel molecular components of the symbiosis has the potential to greatly enhance understanding of this widespread and important mutualistic relationship (33). Following the identification of two maize mutant lines that appeared unable to form a functional symbiosis with *R. irregularis* (240), this PhD project aimed to understand the biological and underlying genetic defect behind the novel *invisible to arbuscular mycorrhizal fungi* (*ina*) mutant, which is unable to associate with *R. irregularis*. Initial observations of this mutant phenotype suggested the possibility of erroneous communication during the initial, pre-symbiotic, stages of the symbiosis (240), and this research intended to examine the cause of such a strong block in fungal colonisation. A core focus of this PhD project has been the phenotypic characterisation of the *ina* mutant through well-established techniques used to understand arbuscular mycorrhizal mutant phenotypes. Initial phenotypic analyses involved plant growth experiments, inoculating mutant plants with the AM fungus *R. irregularis* and examining the effect of growing *ina* mutants with WT nurse plants. Visual phenotyping required microscopic analyses to assess the extent of fungal colonisation and fungal structures associated with mutant roots. Research into the *ina* phenotype led to the conclusion that an analysis of how *R. irregularis* responds to the presence of *ina* mutant plants is required, and this was carried out by RNA-Sequencing experimentation on spores of *R. irregularis*. Another important objective of this project has been the elucidation of the underlying genetic defect in the *ina* mutant line through positional cloning methods. Identification of the gene behind this mutant line is required to establish whether a known AM symbiosis component is the causal candidate. This work aims to identify the causal genetic defect in the *ina* genome to further understand the biological mechanisms of this novel phenotype, and to establish where this molecular component may fit into known pathways that regulate the AM symbiosis.

1.8 Contribution of others

All research described in this thesis was the work of myself, with the exception of elements of the positional cloning work described in Chapter 4. All plant growth and phenotyping for positional cloning purposes was carried out by myself in Cambridge, UK. Genotyping for rough

mapping of the *INA* locus, and subsequent genotyping by seed chipping, (4.2.3) was carried out by Corteva AgriScience (IA, USA). Analysis of the genotyping data was carried out by myself (4.2.4) using the facilities at Corteva AgriScience (IA, USA) as part of the BBSRC iCASE studentship program. All other experimentation described in Chapter 4 was carried out by myself.

CHAPTER 2

Materials and Methods

2.1 Plant growth

2.1.1 *Z. mays* material and sterilisation

Initial seed lines containing the *ina* mutation were provided by Istituto Sperimentale per la Cerealicoltura, Sezione di Bergamo (240). The mutant individuals were crossed to *Z. mays* inbred lines B73 and W22, and to a *Mu* killer line in the W22 background (244). For positional cloning, F_2 populations segregating for the *ina* mutation were used. For all experiments requiring the homozygous (HMZ) *ina* mutant and a control WT line, F_3 seed lines produced by self-pollination of HMZ *ina* or HMZ WT individuals from segregating populations were used.
A maize seed line segregating for a *Dissociation* (*Ds*) (245) transposable element-generated insertion mutation within *ZmNOPE1* was used to obtain HMZ *Zmnope1* material for this study (33). Maize inbred line W22 was used as a WT control for this material.
Before growth, all *Z. mays* kernels were sterilised by washing with 3% sodium hypochlorite for 5 minutes, followed by washing with autoclaved de-ionised water (diH_2O) 3 times. Seeds were then pre-germinated for 3 days on moist filter paper at 30°C in the dark.

2.1.2 *O. sativa* material and sterilisation

The rice *d10* mutant used in this research, harbouring point mutations, was previously described (88, 246), as was the rice *d27* mutant material, caused by a deletion resulting in a truncated translation product (247). WT rice used in this study was the cultivar Shiokari, as the *d10* and *d27* mutants were backcrossed into this background (88). Rice seeds were manually de-husked and washed with 3% sodium hypochlorite for 30 minutes on a Heidolph Plymax 1040 platform shaker (Schwabach, Germany). Following bleaching, seeds were

washed 3 times with diH_2O. Sterile seeds were pre-germinated on 0.7% agarose plates sealed with micro-pore tape at 28°C for four days.

2.1.3 Production of fungal crude inoculum

R. irregularis 'crude' inoculum was produced by inoculating *Tagetes patula* plants grown in 5L pots of sand and Terra Green (1:0.5 v/v) with approximately 3,000 *R. irregularis* spores per pot. Following growth for two weeks and watering with Reverse Osmosis (RO) water, plants were watered twice weekly with ½ Hoagland's Solution (Appendix: Table A1). After two months of growth, colonisation of *T. patula* roots was examined microscopically. When high colonisation levels (approximately 80%) were achieved, watering of the *T. patula* plants ceased, and the growth medium was dried out over a period of roughly three weeks. Dried above-ground plant material was cut and removed, and the growth mixture containing fungal spores, hyphae, and pieces of colonised root was sieved and used as a source of inoculum.

2.1.4 Fungal inoculation and maize planting

1L pots with drainage holes were used for *Z. mays* colonisation assays. The drainage holes were covered by a nylon filter, and then filled with damp sand. A 30mL hole was bored into the sand and 5mL of crude inoculum was placed inside. Pre-germinated kernels were placed atop the crude inoculum and covered by sand. Plants planted for the non-inoculated control condition were planted without the addition of *R. irregularis* crude inoculum.

2.1.5 Plant cultivation conditions for colonisation assay

Plant growth took place under a 12-hour light/12-hour dark cycle at 28°C during the day, 23°C during the night, and 60% humidity. Following two weeks of initial growth post inoculation with *R. irregularis*, 100mL of Hoagland's solution (Appendix: Table A1) was added twice a week to each plant. Plants were checked daily for watering requirements and were watered using RO water when the sand medium was not sufficiently damp.

2.1.6 Nurse plant cultivation conditions

Germinated seeds were placed into 5L pots of sand with a nylon filter covering drainage holes. The 'experimental' maize plants were placed into the centre of a pot and surrounded by 3 'nurse' plants, rice or maize. All seeds were placed into a 30 mL hole and inoculated with 5 mL of crude inoculum. Maize nurse plant experiments were fertilised with full Hoagland's Solution containing 100µM Pi (Appendix: Table A1), while rice nurse plant experiments were fertilised with ½ Hoagland's Solution containing 50µM Pi (Appendix: Table A1).

2.1.7 Maize exudate complementation

Non-inoculated exudate donor maize plants were pre-germinated and cultivated for six weeks according to the previously-described plant growth protocol (2.1.5). For exudate collection, six week-old plants were harvested, roots washed with autoclaved diH_2O, and placed into 500mL conical flasks of 400mL full Hoagland's solution. Two maize plants were added to each flask, with root systems completely submerged. Flasks were covered with aluminum foil to avoid light exposure and the opening was covered with Parafilm Tape (Sigma-Aldrich, USA) to minimise water loss. The conical flasks containing plants were then placed onto a mechanical shaker (IKA Basic Variable-Speed Digital Orbital Shaker, 230V) and shaken at 50 shakes/min for 3 days, in the previously described growth conditions (2.1.5).
Experimental plants were pre-germinated and grown for two weeks (2.1.5). At two weeks, plants were inoculated with 5mL of *R. irregularis* crude inoculum, and received 100mL of exudates from donor plants once every three days as an alternative to receiving full Hoagland's fertiliser. After six weeks of receiving exudates, experimental plants were harvested (2.1.8).

2.1.8 Plant harvest and sampling

Plants were carefully removed from the pots and the root systems rinsed with RO water. The embryonic root was cut away and the remaining root system cut into pieces of 1-2cm. The root cuttings were mixed to ensure a diverse collection of root types were taken for each sampling method. A sample of root pieces were placed into 2mL Eppendorf tubes containing

10% (w/v) KOH for Trypan Blue analysis (2.2.2). Root pieces were also collected in 2mL Eppendorf tubes of 50% Ethanol (v/v) for later Wheat Germ Aglutenin (WGA) analysis (2.2.3). Finally, root pieces were placed into 2mL Eppendorfs containing 2x 2mm stainless steel beads and immediately frozen in liquid nitrogen and stored at -80°C for molecular analyses (2.3).

2.2 Visual maize mutant phenotyping

2.2.1 Screening mutant phenotypes

Z. mays plants were phenotyped at 6-7-weeks post-inoculation (wpi). For inspection, plants were removed from the pots and mycorradicin accumulation in roots was categorized based on the colour of the roots. Root systems were scored as either 1) 'Yellow'; obvious yellow pigmentation visible, 2) 'Intermediate'; possible or faint yellow pigmentation, 3) 'Pale'; complete lack of yellow pigmentation.

2.2.2 Microscopic quantification of colonisation using Trypan Blue staining

Quantification of *R. irregularis* colonisation was carried out by staining root samples with Trypan Blue. Samples that had been collected in 10% KOH (2.1.5) were incubated at 90°C for 30 minutes, followed by removal of KOH and rinsing twice with diH_2O. A solution of 0.3M Hydrochloric acid (HCl) was added for 15-30 minutes at room temperature. Upon removal of HCl, a 0.1% solution (100 mg trypan blue in 50mL:25mL:25mL – lactic acid:glycerol:diH_2O) of Trypan Blue (Sigma-Aldrich, USA) was added and the sample boiled at 90°C for five minutes. Root pieces were then removed from solution, rinsed with acidic glycerol (50% (v/v) glycerol in 0.3M HCl) and transferred to slides. Colonisation was quantified with an Olympus CH40 light microscope (Olympus, Japan) using ten root pieces from each individual, where ten microscopic viewpoints at 200X magnification were examined per root piece for the presence of fungal colonisation and structures (Figure 2.1). Representative images of root colonisation were captured using a Keyence VHX-1000 microscope (Keyence, Japan).

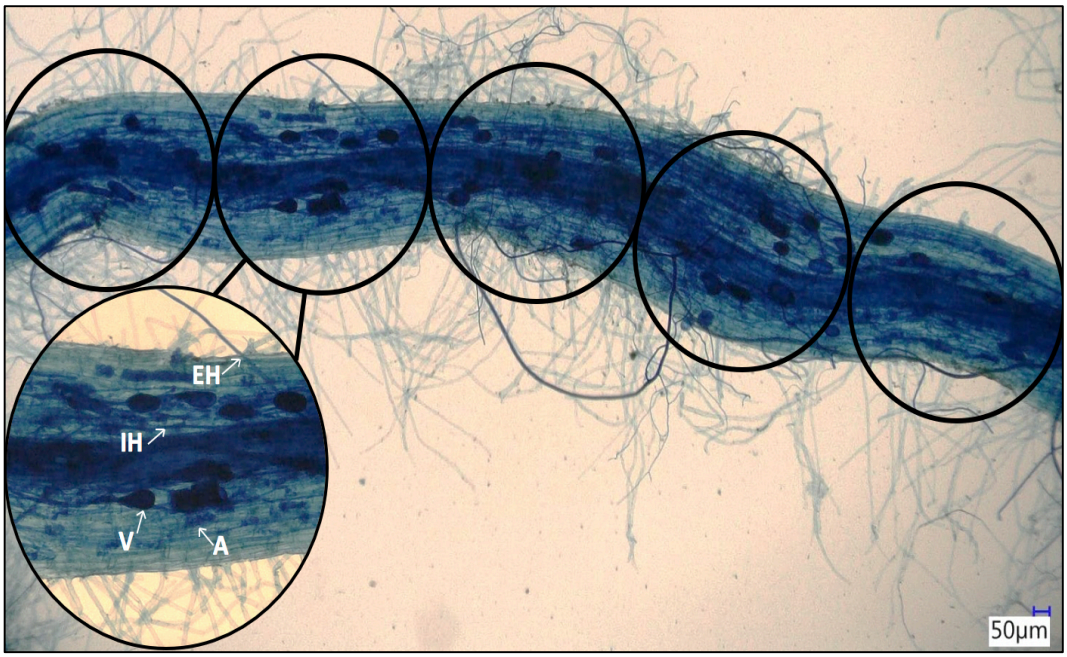

Figure 2.1: Quantification of *R. irregularis* colonisation levels of maize roots stained with Trypan Blue. One representative maize root piece is displayed, and six of the ten viewpoints used to quantify colonisation per root piece are circled. An enlarged example of a viewpoint observed through microscopic analysis of colonisation at 200X magnification is displayed, and the fungal structures are indicated with arrows. These fungal structures observed in this viewpoint would be classified as present at that singular section of ten of the viewpoints assessed per root piece.

2.2.3 Assessment of fungal structures using WGA staining

To visualize fungal structures in higher resolution for a qualitative assessment of the *ina* phenotype, roots were stored in 50% EtOH for up to seven days before incubation in 20% KOH at room temperature for two days. Root samples were then rinsed with diH_2O and 1x phosphate buffered saline (PBS). Rinsed roots were then incubated for up to two weeks in the dark at 4°C in a solution of 0.2µg/ml Alexa Fluor 488 Wheat Germ Agglutinin (WGA) (Sigma-Aldrich, USA) diluted in 1x Phosphate-Buffered Saline (PBS). Immediately prior to imaging, root pieces were stained for three minutes in a solution of 10µg/ml of Propidium Iodide (Fisher Scientific, UK) to stain plant cell walls. Fluorescence of fungal and plant structures was examined and imaged using a Leica SP8 microscope (Leica Microsystems, Germany).

2.3 Molecular analyses of maize mutants

2.3.1 gDNA extraction

For plant genotyping, ~2cm of leaf tissue was taken from three week-old individuals, placed into 2mL Eppendorf tubes with 2x 2mm stainless steel beads and frozen in liquid nitrogen. Samples were ground using a Qiagen TissueLyser II (Quiagen, Germany) at 30 shakes/second for three minutes. For extraction of genomic DNA (gDNA), 300µl of extraction buffer (3.727g KCl in 5mL TRIS pH7.5, 1mL EDTA, and MilliQ H_2O to 50mL total volume) was added to each sample. The samples were then vortexed and transferred to a heat block at 98°C for ten minutes, followed by two minutes of centrifugation (13,000 rpm) at room temperature. Supernatant was then transferred to 1.5mL tubes containing 300µl of 100% isopropanol. After another centrifugation step at room temperature for 15 minutes (13,000 rpm), the pellet was washed twice using 300µl of 70% EtOH. EtOH was removed and the pellet air-dried for ten minutes, before finally dissolving the gDNA pellet in 50µl of MilliQ H_2O. Final concentrations of gDNA were estimated using a Nanodrop Spectrophotometer (Thermofisher Scientific, USA).

2.3.2 PCR genotyping

Genotyping of the maize mutants used in this thesis, *ina* and *nope1,* was carried out using a standard PCR mix and protocol (5x GoTaq Buffer, 10mM dNTPs, 25mM $MgCl_2$, 10µM forward and reverse primers, and Promega GoTaq G2). Reactions were carried out using a Thermocycler with extension time adjusted for the size of the desired amplicon, and annealing temperature was adjusted for the melting temperature of the primers used. All PCR products were run on a 0.8% agarose gel made with 1µl/mL ethidium bromide at 120mV. Gels were imaged under UV light and images captured to genotype biological samples.

To obtain HMZ *nope1* individuals, segregating material was genotyped for the WT allele using gene-specific primers (33), and for the mutant allele using a gene-specific primer and primer specific for the *Ds* insertion (Appendix: Table A2, Figure A1).

2.3.3 RNA extraction and quality checking

During harvesting of maize root systems, root samples were frozen and stored at -80°C (2.1.8). A Qiagen TissueLyser II (Quiagen, Germany) set to 30 shakes/second for three minutes was used to grind these frozen samples into a powder. For RNA extraction, TRIzol reagent (Guanidium Thiocyanate 23.63g, Ammonium Thiocyanate 7.6g, Sodium Acetate pH5 8.33mL, Glycerol 12.5mL, Phenol pH5 95mL, dilute to 250mL with diH_2O) was used with a modified TRIzol extraction protocol (Invitrogen Life Technologies). The modified protocol included a suspension of the RNA pellet in 60µl H2O and 60µl LiCl buffer (4M LiCl, 2mM trisHCl pH7.5, 10mM EDTA), incubation at -20°C for 1h, and centrifugation for 20 minutes (13,000rpm). Finally, the samples were washed twice with ice-cold 75% EtOH and air-dried. Following extraction, RNA pellets were suspended in 25µl of RNase-free H_2O for use and quantity and purity estimated using a Nanodrop Spectrophotometer (Thermofisher Scientific, USA). To assess integrity of extracted RNA, 2µl of each sample of total RNA was run on a 2% agarose gel and examined for integrity.

2.3.4 cDNA synthesis

Prior to complementary DNA (cDNA) synthesis, a total RNA quantity of 1.1µg for each sample was treated with DNase I (Sigma-Aldrich, USA) to remove contaminating gDNA, followed by deactivation of the DNase I enzyme by incubation with EDTA at 65°C for five minutes. A standard PCR analysis (5x GoTaq Buffer, 10mM dNTPs, 25mM $MgCl_2$, 10µM forward and reverse primers, and Promega GoTaq G2) was carried out using the RNA samples as templates to confirm removal of all contaminating gDNA using primers for *ZmGAPDH*. Lack of amplification visualised by running the PCR product on a 0.8% agarose gel confirmed the absence of contaminating gDNA in DNase I-treated RNA samples. cDNA synthesis was then carried out using a SuperScript II Reverse Transcriptase (Invitrogen, USA) standard protocol.

2.3.5 qRT-PCR analysis

Primer design used sequence information from the Maize W22 v2.0 genome, MaizeGDB. Primers were designed using NCBI Primer-BLAST (Appendix: Table A3) and were designed to

anneal to the 3' UTR of selected genes for specificity. Primer efficiency for new primer sets was assessed by carrying out a qRT-PCR using five two-fold dilutions of maize cDNA as a template. The Ct values obtained were plotted as a linear standard curve and efficiency obtained from the slope of this curve using the equation: $Efficiency = \left(10^{\frac{-1}{slope}} - 1\right) \times 100.$ Primer sets with an efficiency of 90-110% were used.

qRT-PCR was carried out to quantify expression levels of genes of interest in maize mutant and WT samples. cDNA samples were diluted 1:10 with MilliQ H_2O and added to a SYBER Green detection-based reaction mix (10x SYBER green, 50mM MgCl2, 10mM dNTPs, 5x GoTaq buffer, 3µM forward and reverse primer mix, MilliQ H_2O, and Promega GoTaq G2). Each biological sample reaction was carried out in triplicate technical replicates, and reactions were carried out in a 96 or 384-well plate (Thermo Scientific) using a Bio-Rad CFX Real-Time PCR Detection System (Bio-Rad, USA) (Appendix: Figure A2). For each maize cDNA sample, expression of three housekeeping genes, *ZmGAPDH, ZmCyclophilin2,* and *Zmβ-actin,* (Appendix: Table A3) was measured to normalise the expression of genes of interest. Expression of these three housekeeping genes in each sample was averaged using a geomean, and this geomean value was then used to normalise the expression results for genes of interest for each sample.

For visualisation of expression data, the average normalised expression value across all three technical replicates per biological sample was taken and plotted on statistical software R using package ggplot2 (248).

2.4 Positional cloning of the *INA* locus

2.4.1 Harvesting and shipping

Maize plants from segregating populations (4.2.2: UP23.3, UP23.4, UP23.9, UP23.10, UP23.11, UP23.15, UP23.17, UP23.18) were grown as previously described (2.1) and eight leaf discs per plant were harvested when plants were three-weeks old using a Leaf Puncher for uniformity and collected into 96-well cluster tubes (Corning, USA). Leaf material was frozen in liquid nitrogen and stored at -80°C in 96-well blocks (Corning, USA). Material was lyophilised before sending to Corteva (Corteva AgriScience, USA) for SNP genotyping.

2.4.2 gDNA extraction

gDNA was extracted from 96-well assay blocks (Corning, USA) of lyophilised leaf material. Eight stainless steel beads were first added to each well, and material was lysed during one minute of shaking in a 2000 Geno/Grinder (SPEX SamplePrep, USA) at 750 strokes/minute. gDNA extraction was then carried out using a Puregene extraction kit and standard protocol (Quiagen, Germany). Following extraction, gDNA was resuspended in 100µl TE + RNase.

2.4.3 SNP marker development and KASP genotyping

SNP markers for positional cloning were chosen using SNPs available from Corteva proprietary resources, and from Maize SNP50 (249). Genotyping of SNPs was performed using allele-specific primers designed using Primer Picker (KBiosciences, UK). SNPs were first tested for polymorphism between WT and *ina* HMZ individuals using control gDNA from these samples. Only SNPs that were polymorphic between WT and *ina* individuals were selected for use in positional cloning.

Genotyping SNPs was carried out using allele-specific amplification via fluorescence detection, using the Kompetitive Allele-Specific PCR (KASP) genotyping method (LGC Group, UK) (Appendix: Figure A3), requiring a standard KASP reaction mix (primer mix of two allele-specific primers and a common reverse primer, KASP master mix, diH_2O). PCR amplifications were carried out in a Thermocycler using a standard KASP PCR program (LGC Group, UK).

Fluorescence was measured following amplification using a Tecan Infinite M1000 PRO plate reader (Tecan, Switzerland). Plate data was analysed using TIBCO Spotfire (Spotfire, USA) by assessing the fluorescence of each DNA sample and comparing this to WT and *ina* HMZ control samples to identify the form of the SNP.

2.4.4 Rough mapping

Rough mapping was carried out by genotyping 31 segregating individuals using SNP markers selected to maximize coverage of the maize genome (SNPs: proprietary Corteva resource). This enabled the identification of the haplotypes most commonly observed in WT or *ina*

individuals. For analysis, genotype at each SNP was scored as 'A' for individuals HMZ for the SNP allele most commonly found in WT plants, 'B' if HMZ for the allele most common in mutant individuals, and 'H' for heterozygotes at the SNP. In a subsequent mapping round, a further 180 individuals were genotyped at 29 SNPs within this region. The R package R/qtl was used for visualisation of distance between SNPs and their genome coverage by inputting genotype scoring of the 180 individuals at each SNP.

2.4.5 Fine mapping

From the seven segregating lines identified through phenotyping, 2,100 seeds were chipped and genotyped for five SNP markers without the need for first growing plants and leaf sampling (seed chipping: proprietary Corteva technology). Of these individuals, 269 individuals were identified as possessing recombination events between these five SNP markers, and these individuals were grown and phenotyped (2.1).

Subsequent rounds of SNP marker design and KASP genotyping were used to identify additional SNPs between markers flanking the *INA*-containing region and to genotype these SNPs in recombinant individuals. This was sequentially carried out until none of the 269 recombinant individuals were identified as having a recombination event between the flanking markers in question, based on phenotyping data.

2.4.6 Candidate gene analysis

Genes that were located within the fine-mapped region containing the *INA* locus were analysed using previously described gDNA extraction and PCR protocols (2.3.2) using primers designed using NCBI Primer BLAST (Appendix: Table A2).

2.5 *R. irregularis* RNA-Sequencing analysis

2.5.1 Preparation of *R. irregularis* material

R. irregularis spores (Agronutrition, Toulouse, France) were washed with MilliQ H_2O to remove citrate storage buffer and sieved using a 40µm cell strainer (Corning, USA). A known

quantity of spores was suspended in 1x M Media (Appendix: Table A4) to a density of 10,000 spores/mL. 8mL of this spore solution was aliquoted to an individual 16.8 mL tissue culture well (Corning, USA), for a total of 80,000 spores/well. Tissue culture dishes containing spores were pre-germinated at 30°C and 2% CO_2 for seven days.

Maize plants were grown according to previous description (2.1) and their root exudates collected as described (2.1.6). Exudates were then sterilized using 0.2µm filters (Sartorius Epsum, UK). Spores were removed from seven-day incubation and sieved using a 40µm cell strainer (Corning, USA) to remove M Media. Spores subjected to the 0h treatment were immediately frozen in liquid nitrogen for analysis. Spores subjected to root exudate treatment received 8mL of the collected maize root exudates. Tissue culture dishes of spores in root exudate solution were then incubated once again at 30°C and 2% CO_2 for 1h or 24h, before removal, sieving to remove exudates, and freezing in liquid nitrogen.

2.5.2 *R. irregularis* RNA extraction and qRT-PCR analysis

R. irregularis spore material was ground using a mortar and pestle cooled with liquid nitrogen, and RNA extraction was carried out using an RNeasy Plant Kit (Quiagen, Germany) according to manufacturer's instructions.

For qRT-PCR analysis of fungal material, DNase treatment, cDNA synthesis, and qRT-PCR expression analysis was carried out as previously described for maize material (2.3). Primers were designed using sequence data from the Joint Genome Institute (JGI) using *R. irregularis* DAOM 197198 v2.0. Primer design was carried out using NCBI Primer BLAST. qRT-PCR expression data from genes of interest were normalised using a geomean obtained from three *R. irregularis* housekeeping genes, *RiEF1α*, *RiGAPDH*, and *Riα-tubulin* (Appendix: Table A5).

2.5.3 *R. irregularis* library preparation and sequencing

Extracted RNA to be analysed using RNA-Sequencing was DNase-treated to remove contaminating gDNA using TURBO DNase (Thermofisher Scientific, USA) according to standard manufacturer's protocol. RNA integrity and purity was assessed using an Agilent

2100 Bioanalyser and RNA 6000 Pico Kit (Agilent, USA). Samples of a RIN score above 7 and with clean, expected RNA peaks were used for further analysis.

RNA-Sequencing libraries were prepared using the Illumina TruSeq Stranded mRNA Kit and standard protocol (Illumina, USA), and used a starting quantity of 1µg from each *R. irregularis* RNA sample. Following library preparation, libraries were quality checked using an Agilent 2100 Bioanalyser and DNA 1000 Kit (Agilent, USA). Library quality was assessed through the Bioanalyser electropherogram output and samples with expected DNA peaks were pooled (minimum three samples per treatment) and the resulting pooled libraries were diluted to 4nM using a Qubit fluorometer (Thermofisher Scientific, USA).

R. irregularis samples were uploaded to the *in silico* application Illumina BaseSpace to identify which adapter sequences used during library preparation corresponded to each sample. The pooled libraries were then sequenced using a NextSeq500/550 High Output v2 Kit (150 cycles) through an Illumina NextSeq 550 system (Illumina, USA).

2.5.4 RNA-Sequencing bioinformatics analyses

Raw sequencing data obtained from Illumina BaseSpace was quality checked using the program MultiQC, which produced a summary report on all samples (250). All samples were of sufficient quality for analysis, thus raw sequencing reads for each sample were aligned against the transcriptome assembly of *R. irregularis* DAOM 197198 v2.0 using the program Salmon, which was then used for transcript quantification of alignment files (251). Mapped and quantified data files were analysed in R using the package DESeq2 (252). DESeq2 was used to carry out pairwise comparisons, where transcripts with an FDR-adjusted P-value of <0.05 were considered as differentially expressed between treatment comparisons. Further analysis of RNA-Sequencing data involved assignment of Gene Ontology (GO) terms to all transcripts from DAOM 197198 using BLAST2GO (OmicsBox, BioBam, Spain), and the identification of GO terms enriched under spore treatment conditions using a Fisher's Test (253). Further detail into the experimental design and bioinformatics analysis of the RNA-Sequencing data is outlined in Chapter 3.

CHAPTER 3

Phenotyping of the *invisible to arbuscular mycorrhizal fungi* mutant

3.1 The *ina* mutant is blocked in its pre-symbiotic interaction with AM fungus *R. irregularis*

3.1.1 Introduction

Research into the genetics underpinning the AM symbiosis has historically been reliant on the characterisation of plant mutant phenotypes that display alterations in their interactions with AM fungi (254). Plant phenotypes defective in AM symbiosis fall into categories based on the stage of their impairment, ranging from defective pre-contact signalling to the altered formation and lifespan of internal fungal structures (255).

Pre-symbiotic mutant phenotypes result from an erroneous communication between plant and fungus, and plant mutant phenotypes of this stage include inabilities to signal to, or 'talk to', the fungus (33, 48), and inabilities to perceive signals from, or 'listen to' the fungal partner (91, 256). Whether the directionality of impairment lies in contacting or perceiving the fungus can be established by the co-cultivation of a pre-symbiotic mutant with WT individuals, a 'nurse plant' experiment. The fungal extraradical hyphae that exist outside the root form a bridge between individual plants (257). As such, any lack of signal or nourishment from the mutant individual that is required by the fungus for colonisation will be provided by WT plants. The *osnope1* and *S. lycopersicum* M161 mutants, which both display reduced colonisation by *R. irregularis*, have the ability to support WT-levels of colonisation when grown with WT nurse plants (33, 258). This is likely due to WT plants providing signalling components required for fungal entry into plant roots, and in the case of *osnope1* this component is a GlcNAc-related compound (33). In contrast, pre-symbiotic perception mutants such as *d14l* are unable to support colonisation in a nurse plant system, as the presence of a WT individual cannot enable mutant perception of fungal signals (91).

During pre-symbiotic signalling, the lack of signal from mutant plant to fungus may be due to an altered composition of root exudates (258). Plant roots exist in a diverse microbiome, and

one way in which they cultivate and control their associations with rhizosphere microbes is through root exudate composition (259). The presence of a suitable host root has a clear effect on the morphological development of AM fungal spores (94, 260), and a number of studies have demonstrated that the presence of isolated host root exudates may elicit fungal morphological development even in the absence of the root system itself (33, 261-264). This ability of isolated exudates enables further study of pre-symbiotic mutant phenotypes by studying the effect of these exudates on AM fungi at the pre-contact stage of development (33, 265).

This chapter describes the exploration and characterisation of a novel mutant phenotype, *invisible to arbuscular mycorrhizal fungi (ina)*. This mutant phenotype was discovered in a screen for maize phenotypes with altered associations with AM fungi, identified due to a potential lack of ability to host colonisation by *R. irregularis* (240). This work utilises methods of phenotyping symbiosis mutants discussed above in order to understand the underlying cause of what is a severe, and unique, AM phenotype.

3.1.2 Results

3.1.2.1 The *ina* mutant displays a block in colonisation by *R. irregularis*

Under standard growth and *R. irregularis* inoculation conditions (2.1), maize roots from a seed family segregating for the *ina* mutation were examined using Trypan Blue staining (2.2.2). At this stage of 7 wpi, the segregating plants looked visibly WT above ground, with no developmental defects (Figure 3.1A). Individuals identified as mutants due to the pale root phenotype displayed a significant lack of root colonisation by *R. irregularis*, no internal fungal structures were observed in these plants under Trypan Blue staining (Figure 3.1B). Extraradical hyphae could occasionally be seen in the vicinity of the mutant roots, but the formation of hyphopodia appeared to be blocked, as no attempts from the fungus to form penetration structures were visible. In contrast, WT roots were highly colonised (Figure 3.1C), and displayed a higher average total root length colonisation level of 87% (Figure 3.1D).

As the AM symbiosis is a dynamic process, a repeat experiment assessing colonisation levels at early (4wpi) and late (9wpi) time-points was carried out to attempt to capture any further aspects of the interaction between the fungus and this mutant phenotype. In WT plants, total colonisation rose from 51% at 4wpi to 91% at 9wpi, though *ina* mutants supported no internal colonisation at both time-points (Figure 3.1E). This further emphasised the inability of *ina* mutant individuals to physically interact with and enable colonisation by *R. irregularis.*

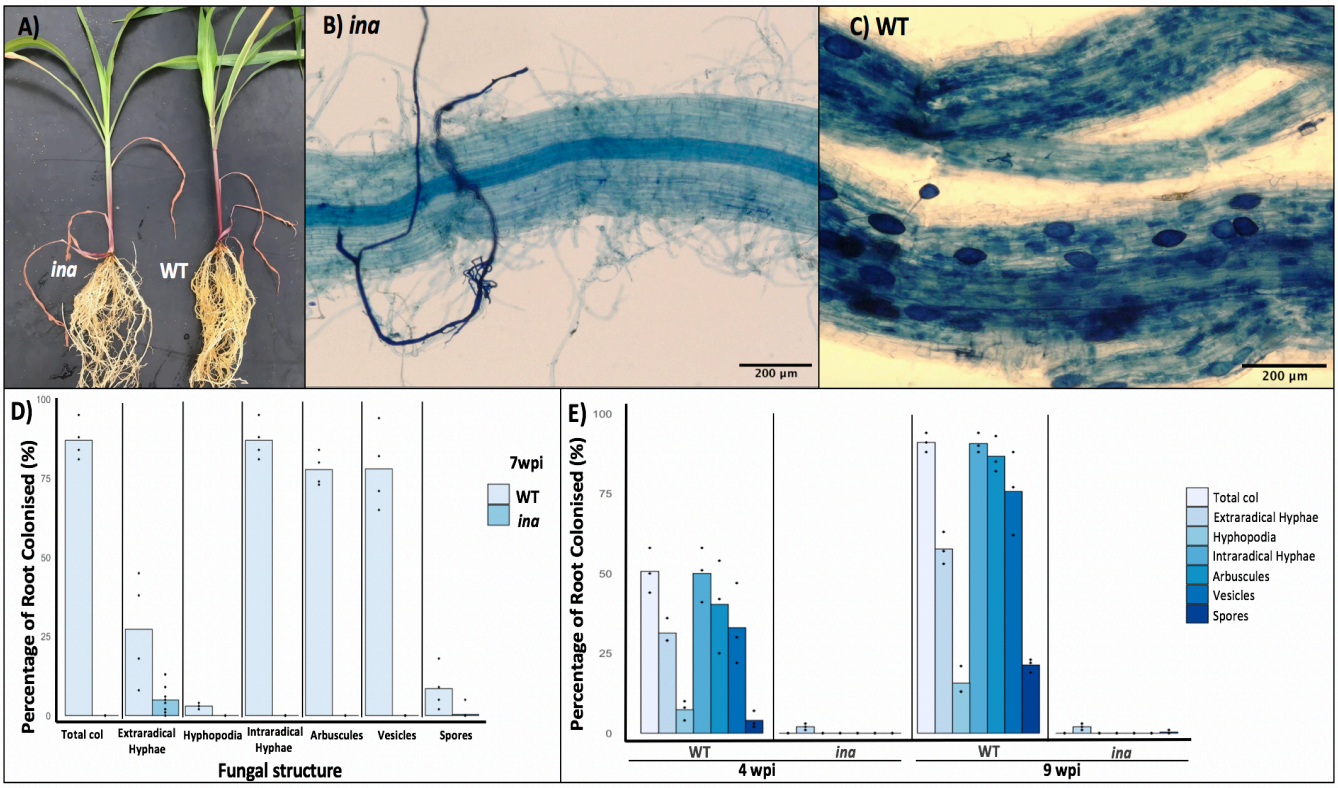

Figure 3.1: ***R. irregularis*** **root colonisation of the** ***ina*** **mutant. A)** Representative image of Trypan Blue stained *ina* and WT plants showing no defects in above-gound growth and development at 7 weeks. **B)** and **C)** Representative images of *ina* mutant roots at 7wpi following Trypan Blue staining. **D)** Representative image of WT maize roots at 7wpi following Trypan Blue staining. **D)** Percentage root colonisation at 7wpi of 13 mutant individuals and 4 WT individuals. **E)** Percentage root colonisation in WT and *ina* plants following 4wpi and 9wpi (3 biological replicates from each genotype per time-point). WT colonisation level increases between time-points, though was not a statistically significant increase (Mann-Whitney-Wilcoxon Test $p<0.05$). No internal colonisation was recorded in *ina* individuals at either time-point, and due to the excess of data points with a value of 0, *ina* readings were excluded from statistical analyses. Bar height represents average colonisation across individuals, and individual plant data points are displayed.

In order to support this quantification phenotype with molecular data, a qRT-PCR experiment was carried out using cDNA from three WT and *ina* individuals from the colonisation assessment experiment. An established system of marker genes expressed exclusively upon AM colonisation exists in rice, and may be used to monitor progression of fungal colonisation through the stages of the symbiosis (91, 266). Included in these established markers is the *R. irregularis* gene *RiEF1α,* encoding elongation factor 1α and serving as an indicator of fungal quantity in the root (267).

The maize homologs of *OsAM3*, (*ZmAM3)* induced early during the symbiosis and encoding a small secreted protein, and *OsPT11 (ZmPT6)*, which encodes a mycorrhizal-specific phosphate transporter (121), have previously been utilised as marker genes in maize (111, 228). The markers *ZmARK1*, encoding a receptor-like kinase localised at the PAM that serves as a later-stage symbiotic marker (216), and *ZmPT14*, an additional mycorrhizal-specific phosphate transporter that exists in some cereals (123), were established as marker genes for the purposes of this study.

All marker genes, including those newly established, showed a significant upregulation in the inoculated condition, and in all expression analyses there were no significant differences between the non-inoculated WT levels and the expression levels in inoculated *ina* plants (Figure 3.2).

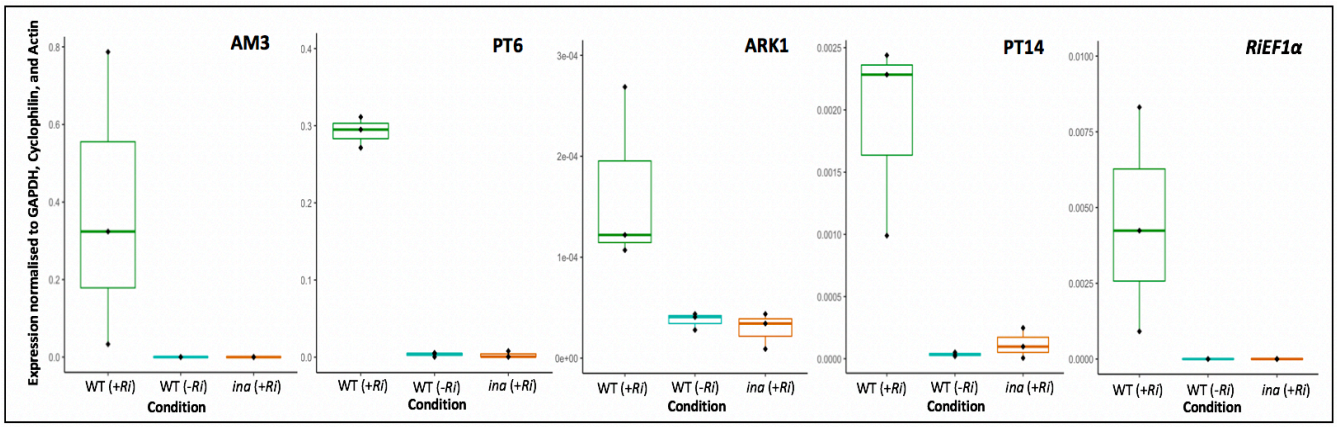

Figure 3.2: qRT-PCR expression analysis of symbiosis marker genes. Expression of symbiosis markers *ZmAM3, ZmPT6, ZmARK1, ZmPT14* in 3 biological replicates of WT inoculated (+*Ri*), WT non-inoculated (-*Ri*), and *ina* inoculated (+*Ri*) plants. Expression of all symbiotic markers was significantly higher in WT inoculated plants than in non-inoculated WT and inoculated *ina* plants. Expression in all samples was normalised against the geomean expression of maize *GAPDH*, *Cyclophilin*, and *Actin* reference genes.

3.1.2.2 Growth of *ina* in a nurse plant system restores fungal colonisation

A nurse plant system provides both a strong inoculum pressure and potential required signals or fungal nourishment from WT plants. Colonisation was quantified through Trypan Blue staining of *ina* plants grown in a monoculture or co-cultivated with three WT plants, and of WT plants grown in a monoculture of four individuals. Co-cultivation with WT plants until 9wpi restored the ability of the fungus to form hyphopodia, penetrate *ina* roots, and produce internal fungal structures (Figure 3.3A). Average total colonisation of *ina* roots that were co-cultivated with WT nurse plants was not found to be statistically lower than the average total colonisation in highly-colonised WT monocultured plants (Figure 3.3B) (Mann-Whitney-Wilcoxon Test, $p<0.05$). Interestingly, though the fungus formed internal structures within *ina* individuals complemented by the presence of WT nurse plants, there appeared to be a defect in arbuscule formation in these plants. The majority of visible arbuscules under Trypan Blue analysis were small and stunted in *ina* roots (Figure 3.3C) compared to highly branched, larger, arbuscules in WT individuals (Figure 3.3D). When *ina* plants were cultivated in a monoculture, no internal colonisation by *R. irregularis* was observed (Figure 3.3E).

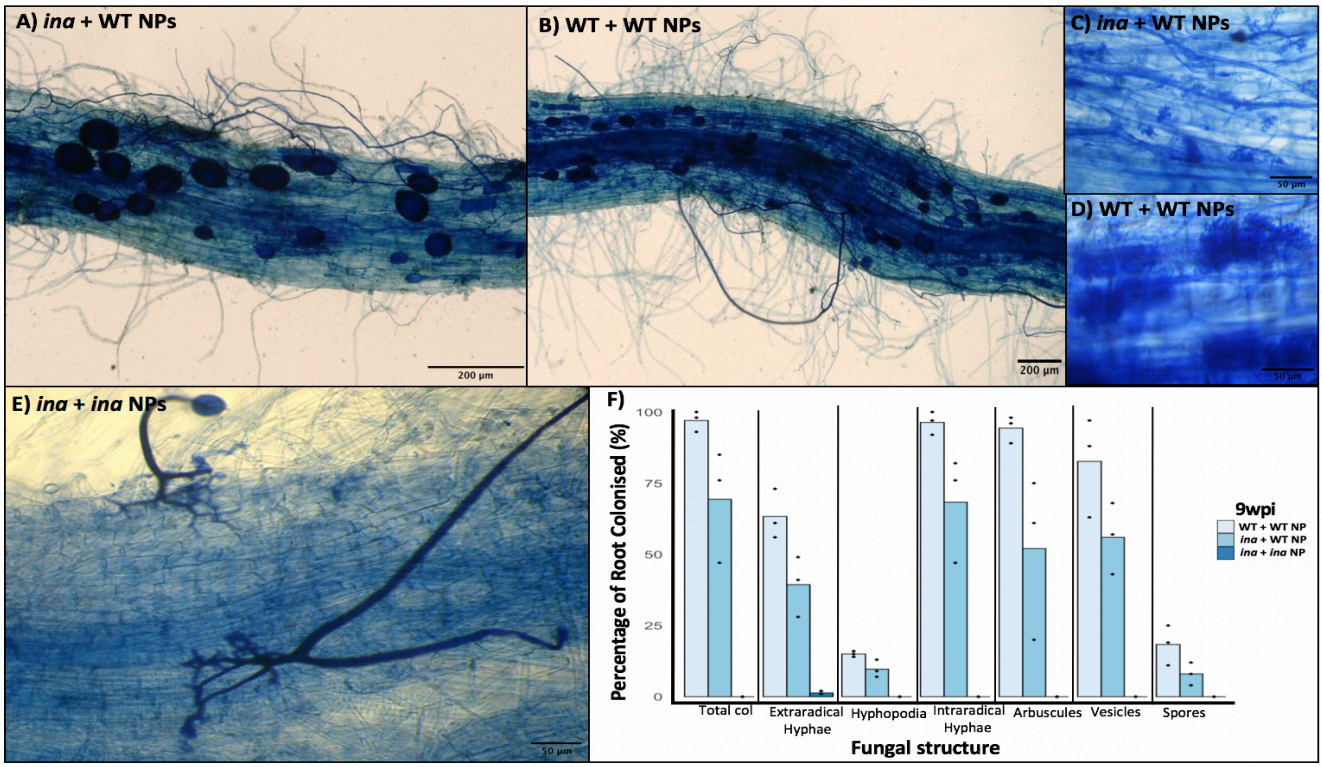

Figure 3.3: ***R. irregularis*** **colonisation of** ***ina*** **plants is restored in a nurse plant system. A)** Representative image of Trypan Blue-stained *ina* roots co-cultivated with WT NPs that enable internal colonisation by *R. irregularis* and the formation of internal fungal structures. **B)** Representative image of a Trypan Blue-stained WT root grown in a monoculture, supporting high fungal colonisation levels. **C)** Representative image of colonised *ina* individuals that display stunted arbuscules visible following Trypan Blue staining. **D)** Representative image of WT, branched, arbuscule in WT individuals visible under Trypan Blue staining. **E)** Representative image of a Trypan Blue-stained *ina* individual cultured in a monoculture that displays a block in colonisation by *R. irregularis*. **F)** Percentage root colonisation for WT monocultured, *ina* co-cultivated with WT nurse plants, and *ina* monocultured individuals (three biological replicates per treatment). No significant difference was found in the quantity of fungal structures in WT monocultured individuals and *ina* individuals grown with WT nurse plants (Mann-Whitney-Wilcoxon Test, $p<0.05$). *ina* individuals grown in a monoculture were excluded from statistical analysis, due to an excess of zero counts in these observations. Bar height represents average colonisation across individuals, and individual plant data points are displayed.

3.1.2.3 Addition of WT exudates to *ina* growth medium restores fungal colonisation

Complementation of the *ina* phenotype in a nurse plant system suggests a directionality in the erroneous communication, where the defect appears to be involved in the plant to fungus signal. This led to a hypothesis that WT and *ina* individuals produced exudates with different compositions. Exudates were harvested from *ina* and WT individuals and added to the growth medium of both *ina* and WT individuals, in all combinations, to examine whether the presence of WT-produced exudates could enable *R. irregularis* to colonise *ina* roots.

Remarkably, addition of WT exudates to *ina* plants twice every week over a 6-week time-period did restore the ability of the fungus to penetrate and colonise *ina* roots (Figure 3.4A). When complementation with WT exudates made fungal penetration possible in *ina* plants, the sparse patches of colonisation supported small, stunted arbuscules (Figure 3.4A). WT plants provided with WT and *ina* exudates remained visibly highly colonised (Figure 3.4B, C). When *ina* exudates were added to the growth medium of *ina* plants, the inability of *R. irregularis* to colonise the roots remained, and no fungal structures were seen (Figure 3.4D).

The average total colonisation level in WT exudate-complemented *ina* plants was very low, at 13% (Figure 3.4E). This was significantly lower than average total colonisation in conditions where WT plants were provided either WT or *ina* exudates (Mann-Whitney-Wilcoxon Test, $p<0.05$). WT plants given WT exudates supported an average total colonisation level that was not significantly different to that observed in WT plants provided with *ina* exudates (Mann-Whitney-Wilcoxon Test, $p<0.05$) (Figure 3.4 E). This finding potentially rules out an inhibitory effect of *ina* root exudates on colonisation.

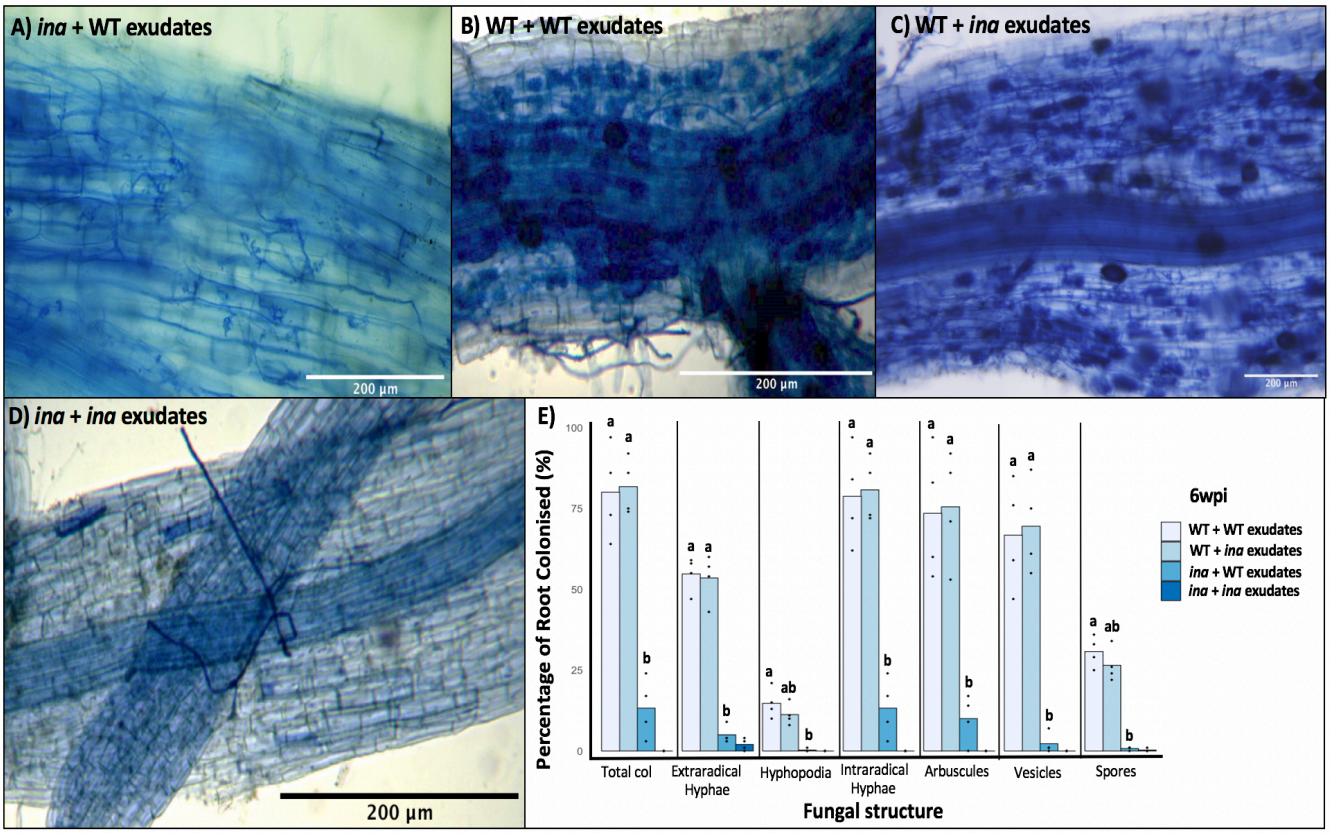

Figure 3.4: ***R. irregularis*** **colonisation of** ***ina*** **plants is restored by addition WT exudates. A)** Representative image of *ina* individuals provided with WT exudates, enabling penetration by *R. irregularis* and internal colonisation, though with stunted arbuscules, visible under Trypan Blue-staining. **B)** Representative image of Trypan Blue-stained WT roots that were provided with WT exudates and display high colonisation levels. **C)** Representative image of WT individuals watered with *ina* exudates displaying dense colonisation visible under Trypan Blue staining. **D)** Representative image of a Trypan Blue-stained *ina* plant provided with *ina* exudates, no internal colonisation was observed. **E)** Percentage root colonisation in WT individuals provided with WT exudates and *ina* exudates, and *ina* individuals provided with WT exudates and *ina* exudates (four biological replicates per treatment). There is no significant difference in average quantity for any of the fungal structures between WT individuals provided with WT and WT individuals provided with *ina* exudates (Mann-Whitney-Wilcoxon Test, $p<0.05$). A significantly different colonisation level across a majority of fungal structures is observed between WT individuals given both exudate treatments and *ina* individuals provided with WT exudates. *ina* individuals provided with *ina* exudates were excluded from the statistical analysis, due to an excess of zero counts in these colonisation observations. Bar height represents average colonisation across individuals, and individual plant data points are displayed.

3.1.2.4 Qualitative analysis of *ina*-supported fungal structures reveals arbuscule abnormality

Roots of individuals grown in the nurse plant system and exudate complementation experiments were stained with WGA to examine the stunted arbuscule phenotype at higher resolution than possible through Trypan Blue staining. Using this staining technique it was possible to qualitatively observe the stunted arbuscules that occurred regularly in *ina* individuals colonised with the aid of a WT nurse plant (Figure 3.5A, B). These structures were smaller in size and displayed a reduced and abnormal branching pattern compared to arbuscules formed in WT individuals (Figure 3.5C, D).

Using WGA staining to observe the intracellular structures produced in WT exudate-complemented *ina* individuals did not reveal any arbuscule-like branches. Commonly, hyphae were seen twisting inside root cells (Figure 3.5E, F). It may be that no arbuscules were seen in these root samples due to the severely low number of arbuscules observed in these exudate-complemented mutants. WT individuals receiving both WT and *ina* exudates supported WT-branching arbuscules (Figure 3.5 G, H).

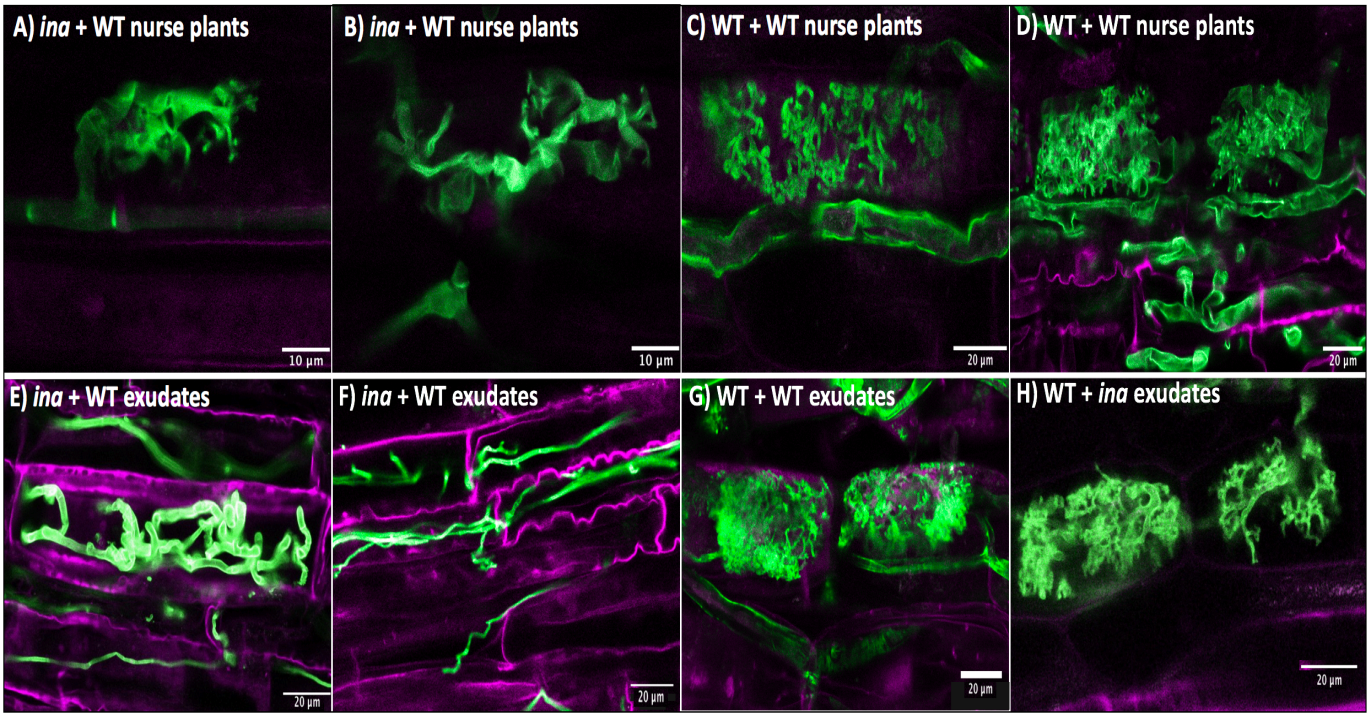

Figure 3.5: ***R. irregularis*** **arbuscules observed under WGA staining in** ***ina*** **and WT genotypes under exudate complementation conditions. A)** and **B)** Representative images of stunted arbuscules in *ina* roots that support fungal colonisation due to complementation by the presence of a WT nurse plant. **C)** and **D)** Representative images of WT arbuscules displaying extensive branching inside WT plants grown in a monoculture. **E)** and **F)** Representative images of internal hyphae within *ina* roots colonised with the aid of WT root exudate application. Colonisation is supported but no arbuscules are visible with WGA staining. **G)** Representative image of WT, highly-branched arbuscules inside root cortical cells of WT plants provided with WT exudates. **H)** Representative image of WT plants provided with *ina* exudates that support WT, branched arbuscules.

3.1.2.5 Co-cultivation of *ina* with rice SL biosynthesis mutants restores colonisation

As SLs are known plant-derived signals that trigger germination and hyphal branching in AM fungi (39), these compounds were a candidate for the missing component from the root exudates of *ina* mutants. In order to establish whether a lack of SL production or exudation causes the inability of *R. irregularis* to colonise *ina* roots, an additional nurse plant experiment was carried out using SL biosynthesis mutants as nurse plants. No maize SL biosynthesis mutants were available, so rice mutants of *d27* (1.2.2.1) and *d10* (1.2.1.2) were used. This experiment also required the use of WT maize and WT rice nurse plants as controls, WT maize

to as a positive control, and the rice variety Shiokare, the corresponding WT cultivar and genetic background of the *d27* and *d10* mutants used.

Co-cultivation of *ina* individuals with WT maize plants once again restored the ability of mutant individuals to host colonisation by *R. irregularis* (Figure 3.6A), as did growth of *ina* plants with WT rice variety Shiokare (Figure 3.6B). Interestingly, co-cultivation of *ina* with rice *d27* mutants enabled *R. irregularis* to penetrate and colonise roots (Figure 3.6C), and so did the co-cultivation of *ina* with rice *d10* mutants (Figure 3.6D). Although colonisation in *ina* individuals co-cultivated with WT maize was high, roughly 81% total colonisation, *ina* individuals grown with rice nurse plants of all genotypes, Shiokari, *d27*, and *d10*, were poorly colonised, with total colonisation rates ranging from 8-10% (Figure 3.6E). One rice nurse plant from each biological replicate experimental pot was assessed for colonisation, and the average root length colonisation percentage was 19% in Shiokari nurse plants, 14% in *d27* nurse plants, and 11% in *d10* nurse plants. This low colonisation level in the rice nurse plants may account for the reduced ability of these rice individuals to restore *ina* colonisation levels compared to WT maize, as maize nurse plants displayed an average total colonisation of 90%.

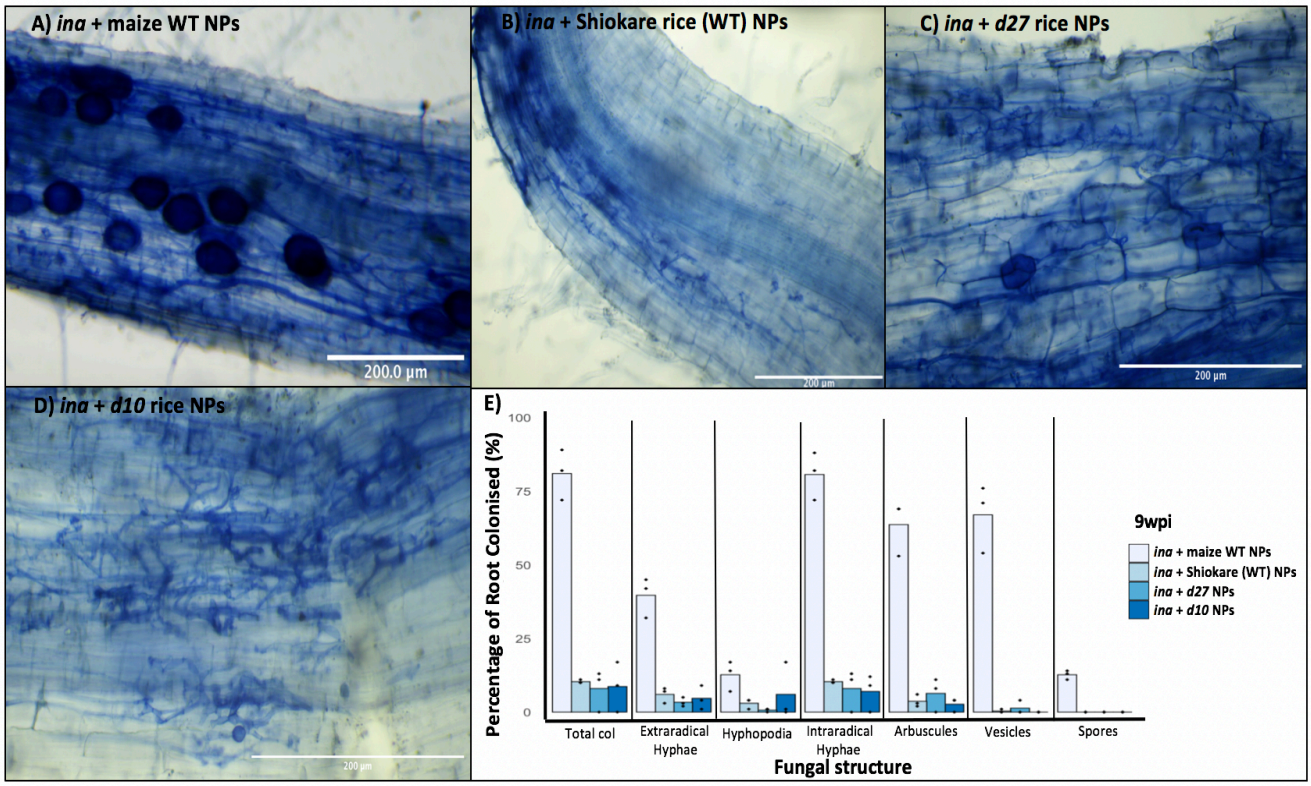

Figure 3.6: ***R. irregularis*** **colonisation of** ***ina*** **is complemented by co-cultivation with SL mutants of rice. A)** Representative image of Trypan Blue-stained *ina* individuals co-cultivated with WT maize plants that support *R. irregularis* colonisation. **B)** Representative image of *R. irregularis* colonisation of *ina* individuals stained with Trypan Blue following co-cultivation with WT rice of the Shiokari variety. **C)** Representative image of a patch of *R. irregularis* colonisation within *ina* individuals that were co-cultivated with rice *d27* mutants in the Shiokari background, visible due to Trypan Blue staining. **D)** Representative image of Trypan-Blue stained *ina* individuals supporting colonisation of *R. irregularis* when co-cultivated with rice *d10* mutants in the Shiokari background. **E)** Percentage of root colonisation in *ina* individuals co-cultivated with maize WT, rice Shiokari WT, and rice mutants of SL biosynthesis, *d27* and *d10* (three biological replicates per treatment). No significant difference was found between any of the treatments carried out (Mann-Whitney-Wilcoxon Test, $p<0.05$). Bar height represents average colonisation across individuals, and individual plant data points are displayed. Rice nurse plant colonisation – (Average total colonisation: Shiokari – 19%, *d27* – 14%, *d10*–11 %).

3.2 The extended phenotype of *ina*: A transcriptomics analysis of the response of fungal spores to *ina* root exudates

3.2.1 Introduction

Key aspects in understanding pre-symbiotic communications during the AM symbiosis involve identifying which signals are passed between host plants and AM fungi, and understanding the response of the symbiotic partner when it perceives these signals. Analyses have been conducted on the response of plants to signalling molecules produced by AM fungi. Fungal signals such as short- and long-chain COs and LCOs elicit a plant symbiotic response, and the responses of plants to these signals can be studied alone or as a component of germinated spore exudates (GSE) (61, 62, 268, 269). This plant response to fungal signals includes the increased production of SLs, a response that may result in an increased signal to the fungal partner (270). Pre-symbiotic mutants with a defect in perceiving fungal signals can be studied using GSE, which provides an optimal experimental design by enabling both WT and mutant plants to be treated with GSE to observe differences in response to fungal signals, rather than using whole spores that would result in the colonisation of the WT control and the vast responses associated with the later stages of the symbiosis (91).

From the perspective of plant-to-fungus signalling, research has identified plant-derived signals that cause a symbiotic response in the fungus. Known components produced by plants that cause a morphological response in the fungus during pre-symbiotic communication include flavonoids (54, 55), 2-hydroxy fatty acids (2-OH-FA) (59), branched-chain fatty acids (60), SLs (29, 39, 271), and the GlcNAc-like molecule transported by the plant transporter *NOPE1* (33). Treatment of fungal spores with the synthetic SL analog GR24, a useful tool in simulating the presence of a host plant, increases the potency of fungal GSE by increasing fungal production of COs and LCOs, a further example of the dynamic nature of pre-symbiotic signalling (61).

This increasing focus on the fungal side of the AM symbiosis has been possible due to a number of genome sequencing datasets from AM fungi (149, 182, 183, 185, 272). There are also several transcriptomic analyses that shed light on fungal gene expression during the different stages of the symbiosis (113, 186, 189, 273). Studies on the transcriptomics response of AM fungi during their interaction with plant hosts include analyses on the response of

spores to GR24 (63, 194), and, recently, branched-chain fatty acids, in an attempt to understand how *R. irregularis* spores react during the pre-symbiosis when they receive plant-derived signals. Notably, comparison of spore response to GR24 and palmitoleic acid, two factors known to induce activity in spores, revealed very little overlap in fungal reaction, suggesting that a number of plant-derived products have the ability to metabolically activate AM fungal spores and produce distinct responses (60). Plant exudates may also be utilised to view the response of fungal spores to plant signals during the pre-symbiosis and to understand the impact on fungi of plant mutants perturbed in the pre-symbiotic pathway (258). The use of exudates has even enabled an analysis of the transcriptomic response of *R. irregularis* spores to WT and *nope1* mutant exudates, revealing the role of the NOPE1 transporter in activating the fungus prior to symbiosis (33).

This section explores the 'extended phenotype' of the *ina* mutant by examining the transcriptomics response of *R. irregularis* spores to exudates produced by *ina* and WT plants, with a comparative analysis of spore response to *nope1*. The analysis of the fungal response to plant-derived signals that are a component of root exudates will enable a deeper understanding of the signal that appears to be lacking from *ina* root exudates.

3.2.2 RNA-Sequencing experimental design and analysis pipeline

Plant growth and exudate collection was carried out as with the exudate-complementation experiment. In order to understand the responses of fungal spores to multiple plant mutant phenotypes with defects in pre-symbiotic signalling, exudates were also collected from *Zmnope1* mutant plants and the associated W22 WT background for spore treatment. Spore plates pre-germinated in M Media were treated to root exudates for time-points of 0h, 1h or 24h, with the 0h time-point requiring spores to be frozen immediately after the 7-day pre-germination period in M Media. For each condition, 3-4 spore plate biological replicates were used. To ensure fungal response was to plant genotype and not simply to individual plants, two plants of the same genotype were placed in flasks together for root exudate collection, and each spore plate biological replicate received exudates from different flasks of plants of the same genotype in a minimum of three replicates (Figure 3.7).

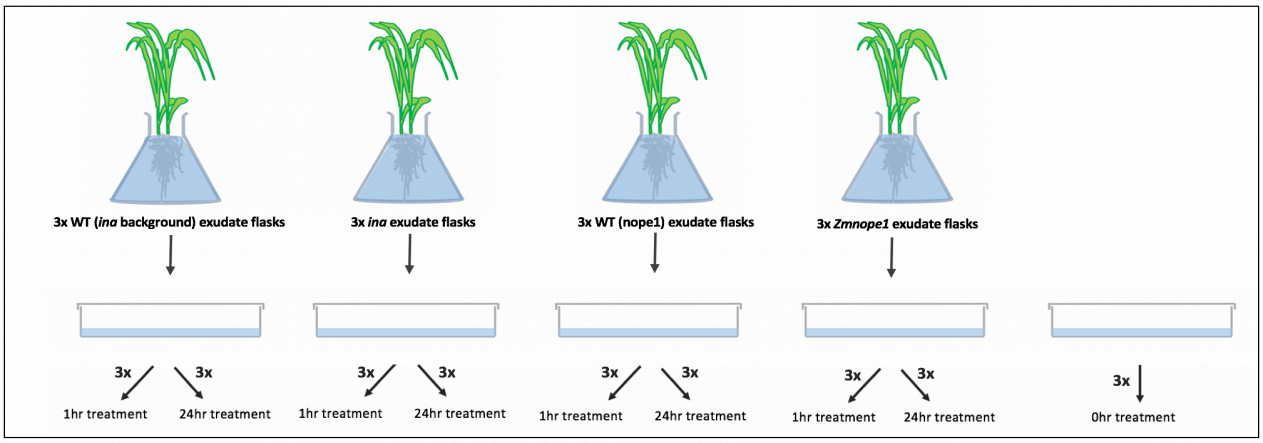

Figure 3.7: Experimental design of the *R. irregularis* RNA-Sequencing experiment. Flasks (3 per genotype) of two maize plants suspended in full Hoagland's solution were used to collect plant exudates of four different genotypes, *ina*, *nope1*, and two corresponding WT backgrounds, WT (*ina*) from a HMZ WT sibling line, and WT (*nope1*), which were plants from the W22 inbred line. 8mL of plant exudates were applied to plates of pre-germinated spores (80,000 spores per plate) for 1h or 24h treatments. 0h time-point spore plates did not receive plant exudates.

RNA-Sequencing libraries produced from RNA samples were submitted for sequencing. Sequencing data in the form of .fastq files was then quality checked by producing a MultiQC report on all samples (Figure 3.8) (250). The MultiQC report output provided a Phred quality score for the samples, and all samples were of a sufficient quality to pass the threshold for continued analysis. The average guanine-cytosine (GC) content across samples was 38%, which is an expected value for the *R. irregularis* genome (149).

Following quality checking, reads were aligned against *R. irregularis* transcriptome assembly 197198 v2.0 (149) using Salmon for alignment and transcript quantification (251). The average mapping percentage across all samples was 81%. Mapped and quantified data .bam files were then analysed using DESeq2, which uses internal normalisation across all genes to control for any differences in sequencing depth across samples (252). Any normalised transcript values described in this analysis were produced from DESeq2 normalisation. DESeq2 was used to carry out pairwise comparisons to identify differentially expressed (DE) genes (Padj <0.05) when comparing fungal responses to different plant genotype-produced exudates (Pipeline described in Figure 3.8A). Pairwise comparisons were checked for separation based on condition using Multi-Dimensional Scaling (MDS) plots to visualise sample separation (Figure 3.8B).

Gene Ontology (GO) terms were assigned to all transcripts within the RNA-Sequencing dataset using BLAST2GO (OmicsBox) (253). BLAST2GO utilised the nucleotide sequences for all transcripts and assigned GO terms to each transcript following BLAST (Fungal Kingdom NCBI BLAST) and database searches using InterPro, UniProt, and Ensembl. BLAST2GO was used to further explore GO term assignments using Fisher's Tests to identify GO terms enriched under specified conditions. Of 26,183 transcripts, 10,609 received at least one GO annotation (Figure 3.8C).

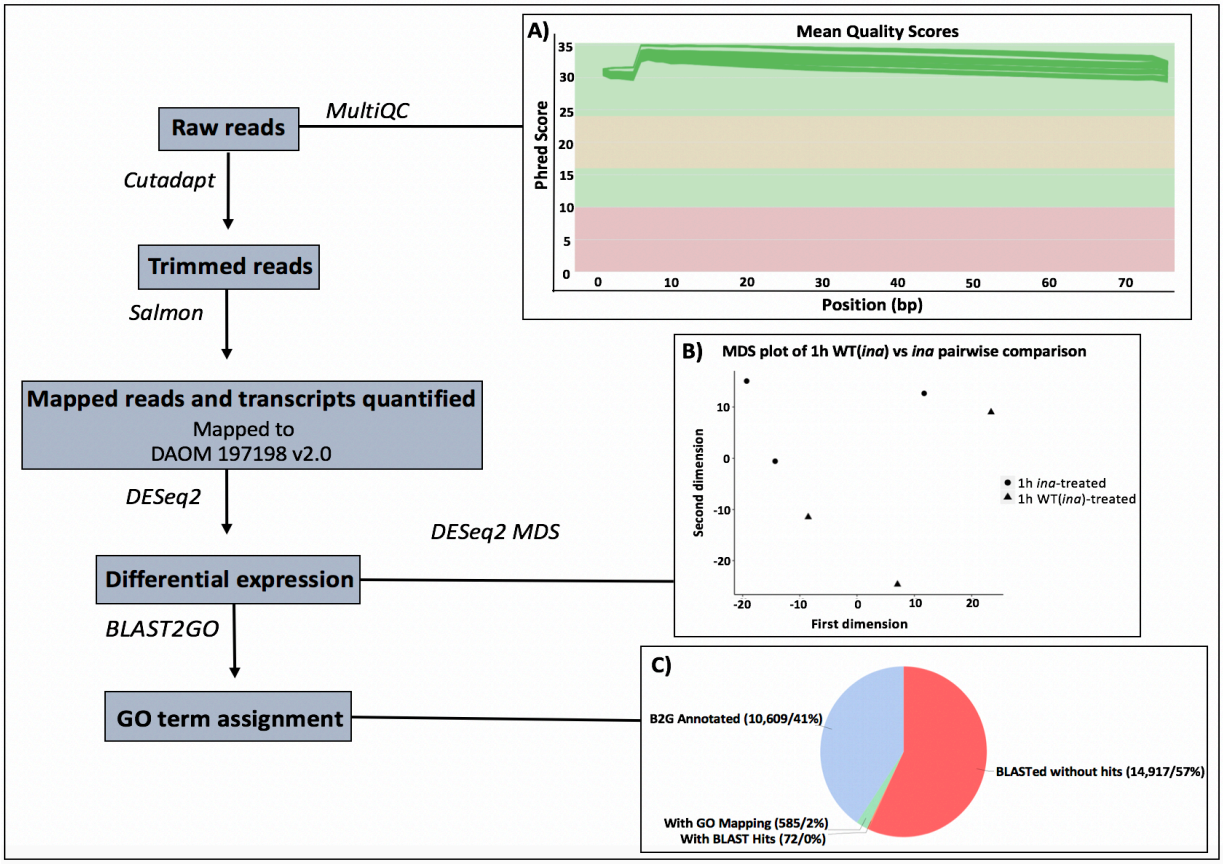

Figure 3.8: Workflow of *R. irregularis* RNA-Sequencing analysis. Displayed in a flow-chart is the pipeline of RNA-Sequencing analysis from receipt of raw sequencing reads, through trimming of adapter sequencing, mapping and transcript quantification, differential expression analysis, and GO term assignment. Software used for analysis are italicised. **A)** MultiQC-generated scores of all *R. irregularis* samples passed the quality threshold Phred score. **B)** Sample MDS plot displaying the separation of samples by treatment condition. **C)** Pie chart depicting percentages of transcripts assigned GO annotation scores by B2G in blue. Transcripts BLASTed but with no hits are indicated in red. Transcripts that were assigned GO terms based on BLAST information, but that received no final annotation score following protein database searches are indicated in green, and the 72 transcripts that produced BLAST hits and received no mapping- stage GO term assignment are indicated in yellow.

3.2.3 Results

3.2.3.1 Fungal transcriptomic responses to maize mutant genotypes

To first understand how spores respond to the different plant genotypes, pairwise comparisons between spores treated to the 0h condition, receiving no exudates, and spores treated to the WT and mutant exudates were carried out. This allowed an analysis of overlap of transcripts induced or downregulated in response to addition of exudates at the different time-points, 1h and 24h. The initial response of spores to the different plant genotypes was largely similar at 1h, with a strong overlap of transcripts. At this stage, the transcripts induced under all exudate treatments are associated with enriched GO terms involving transport and metabolism (Figure 3.9A). When looking at downregulated transcripts compared to the 0h time-point, there was again a large overlap in spore response to the different plant exudates, though *ina* treatment produced a larger downregulation response than other conditions. Oxidoreductase activity and catalytic activity were some overlapping GO terms downregulated by 1h exudate treatments compared to 0h (Figure 3.9B).

Following prolonged incubation for 24h, the different exudate treatments tended to cause the induction of more unique transcripts in their pairwise comparisons to the 0h time-point, though a large number of common transcripts were induced by all exudate treatments. There appeared to be a large response in spore transcript induction to the presence of *nope1* exudates following the 24h treatment. At this later stage, it appears that WT(*nope1*)-treated spores displayed a reduced response compared to WT(*ina*)-treated spores (Figure 3.9C), suggesting a different effectivity of exudates produced by the different maize inbred lines. Following the 24h treatment, the common transcripts that were induced regardless of exudate genotype were associated with GO terms describing metabolic activity. A small number of overlapping transcripts were identified as downregulated in response to all plant exudate treatments at 24h compared to the 0h time-point (Figure 3.9D), and, as with the downregulated transcripts at 1h, associated GO terms included oxidoreductase activity.

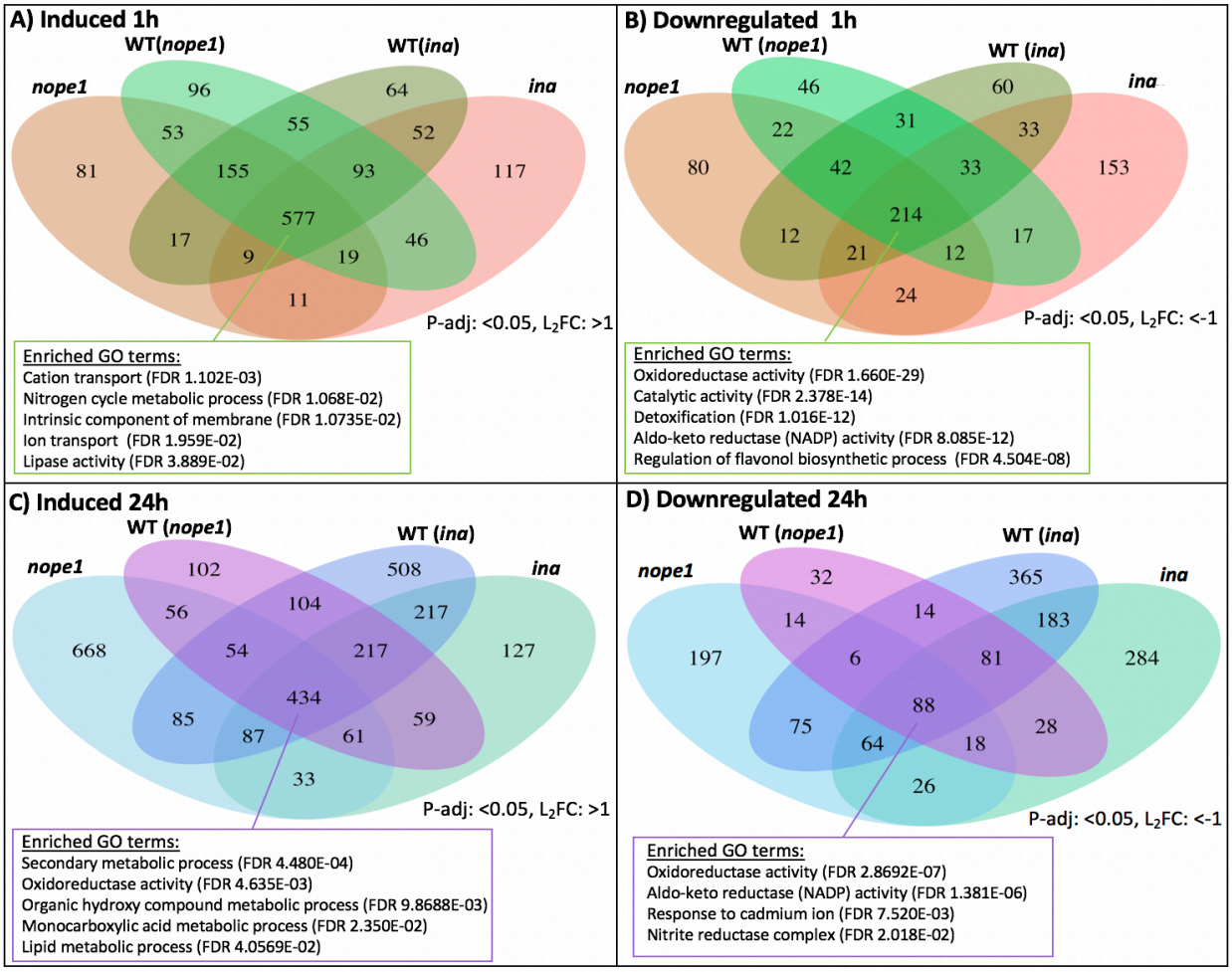

Figure 3.9: Venn diagrams displaying overlapping transcripts identified from pairwise DE lists induced or downregulated after 1h and 24h in WT (*nope1*), WT (*ina*), *nope1*, and *ina* compared to the 0h non-treated time-point. A) Number of transcripts DE between 1h treatments of different plant genotype exudates vs 0h. **B)** Number of transcripts downregulated by plant exudates after 1h vs 0h. **C)** Volume of transcripts induced after 24h exudate treatments vs 0h. **D)** Volume of transcripts downregulated after 24h of exudate treatments vs 0h.

As a previous transcriptomics analysis was carried out that identified GR24-induced transcripts in *R. irregularis* spores (63), this dataset was examined against these GR24-responsive transcripts to view responsivity of mutant and WT-treated spores using SL-induced transcripts. DE lists of all exudate treatments at both time-points compared to the 0h time-point were compared against the top 15 most highly induced GR24-responsive transcripts reported in Tsuzuki et al. (63). Of the 15 chosen GR24-responsive transcripts, 6 were identified that were significantly induced by at least one exudate treatment from any time-point (Padj <0.05) (Table 3.1). All treatments, usually following 24h of exudate exposure, were capable

of inducing these GR24-induced transcripts to some extent, which potentially suggests that SL production and exudation is intact in all plant genotypes tested. The characterised SL-responsive gene *SIS1* was not found to be induced by any exudate condition compared to the 0h timepoint, though *SIS1* has previously been described as responding to SL treatment following five days of incubation, and no earlier (63). Another well-known fungal protein with a predicted role in colonisation of host plants, *SP7*, was not found to be induced by any of the exudate treatments over the 0h timepoint. This is to be expected, as *SP7* has been studied in colonised plant tissue with no described role in pre-symbiotic interactions (196).

The variance between samples of all conditions is displayed through a Principal Component Analysis (PCA), and shows that samples cluster closely together at 1h, regardless of exudate treatment genotype, and that variance between samples increases at 24h (Figure 3.10).

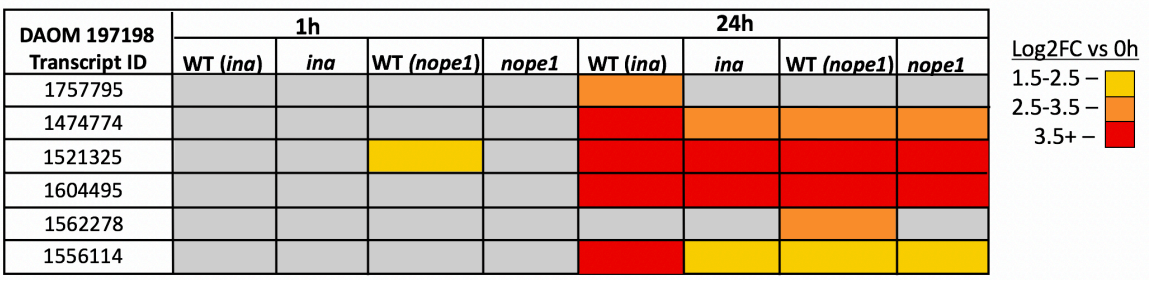

Table 3.1: Fungal spore RNA-Sequencing normalised expression of GR24-induced transcripts. The top 15 (by L_2FC) transcripts induced by GR24 were extracted from Tsuzuki et al. (47) and examined against the fungal exudate RNA-Sequencing dataset of DE transcripts induced in DESeq2 pairwise comparisons of each exudate treatment vs the 0h time-point. Only transcripts where at least one root exudate treatment condition significantly induced transcript expression are shown (Padj <0.05). Induction of GR24-induced transcripts is largely similar across treatment conditions. Transcript IDs included are from DAOM 197198 v2.0, and thus have been converted from the v1.0 protein IDs included in Tsuzuki et al. (47).

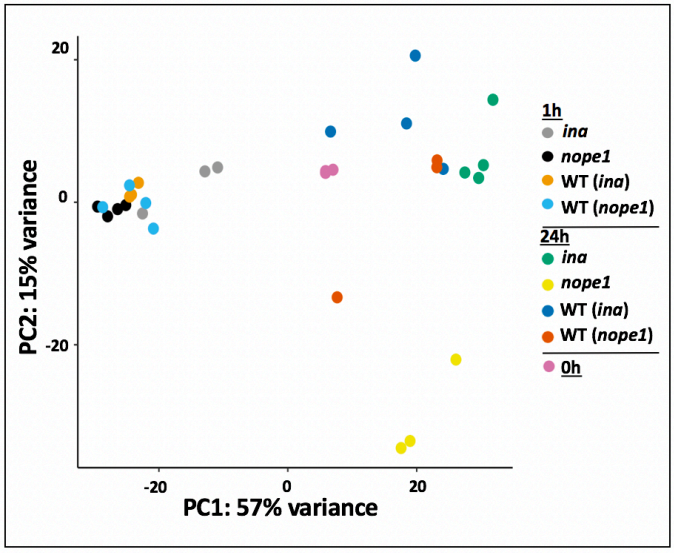

Figure 3.10: PCA plot depicting clustering of *R. irregularis* samples subjected to all treatments based on sample similarity. Plot was generated using R package ggplot2, using a dataset of quantified transcripts from Salmon. 0h samples not treated to plant exudates cluster closely together. *R. irregularis* samples treated for 1h tend to cluster together regardless of plant genotype that exudates were collected from. At 24h, samples appear to disperse based on the plant exudate genotype that spore samples were treated to.

3.2.3.2 The effect of mutant exudates on fungal transcriptomics

Further pairwise comparisons were carried out between WT-treated spores and spores treated with the exudates of corresponding mutants. For the 1h time-point treatments, the *ina* and *nope1* maize exudates caused a strongly overlapping response when compared with their respective WT exudates, as displayed by very few significantly induced or downregulated transcripts between WT exudate-treated spores and their corresponding mutant exudate-treated spores (P-adj <0.05, $L_2FC > 1$ or <-1) (Figure 3.11A). However, at 24h, the spores show a larger number of transcripts induced and downregulated when WT exudate-treated samples were compared to their respective mutants (Figure 3.11A). This trend can also be seen in the form of a volcano plot, where transcripts that pass the set threshold are highlighted (P-adj <0.05, $L_2FC > 1$ or <-1), and those most strongly and significantly induced or downregulated transcript IDs are indicated. Again, there were very few significantly DE genes between WT and mutant exudate-treated samples at 1h (Figure 3.11B). A larger difference in expression patterns is observable at 24h (Figure 3.11C). At this

stage, differences in the fungal response to WT exudate counterparts compared to *ina* and *nope1* exudates become visible. The spores respond to *nope1* exudates with a strong induction of unique transcripts that are not induced in the corresponding WT (*nope1*) treatment. The spore sample response to *ina* involves the induction of fewer *ina*-unique upregulated transcripts that are missing in WT (*ina*) exudate-treated spores. A large number of transcripts are induced in the WT(*ina*) exudate-treated samples that do not respond similarly in the response to *ina* exudates (Figure 3.11C).

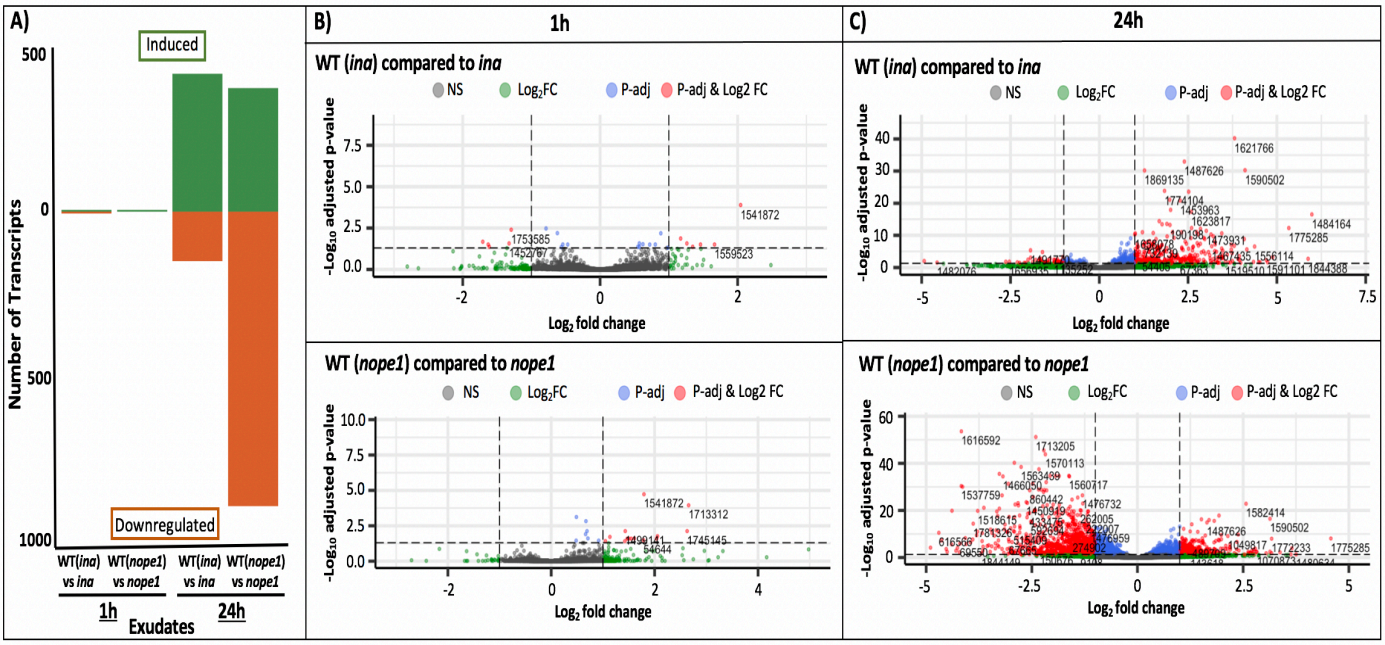

Figure 3.11: Visualisations of transcript induction and downregulation in pairwise comparisons between WT genotypes and their corresponding mutants at both treatment time-points, 1h and 24h. A) Barplot displaying the very few transcripts induced or downregulated at 1h. At 24h, a large number of transcripts are DE between WT genotype treatments and their corresponding mutant exudate treatments. **B)** Volcano plot displaying the small number of transcripts DE at 1h between WT-treated and the corresponding mutant-treated spore samples. **C)** At 24h, the volcano plot displays a large number of DE transcripts visible in pairwise comparisons between WT exudate-treated spores and spores treated to exudates produced by the corresponding mutant genotypes. Transcripts induced above a L_2FC increase of 1 and with a Padj of >0.05 are significantly induced in WT-treated spores compared to mutant-treated, and transcripts where expression was reduced below a L_2FC of -1 and with a Padj of >0.05 are significantly downregulated in WT compared to mutant-treated samples.

3.2.3.3 Fungal response to *nope1* and WT exudates examined with GO enrichment

Lists of significantly induced transcripts (P-adj <0.05, L_2FC >1) induced in WT over *nope1*, and vice-versa, induced in *nope1* compared to WT-treated samples, were assessed for GO enrichment against the whole GO-annotated transcriptome dataset using a Fisher's Exact Test (FDR <0.05).

Following 1h exudate treatment, only one term, 'glutathione metabolic process' was enriched in the transcripts induced in WT-treated spores compared to the corresponding *nope1* mutant exudate treatment, and no significantly enriched terms emerged when examining lists

of induced transcripts in *nope1* compared to WT-treated samples. After the 24h treatment, 'membrane' and 'transporter'-associated terms are enriched in the transcripts that are induced in response to WT(*nope1*) compared to *nope1*-treated spores (Table 3.2). In this gene list, there is also an enrichment of terms associated with metabolic processes, including 'organonitrogen compound metabolic process', which supports a role of NOPE1 in providing fungal spores with a nitrogen-based compound. GO terms that are significantly enriched when spores are treated to *nope1* over WT (*nope1*) exudates at 24h include terms associated with regulating cell division such as 'regulation of mitotic nuclear division' (Table 3.2). This may support a hypothesis that the GlcNAc-related compound is required for activation of AM fungal spores, at is has previously been identified that GlcNAc may cause hyphal growth and extension in fungi that have stages of filamentous growth (49, 51, 274, 275). In this scenario, where the spores have not received the required GlcNAc signal, it would be expected that these terms associated with the 'regulation' of filamentous growth are showing an induction in transcripts associated with the negative regulation of growth.

GO term	FDR	Count
1h		
Enriched in transcripts induced in WT (*nope1*) compared to *nope1*		
Glutathione metabolic process	2.114E-02	3
24h		
Enriched in transcripts induced in WT (*nope1*) compared to *nope1*		
Membrane	5.02E-11	157
Cell periphery	9.80E-06	107
Inorganic molecular entity transmembrane transporter activity	1.60E-05	26
Cation transmembrane transport	2.09E-04	19
Organic substance metabolic process	1.61E-03	171
Organonitrogen compound metabolic process	2.15E-03	138
Positive regulation of intracellular signal transduction	5.91E-03	65
Active transmembrane transport	8.65E-03	13
Response to stimulus	8.97E-03	143
Primary metabolic process	8.97E-03	161
Enriched in transcripts induced in *nope1* compared to WT (*nope1*)		
Regulation of chromosome separation	2.11E-06	30
Mitotic sister chromatid segregation	2.92E-03	32
Regulation of mitotic nuclear division	3.34E-03	33
Negative regulation of fatty acid biosynthetic process	3.34E-03	8
Regulation of filamentous growth of a population of unicellular organisms	7.88E-03	7
Small molecule metabolic process	9.82E-03	102
Monocarboxylic acid metabolic process	2.29E-02	42
Response to heat	2.68E-02	33
Carboxylic acid metabolic process	4.78E-02	63
Regulation of glycogen catabolic process	4.78E-02	4

Table 3.2: Table of GO terms enriched in DE transcripts identified from pairwise comparisons between WT *(nope1)* and *nope1.* At 1h, only the term 'Glutathione metabolic process' was enriched under WT-treatment of spores compared to *nope1*-treatment. At 24h, terms such as 'membrane' and transporter-associated terms were enriched in DE transcripts induced by WT-treatment compared to *nope1* treatment. From DE transcripts induced by *nope1* treatment over WT treatment, GO terms involved in cell division were enriched. Count values are the number of transcripts in the DE lists that are associated with that GO term.

3.2.3.4 Fungal response to *ina* and WT exudates examined with GO enrichment

GO enrichment using Fisher's Exact Test (FDR<0.05) was carried out on the lists of significantly induced transcripts in WT (*ina*) compared to *ina*-treated spores, and *ina* compared to WT-treated spores (P-adj <0.05, L_2FC >1).

At 1h, there were no significantly enriched GO terms, due to the fact that only a small number of transcripts were induced in either WT (*ina*)-treated samples compared to *ina*-treated, or vice versa. At 24h, transcripts induced in WT (*ina*) compared to *ina*-treated samples were significantly associated with GO terms involving transporter activity. 'Intracellular sterol transport' and 'intracellular lipid transport' are two of the transporter-related terms significantly enriched in transcripts from this comparison (Table 3.3). As this result could

suggest the reduction in uptake of lipids in *ina*-treated spores, a dataset comparing spores treated with the fatty acid pamitoleic acid and control untreated spores was cross-compared to examine whether any of the DE genes between WT (*ina*) and *ina*-treated spores appeared. Of the 25 genes induced by palmitoleic acid treatment over control treatment (60), 3 were identified as induced in WT (*ina*) treated spores compared to *ina*, with the transcript IDs 1491586 (GO: Thiamine pyrophosphate-requiring enzyme), 1781769 (GO: none), and 1488254 (GO: none).

GO term	FDR	Count
24h		
Enriched in transcripts induced in WT (*ina*) compared to *ina*		
Intracellular sterol transport	8.30E-03	5
Ion transmembrane transporter activity	1.89E-02	17
Transmembrane transporter activity	2.12E-02	16
Intracellular lipid transport	2.26E-02	5
Transporter activity	2.44E-02	19
Cation transmembrane transport	2.60E-02	14
Hyperosmotic salinity response	3.13E-02	6
Inorganic molecular entity transmembrane transporter activity	4.06E-02	15
Enriched in transcripts induced in *ina* compared to WT (*ina*)		
Oxidoreductase activity	1.51E-13	21
Monooxygenase activity	5.50E-12	13
Cellular hormone metabolic process	1.08E-10	11
Oxidoreductase activity, acting on paired donors	2.89E-10	12
Fatty acid metabolic process	2.89E-10	14
Monocarboxylic acid metabolic process	3.25E-10	16
Steroid metabolic process	9.09E-10	13
Cellular lipid metabolic process	6.65E-09	18
Lipid metabolic process	1.71E-08	19
Hormone metabolic process	4.85E-08	12

Table 3.3: Table of GO terms enriched in DE transcripts identified from pairwise comparisons between WT *(ina*) and *ina.* Following 1h treatment, no GO terms were enriched in the transcript lists of DE genes between WT (ina) and *ina*. At 24h, GO terms involved in transport, particularly ion and cation transport, were identified as enriched in DE transcripts induced by WT-treatment compared to *ina* treatment. When DE transcripts induced by *ina* treatment over WT treatment were examined for GO enrichment, terms associated with oxidoreductase activity were found. Count values are the number of transcripts in the DE lists that are associated with their corresponding GO term.

In order to further understand some of these GO terms and their implications, specific DE transcripts were extracted that fall under these terms. The two GO terms 'Intracellular lipid transport' and 'Intracellular sterol transport' enriched under WT (*ina*) treatment were flagged due to the annotation of the same five transcripts (Table 3.4), and these included two MD-2-

related lipid-recognition (ML) domain encoding genes. ML domain-encoding proteins have been implicated in recognition of lipids, and in lipid metabolism (276). The terms 'Transmembrane transporter activity' and 'Ion transmembrane transporter activity' were also examined for specific transcripts, and a majority of transcripts associated with one of these terms were also assigned the other. DE transcripts underlying these terms consisted of major facilitator superfamily-encoding transcripts, ABC superfamily-encoding transcripts, and cation transporters (Table 3.4).

Intracellular lipid/sterol transport	Transmembrane transporter activity	Ion transmembrane transporter activity	Transcript ID	Description (JGI)	L_2FC	WT Count	*ina* Count
	✓	✓	1783273	Major facilitator superfamily	3.46	18.81	2.01
✓	✓		1767688	Pleiotropic drug resistance proteins, ABC superfamily	3.45	31.83	2.84
	✓		1616147	Proteolipid membrane potential modulator	3.23	389.34	41.62
	✓	✓	1850033	Major Facilitator Superfamily (nitrate transporter)	2.99	156.73	16.44
✓			1788903	MD-2-related lipid-recognition domain (ML)	2.74	25.20	3.89
	✓	✓	1556138	Major Facilitator Superfamily (nitrate transporter)	2.72	877.96	145.86
	✓	✓	1731591	OPT oligopeptide transporter protein	2.54	218.82	38.15
	✓	✓	1727319	Ca2+ transporting ATPase (P-type)	2.49	12.80	2.64
	✓	✓	1561087	Sodium/calcium exchanger protein	2.45	1699.54	340.53
	✓	✓	1684237	Pleiotropic drug resistance proteins, ABC superfamily	2.27	17.63	4.23
	✓	✓	1510807	Magnesium transporter NIPA	2.25	95.21	18.91
	✓	✓	1687292	Na+/K+ ATPase (P-type)	2.18	2057.01	492.03
	✓	✓	1575284	Aquaporin (major intrinsic protein family)	1.89	169.98	55.04
✓			1613657	MD-2-related lipid-recognition domain (ML)	1.80	59.06	20.07
✓			1726969	Ca2+-dependent lipid-binding protein CLB1/C2 domain	1.61	113.05	31.07
	✓	✓	1726618	Iron permease FTR1 family	1.58	794.39	256.74
	✓	✓	1519111	The Sulfate Permease (SulP) Family	1.5	40.68	24.57
	✓	✓	1656212	Calcium-dependent channel	1.47	487.93	181.02
	✓	✓	1497124	Plasma membrane H+-transporting ATPase (P-type)	1.26	628.27	220.93
✓			1534754	GRAM domain	1.0	530.05	259.56

Table 3.4: Table of transcripts associated with selected GO terms enriched in transcripts induced by WT (*ina*) treatment over *ina* treatment. Transcript IDs (DAOM 197198 v2.0) associated with transmembrane GO terms are displayed along with descriptions from JGI Mycocosm and L_2FC values for the increase in expression caused by WT treatment compared to *ina* treatment. Average count values across *R. irregularis* samples for both exudate treatments are shown. Count value has been normalised using DESeq2.

When transcripts induced in *ina* compared to WT (*ina*)-treated spores were analysed for GO enrichment, an overrepresentation of terms associated with lipid metabolic processes such as 'Cellular lipid metabolic process' and 'Fatty acid metabolic process' were found to be induced (Table 3.5). These lipid-related terms were examined in more detail, and specific transcripts were identified that fall under these GO terms. A majority of these transcripts, 10 out of 18, were annotated as Cytochrome P450 (Cyp)-encoding. These transcripts also tended

to be associated with the related enriched GO terms 'monoxygenase activity' and 'oxidoreductase activity'. It should be noted, however, that almost all transcripts associated with the lipid/fatty acid metabolic process GO terms displayed a less than 2 L_2FC compared to WT(*ina*)-treated individuals, thus although *ina* treatment is causing a higher induction in these lipid metabolic-associated transcripts, the WT(*ina*)-treated samples still express these transcripts and are likely also metabolically active in respect to lipid-related processes.

Oxidoreductase activity	Monooxygenase activity	Lipid metabolic process	Transcript ID	Description (JGI)	L_2FC	*ina* Count	WT Count
✓	✓	✓	1776235	Cytochrome P450	2.07	76.91	18.78
✓		✓	1650925	Predicted NAD-dependent oxidoreductase	1.89	144.00	38.98
✓		✓	1650942	Predicted NAD-dependent oxidoreductase	1.79	237.86	68.77
✓	✓	✓	1776231	Cytochrome P450	1.74	175.01	52.72
✓	✓	✓	1645507	Cytochrome P450	1.77	749.35	220.21
		✓	1871689	UDP-glucosyl transferase	1.63	1061.70	343.90
✓	✓	✓	1619141	Cytochrome P450	1.48	1315.08	555.62
✓		✓	1712279	Short-chain dehydrogenases	1.39	83.89	36.66
✓	✓	✓	1619129	Cytochrome P450	1.37	1362.43	603.36
✓	✓	✓	1779276	Cytochrome P450	1.35	1446.38	655.06
✓	✓	✓	1619088	Cytochrome P450	1.35	415.76	190.12
✓		✓	1544564	Peroxidase/oxygenase	1.34	6843.77	3038.43
✓	✓	✓	1645174	Cytochrome P450	1.28	230.465	99.28
✓	✓	✓	1549979	Cytochrome P450	1.27	1120.81	522.28
✓		✓	1543476	Short-chain dehydrogenase	1.26	1482.07	698.85
✓	✓	✓	1619234	Cytochrome P450	1.20	146.22	70.77
		✓	1720944	Acyl-CoA synthetase	1.18	79.49	38.87
✓	✓	✓	1773521	Cytochrome P450	1.17	46.07	20.46
✓	✓	✓	1557915	Cytochrome P450	1.17	2701.70	1278.68

Table 3.5: Table of transcripts associated with selected GO terms enriched in transcripts induced by *ina* treatment over WT (*ina*) treatment. Transcript IDs (DAOM 197198 v2.0) associated with transmembrane GO terms are shown, as are associated descriptions from JGI Mycocosm. L_2FC values show the increase in expression caused by treatment of spore samples with *ina* exudates compared to WT exudate treatment. Average count values across *R. irregularis* samples for both exudate treatments are shown. Count value has been normalised using DESeq2.

3.2.3.5 Validation of responsive transcripts using qRT-PCR

In order to validate the biological findings from the transcriptomics experiment, qRT-PCR analysis was performed from selected fungal transcripts using cDNA produced from the same RNA samples used to carry out the RNA-Sequencing analysis. An independent repeat of the

initial experiment was carried out to further validate chosen transcripts that were flagged as DE from the transcriptomics analysis.

A transcript strongly and significantly induced by WT (*ina*) exudates compared to *ina*-treated exudates at 24h, 1590502 (L_2FC 4.2, Padj 4.33E-28), was selected for validation by qRT-PCR. This transcript encodes a HMG-box-containing protein which often serve as transcription factors and as subunits of chromatin-remodelling complexes (277). This transcript was also identified to be strongly and significantly induced in 24h WT (*nope1*) compared to *nope1*-treated spores (L_2FC 3.13, Padj 4.70E-18).

The aquaporin-encoding transcript 1575284 and proteolipid membrane potential modulator 1616147 were two transcripts identified due to their strong and weak induction in WT (*ina*) and *ina* exudate-treated samples at 24h, respectively (Table 3.4). It should also be noted that, in the transcriptomics analysis, the transcript 1575284 is also flagged as DE transcript from a pairwise comparison between 24h WT (*nope1*)-treated spores and *nope1*-treated spores, as it is induced under WT (*nope1*) treatment and displayed reduced induction by the exudates of *nope1.* Aquaporin-encoding transcripts have previously been described in immature *R. irregularis* spores (278), and yeast spores express an aquaporin that may have a function in maturation of spores (279).

Transcript 1590502 displayed similar trends of expression level across RNA-Sequencing read count, and qRT-PCR experiments, with reduced expression in mutant-treated spores compared to corresponding WT treatment following 24h (Figure 3.12A). Transcript 1616147 likewise displays similar expression patterns across experiments (Figure 3.12B). This transcript was not found in the DE gene list from the transcriptomics pairwise comparison between WT (*ina*) and *ina*-treated spores at 1h due to a P-adj value of 0.5, yet transcript 1616147 appears to be induced at 1h in WT (*ina*)-treated samples in both qRT-PCR analyses compared to *ina*-treated samples, to a higher extent than at 24h. The transcript 1575284 shows an expression pattern that is largely conserved between RNA-Sequencing and qRT-PCR experiments, though induction by treatment with WT exudates compared to mutant exudate-treatment is more visible in the RNA-Sequencing normalised expression values and slightly reduced in qRT-PCR analyses (Figure 3.12C).

The validation data produced from qRT-PCR experimentation on the same set of samples used for RNA-Sequencing confirms the sequencing data by displaying similar expression trends. Additionally, the RNA-Sequencing results have been validated through an independent repeat

of the experiment, producing expression data on additional biological samples. The data shown here supports RNA-Sequencing data regarding the expression patterns of the three validated genes.

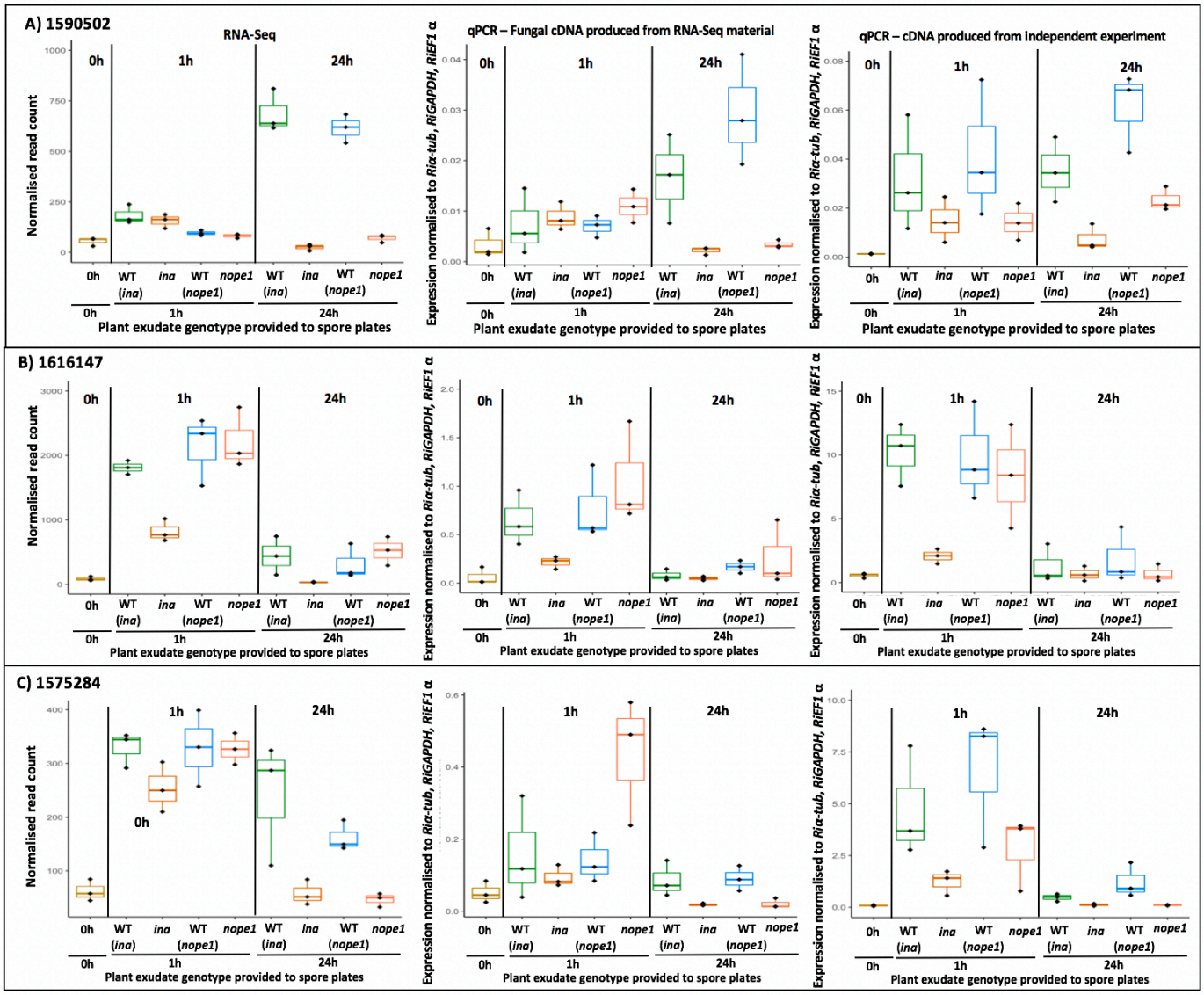

Figure 3.12: Validation of three *R. irregularis* transcripts identified as DE between WT (*ina*)-treated and *ina*-treated samples. DESeq2 normalised counts from RNA-Sequencing data are displayed, as is expression data from qRT-PCR analysis of RNA samples used for the RNA-Sequencing experiment, and expression data from qRT-PCR analysis of cDNA produced from an independent repeat of the experiment. **A)** Transcript 1590502 displays a similar expression pattern between RNA-Sequencing data and qRT-PCR data, and induction in WT plants compared to their corresponding mutants is maintained at 24h in the repeat experiment. **B)** Transcript 1616147 shows downregulation in *ina*-treated samples compared to other exudate-treated samples at 1h, and this is maintained across experimental analyses. **C)** Transcript 1575284 is downregulated by mutant treatment at 24h, and this appears to be consistent across all experimental replicates.

3.3 Discussion

The *ina* phenotype is unique among the more severe AM symbiosis mutant phenotypes. Although mutation of *D14L* produces a similarly severe block in colonisation, the two phenotypes are revealed to be distinct when *ina* individuals are grown in a nurse plant system, enabling fungal penetration into the mutant roots. Mutants of *D14L*, in comparison, maintain a lack of colonisation under co-cultivation with WT individuals (91). The fact that the *ina* presymbiotic phenotype may be overcome in a nurse plant system groups *ina* with *nope1,* which harbours a defect in plant-to-fungal communication (33). It is likely that *INA*, too, is involved in producing a signal to the fungus that is required for colonisation, rather than forming a component of perception of fungal signals.

A further aspect that sets *ina* apart from known AM mutant phenotypes is the second facet of this mutant phenotype; the malformation of arbuscules when the fungus is enabled entry into the root in a nurse plant system. Stunted arbuscules visible in nurse plant-complemented *ina* individuals are comparable to mutants of the AM-specific phosphate transporters *MtPT6/OsPT11,* where arbuscule degradation occurs prematurely (123), and a mutant of H^+-ATPase *MtHA1* that may be required to produce a proton gradient in the arbuscule required for phosphate transfer (280). Stunted arbuscules similar to those seen in colonised *ina* roots are also visible in mutants of a number of genes involved in producing and providing lipids to AM fungi. Mutants of lipid biosynthetic enzymes *FatM, DIS1* and *RAM2* (153, 156) and hypothesised transporters of lipids to the fungus, *STR1* and *STR2* (165, 166) display arbuscules that are also stunted and unable to form fine branches. The mutant of GRAS-family transcriptional regulator *RAM1*, which regulates a number of genes involved in the AM symbiosis including *STR1*, is an additional mutant phenotype where these stunted arbuscules are seen (168). All of these phenotypes that produce erroneous arbuscules enable initial colonisation by the fungus, though it may be reduced, and the commonality between these phenotypes is a role of providing a nutrient or signal at the arbuscule. It is yet unclear why *ina* would display both a pre-symbiotic phenotype and an arbuscule phenotype, and this dual dysfunction in *ina* adds to the uniqueness of this phenotype.

A key finding from the phenotyping of the *ina* mutant has been the complementation of colonisation ability when WT exudates are added to *ina* individuals. This is an important finding as it suggests that the signal missing from *ina* exudates is constitutive, rather than a

signal produced in response to nearby fungal presence, as WT plants grown without fungal inoculum produce exudates that are able to allow penetration into *ina* roots.

SLs are a well-studied and potent activator of AM spore germination (39), and their production does not require the presence of the fungus. However, mutants perturbed in SL biosynthesis do allow colonisation by AM fungi, though it is reduced (45-47). The *ina* phenotype producing a block in *R. irregularis* colonisation does not match that of known mutants within the SL biosynthesis pathway. Indeed, growth of *ina* individuals with rice SL-biosynthesis mutants *d10* and *d27* enabled *R. irregularis* to colonise *ina* roots, suggesting that the defect in *ina* root exudates that prevents fungal entry is not a lack of SL exudation. The *d10* and *d27* plants that do not produce and exude SLs seem to be providing a signal required for colonisation that is lacking from *ina* roots, and thus it is likely that the defect in *ina* pre-symbiotic signalling is not due to a perturbation in SL production or export. Additionally, HMZ *ina* mutants display a normal developmental phenotype, suggesting that at least SL biosynthesis is intact, as defects in SL biosynthesis and regulation in maize causes visible phenotypic effects in above-ground plant architecture (281).

Flavonoids are another compound produced by plants to signal to their fungal counterparts, though maize mutants unable to synthesise flavonoids still allow initial colonisation, suggesting that flavonoids are unessential for colonisation by AM fungi (58). These findings imply that additional compounds are required for colonisation by AM fungi, and recently *NOPE1* was identified as the transporter of an essential GlcNAc-related molecule that enables successful colonisation of roots by AM fungi (33). Although there are strong similarities between the *nope1* and *ina* phenotypes, such as the possibility of complementing both phenotypes using nurse plant systems, the *ina* phenotype is still visibly more severe, as no hyphopodia are ever seen on *ina* inoculated roots. As such, it is unlikely that the *ina* phenotype is caused by an interruption of *ZmNOPE1*, and likely there are still further unknown compounds produced and exuded by plants that are required for AM colonisation.

It can be inferred from the exudate complementation experiment that WT and *ina* plants produce exudates that differ in their composition, and this is supported by data from a transcriptomics analysis on *R. irregularis* spores exposed to these plant root exudates. Although spores responded with a largely similar response to different plant root exudates at 1h, they displayed distinct reactions to mutant and WT genotypes at 24h. This finding supports a previous *R. irregularis* transcriptomics experiment carried out on exudate-treated

spores, where *nope1* and WT exudates elicited an overlapping response at 1h but distinct responses following 24h and 7 days of exudate treatment (33). Spore samples showed distinct DE responses to *ina* exudates and to *nope1* exudates compared to their respective WT genotypes, further discounting the possibility that these phenotypes are caused by interruption of the same underlying gene.

A strong observation from the comparison between WT and *ina*-treated samples is the comparative induction of transporter-encoding transcripts in WT-treated spores. This induction may suggest that the missing component from *ina* is a compound that needs to be transported or taken up by the fungus, or is required for transcriptional regulation of transporter-encoding genes, and that, in its absence, the spores do not induce transcripts for this substance's uptake. Notably though, ion, and particularly cation, transporter-encoding transcripts were overrepresented. Three of the transcripts identified as ion transporters induced under WT treatment are P-type ATPases, a family of transporters that use ATP hydrolysis to transport cations, including H^+, Ca^{2+}, and Na^+, across their electrochemical gradient (282). Previous work has implicated the involvement of electrochemical fluxes in the pre-symbiotic response of fungi to the presence of host exudates, and these fluxes have been linked to hyphal growth in germinated spores of AM fungi (283, 284). Additionally, H^+-ATPase symporters have been identified and their expression patterns at different stages of the symbiosis characterised in *R. irregularis* (285), and in *Glomus versiforme,* in which a high-affinity H^+/Pi symporter was identified that likely enables uptake of phosphate from the soil by the AM fungus (286). ATPase transporters were also identified as critical in fission yeast for the regulation of uptake of nutrients such as calcium, phosphorus, potassium, iron, and magnesium (287, 288). These ATPases in *R. irregularis* may be involved in a swathe of responses to the presence of a suitable plant partner, including the uptake of nutrients. It is known that AM fungi accumulate and transport phosphate as polyphosphate, and this anion uptake is likely countered by intake of cations (113). It is unclear whether such an induction of transcripts for the uptake of substances in WT (*ina*)-treated spores would be occurring to receive plant signals, take up nourishment for the fungus itself, or to begin collection of nutrients such as phosphate for a partner it believes is nearby. Additionally, a number of transcripts induced in WT-treated samples compared to those treated to *ina* exudates are lipid transport-related. This is potentially interesting, as it has recently been discovered that, not only are lipids a hugely important carbon source provided by plants to AM fungi (153,

156, 170), but also that fatty acids including the C16 monounsaturated fatty acid palmitoleic acid can stimulate hyphal branching, higher oxidative status, and even secondary spore formation in *R. irregularis* spores without the presence of a host plant (60). It appears that *ina* treatment, which causes a significantly reduced induction of transporters, may cause a reduction in the uptake or transport of a yet unknown compound or signal required for fungal colonisation of roots, and this would fit with a theory of a different composition of *ina* and WT exudates.

From the transcriptomics analysis on fungal spores it was deduced that spores appeared to induce Cyp-encoding transcripts to an increased extent when treated with *ina* exudates over WT exudates for 24h. *R. irregularis* has an unusually large Cyp-encoding repertoire for a member of the fungal kingdom (149, 189). Although the function of a large number of these *R. irregularis* Cyps is unknown, Cyps are known to catalyse lipid and sterol oxidation, so it is plausible that some of the numerous Cyp-encoding genes in *R. irregularis* are involved in metabolic pathways (289). As Cyp proteins usually work in concert with protein components that transfer electrons from NADH or NADPH, the enrichment of oxidoreductase-encoding transcripts in *ina*-treated spores also fits with this enrichment of Cyp-encoding transcripts (290). As spores are known to store lipids, likely to provide the required energy for germination and location of a host (140), it is interesting to note that *ina*-treated samples are metabolically active, at least in lipid metabolic pathways. This finding may further discount any impairment in SL synthesis or exudation in *ina* mutants, as SLs have previously been shown to activate mitochondrial activity in AM fungi, and likely cause oxidation of lipids (39), a response that seems intact when spores are exposed to *ina* exudates.

Due to the fungal metabolic activity in *ina*-treated spores, and due to the fact that no hyphopodia have ever been seen on inoculated *ina* roots, it could be that an initial priming or signalling compound is missing that may enable the ability of the fungus to form hyphopodia and successfully colonise, even if the fungal spores are branching and active. The combined data from the colonisation phenotype and spore-response extended phenotype have revealed a great deal about the functioning of the genetic component that is missing in *ina* mutant plants. However, further experimentation is needed to confirm a concrete function of *INA* that fits into known models of the regulation of AM symbiosis.

CHAPTER 4

Positional cloning of the *INA* locus

4.1 Introduction

Forward genetics screens have thus far proven highly useful in identifying new molecular components of the AM symbiosis. Although initial forward genetics approaches focused on identifying AM phenotypes in known legume nodulation mutants (291-293), in more recent years attention has turned to directly identifying components of the plant genetic regulation of the AM symbiosis. The half-sized ABC transporters *STR1* and *STR2* predicted to be involved in transporting lipids to AM fungi were identified through a screen for AM mutants phenotypes (166), as were *RAM1* and *RAM2*, encoding a GRAS-transcription factor and GPAT important in AM molecular functioning, respectively (159, 161, 294). These forward genetics screens used dicotyledonous plants and, to date, only one forward genetics screen has been carried out in a monocotyledonous species, maize (240).

This screen discovered seven maize lines with potential AM mutant phenotypes, and it was this screen that enabled the discovery of the major facilitator transporter *NOPE1* (33, 240). Another mutant line, *ina*, identified during this screen is the focus of this thesis. The mutant phenotype described lacks accumulation of the yellow pigment mycorradicin, despite the presence of *R. irregularis* fungal inoculum.

Positional cloning is a tool for identifying the unknown gene underlying a mutant phenotype, and is carried out in a series of steps that narrow the mutation-containing area to smaller and smaller intervals (295). Despite its sizeable genome that consists largely of repetitive DNA, it is possible to carry out positional cloning in maize, as the repetitive areas tend to group together in vast seas, leaving islands of functional and genic areas of the genome, where a majority of recombination events occur (220, 221). During positional cloning attempts to map genes, the areas with low recombination rates are usually invisible due to the reliance on identification of recombination events for mapping (296, 297). The initial stage of positional cloning involves the crossing of different accessions, usually an accession homozygous for the mutant phenotype of interest (in the case of mapping a recessive allele), and a suitably

distinct plant accession line, to create a mapping population that can then be phenotyped for the trait of interest. The mapping population enables identification of the mode of inheritance, and the number of loci, behind the mutant phenotype. In this mapping population, a rough position containing the mutant allele or causal genetic alteration is identified using linked markers that cosegregate with the mutant phenotype (295, 298). Once linkage of the mutant phenotype to known markers has narrowed the region containing the mutant allele, a common method to identify the causal gene is termed a 'candidate gene' approach. This method relies on existing knowledge of gene functions in order to identify a gene within the mutation-containing region that could plausibly be causing the observed mutant defect (299). Single Nucleotide Polymorphisms (SNPs) are a favoured genetic marker for positional cloning due to their high frequency in the genome and their existence as one of only two codominant variants (300). The maize genome has a high density of SNPs, with an estimation of one SNP per 100-200 bp (224, 301). There is a wealth of known SNP sequences present in different maize inbred lines, and such a dense map of sequence polymorphisms is ideal for the mapping of mutant alleles (249, 302).

Positional cloning methods have been successfully employed to identify novel genes in maize from mutant phenotypes (303, 304). This chapter follows the positional cloning and candidate gene analysis used to identify the underlying defect behind the *ina* mutant phenotype.

4.2 Results

4.2.1 Stability and mode of inheritance of the *ina* mutant phenotype

The *ina* phenotype was first identified as displaying a lack of interaction with *R. irregularis*, a phenotype that was identified due to a lack of yellow mycorradicin accumulation in the root systems of these inoculated plants. The mutant phenotype was found to be stable after crossing the mutant-containing line to the inbred line W64A, thus further study could be carried out to investigate the causal allele (240).

Seeds from lines predicted to be segregating for the *ina* mutation were planted, inoculated with *R. irregularis,* and examined at 7wpi for their mycorradicin phenotype. Individuals were identified that clearly displayed no accumulation of mycorradicin in any part of the root system, displaying the 'pale' root phenotype (Figure 4.1). These individuals were examined

microscopically following Trypan Blue staining to confirm the phenotype that these plants cannot host *R. irregularis* and that this is the cause of the lack of mycorradicin accumulation. Indeed, the fungus was unable to colonise the roots of the individuals phenotyped as 'pale', and no internal fungal structures were observed in these plants (3.1.2.1). The identification of mutant individuals in these segregating lines further confirmed the stability of this mutant phenotype through generations.

Individuals from one such segregating line were phenotyped to initially identify the mode of inheritance of the mutant phenotype. Of the 87 individuals screened at 7wpi, 70 were phenotyped as 'yellow', where the root systems accumulated mycorradicin, and 17 were phenotyped as 'pale' mutant individuals. The Mendelian ratio identified here follows a 3:1 pattern ($X^2 = 1.92$, $p > 0.70$), suggesting that *ina* is a recessive mutation at a single locus.

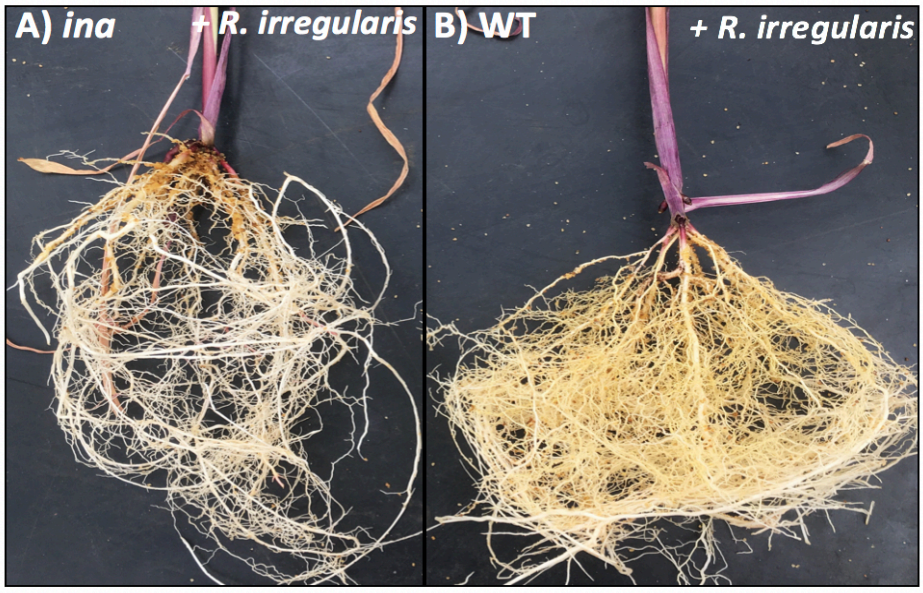

Figure 4.1: Mycorradicin accumulation in *R. irregularis*-inoculated *ina* and WT root systems at 7wpi. A) The *ina* mutant displays no accumulation of the visibly yellow pigment, mycorradicin, when inoculated with *R. irregularis*, making this an ideal phenotype for screening large numbers of plants during positional cloning. **B)** WT root systems accumulate mycorradicin following inoculation with *R. irregularis.*

4.2.2 Mapping and experimental material

Previous members of the Paszkowski group crossed the original HMZ *ina* mutant line to an individual from the B73 inbred line and self-pollinated the HTZ progeny. A HMZ *ina* individual from the self-pollinated progeny was then crossed to a Mu-Killer line in the W22 background

(prior to onset of this PhD) in order to reduce the chances of excision and movement of *Mu* insertions within the genome (244). Once again, the progeny produced by crossing this HMZ *ina* individual to a HMZ WT *Mu*-Killer line was self-pollinated to produce a segregating population, and individuals from this population were self-pollinated, producing seed bags that were either segregating for the *ina* mutation, HMZ WT, or HMZ *ina.* To identify material for use in mapping and experimental work, the identity of this genetic material had to be confirmed, and 16 individuals of each of these lines were planted and phenotyped. Of this selfed material, 7 bags of segregating seed, 2 of *ina* HMZ, and 4 of WT HMZ material were identified (Figure 4.2). For all experimental analyses, any *ina* individuals used were from these HMZ *ina* lines (UP23.7, UP23.12), WT individuals were from these WT HMZ lines (UP23.1, UP23.9, UP23.14, UP23.16), and segregating mapping populations were from these segregating lines (UP23.3, UP23.4, UP23.9, UP23.10, UP23.11, UP23.15, UP23.17, UP23.18).

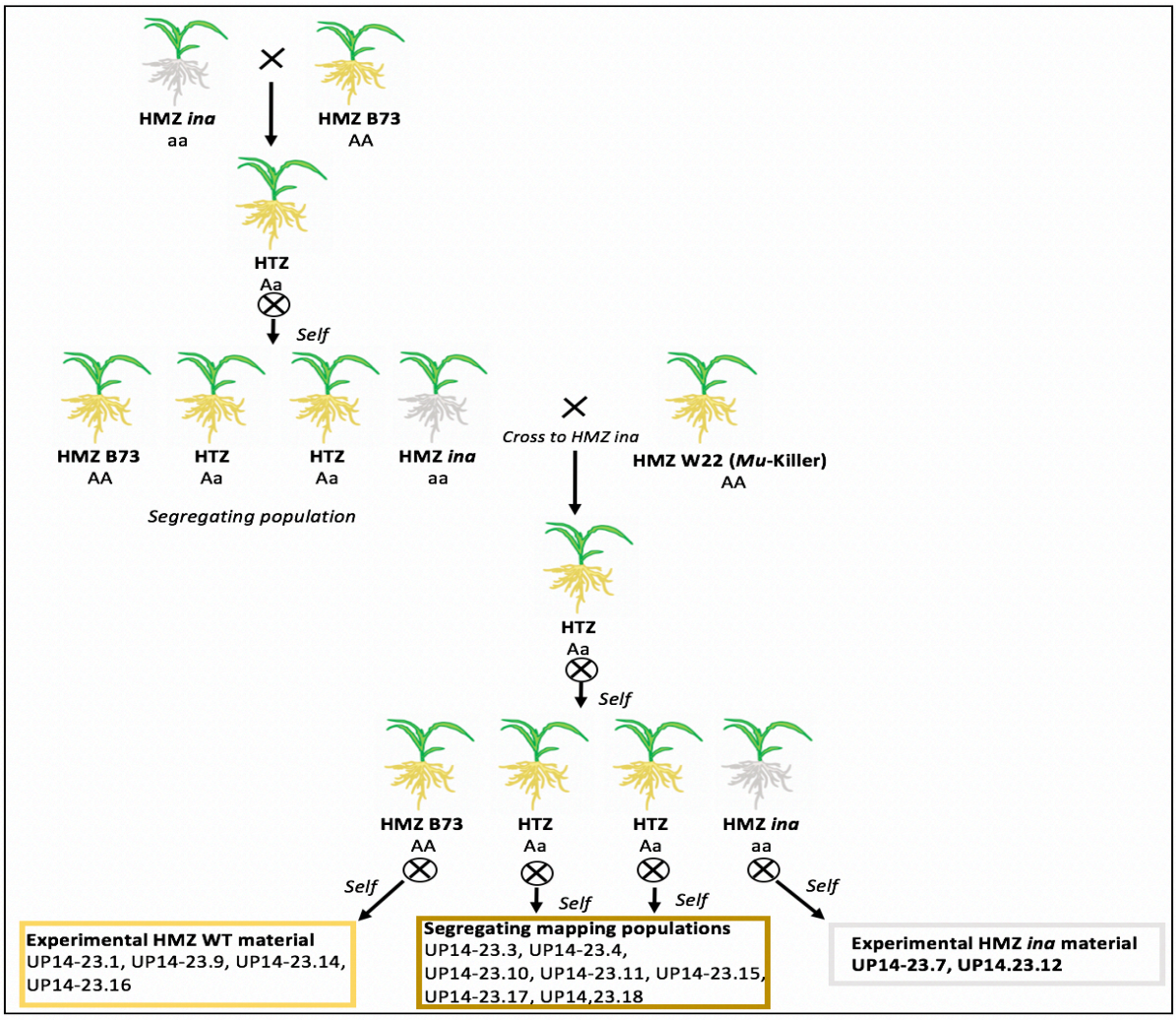

Figure 4.2: Pedigree of the *ina* mutation. An *ina* HMZ individual was crossed to the inbred line B73, and HTZ F_1 progeny self-pollinated to generate a segregating population. A HMZ *ina* individual from this segregating family was crossed to the inbred line W22 containing *Mu*-Killer activity to disable transposition of the *Mu* transposable elements. HTZ progeny was self-pollinated to produce a further segregating line. Individuals from this segregating line were crossed to produce: 1) HMZ WT progeny for use as an experimental control for phenotyping analyses, due to its strongly related background to the *ina* material. 2) Segregating populations for mapping the *ina* mutation. 3) HMZ *ina* material for use in phenotyping analyses.

4.2.3 Rough mapping of the region containing *INA*

Initial mapping required the identification of a rough chromosomal location for *ina,* and this was carried out using 31 individuals from a segregating population that had been phenotyped based on accumulation of mycorradicin in roots. These 31 individuals were genotyped for SNP

markers spread throughout the maize genome (SNPs: proprietary Corteva resource) (Figure 4.3). This genotyping enabled narrowing of the *ina*-containing region, based on SNP genotypes that co-segregated with the mutant phenotype, to 43Mb on the long arm of maize chromosome 3. A subsequent round of mapping used 180 phenotyped segregating individuals that were genotyped for a further 29 SNPs in this region (SNPs: proprietary Corteva resource), enabling the narrowing of the *ina*-containing region to 8Mb, between the markers PZA7848-27 and PZA16021-9.

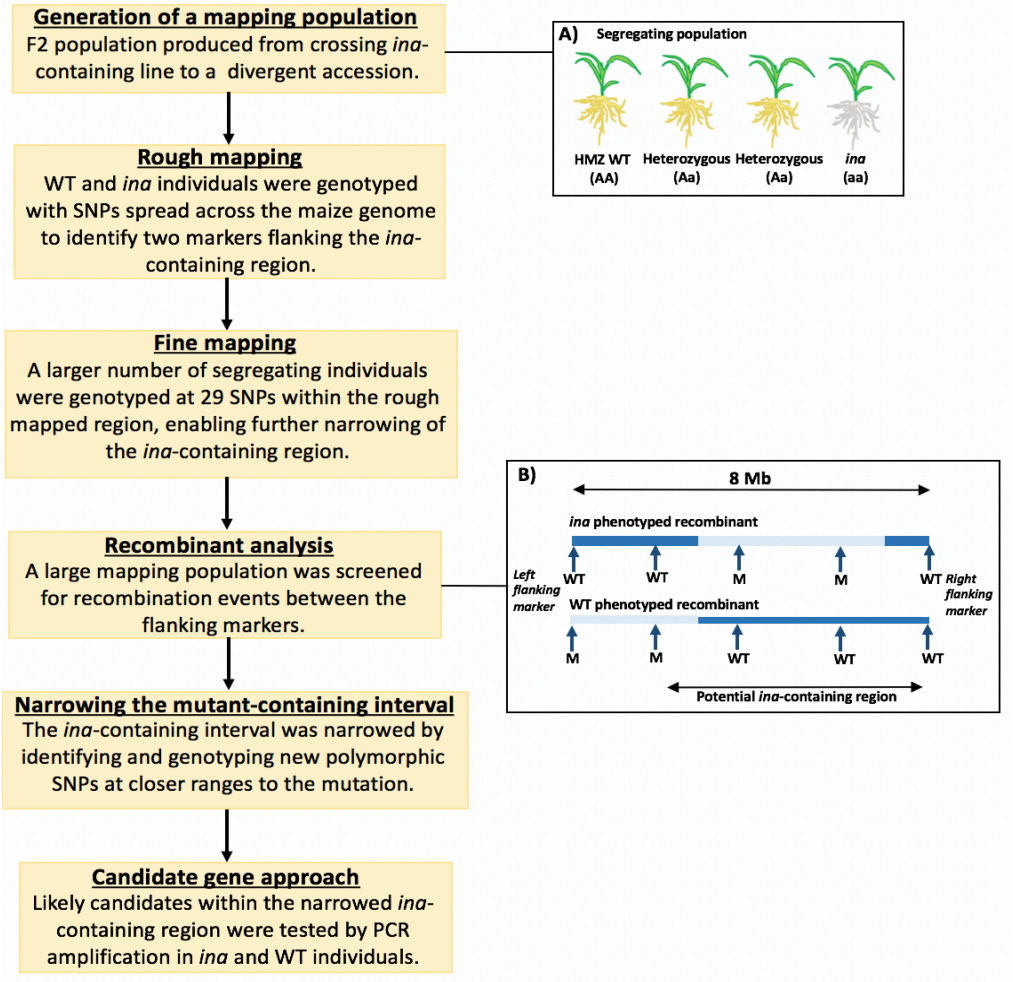

Figure 4.3: Summary of positional cloning methods used to identify the genomic region containing the *ina* allele. Positional cloning using SNP markers were used to narrow the *ina*-containing region to an interval small enough to use a candidate gene approach to explore potential causal genes. **A)** Populations segregating for the *ina* 'pale root' phenotype were used as mapping populations. **B)** A simplification of the process of narrowing the *ina*-containing region using phenotyping data on individuals that were genotyped at a number of SNPs between markers known to flank the *ina* allele.

4.2.4 Fine mapping of the region containing *INA*

From the 7 segregating mapping seed lines previously identified (Figure 4.2), 2,100 seeds were sampled by removing a small portion of seed tissue and genotyped for five SNP markers (PZA7848-27, PZA17811-22, PZA16757-14, PZA4952-7, and PZA16021-9) within the 8Mb region known to contain *ina*. This genotyping revealed any recombination events that had occurred between any of the five SNPs (Figure 4.3). Recombination events have the potential to narrow down the known mutation-containing region in individuals where the phenotype is known, as recombination can separate linked SNPs from the mutant allele in question. There were 269 individuals with recombination events between the flanking markers, the 'recombinants'. Following phenotyping of these individuals, it was possible to use the phenotype and SNP genotype information of these 269 individuals to narrow the *INA*-containing region to the area between two of the five markers, PZA17811-22 (B73 v4 location- Chr3:205,004,996) and PZA16757-14 (B73 v4 location- Chr3:208,693,169) (Figure 4.4).

To further narrow this region, additional SNP markers were identified within this *INA*-containing area, utilising Corteva resources and SNPs available from Maize SNP50 (249). Three subsequent rounds of marker identification and genotyping enabled the further narrowing of the *INA*-containing region until no further recombination events had occurred between new SNP markers in the 269 phenotyped individuals. This placed *INA* in a 173 kbp genomic region between two Corteva markers GTR4M1 (B73 v4 location – Chr3:208,146,460) and GTR4M5 (B73 v4 location – Chr3:208,319,903).

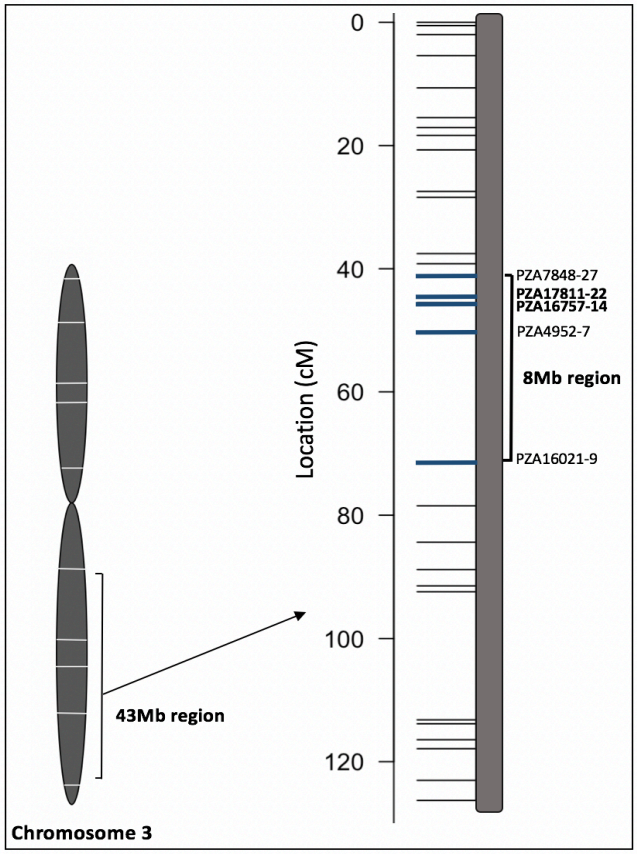

Figure 4.4: Depiction of the 43Mb region on maize chromosome 3 containing *INA* identified during initial rough mapping. SNP sequence information from 180 mapping individuals were used to generate the cM spacing of 29 SNPs (indicated as grey lines) using R/qtl. The five SNPs highlighted in blue were utilised for fine mapping by analysis of recombination events between these markers, and fall within the 8Mb region containing *INA*. The SNP markers labelled in bold (PZA17811-22 and PZA16757-14) were identified as flanking markers containing *INA*.

4.2.5 A candidate gene approach to identifying the causal *ina* allele

The MaizeGDB genome browser was used to identify the gene models within this 173 kbp region in the W22 genome, and the high-confidence gene models identified within this region were *GRMZM2G107754*, *GRMZM2G333833*, *GRMZM2G035276*, *GRMZM2G035222*, and *GRMZM2G034975* (Figure 4.4). MaizeGDB was once again used to identify the gene models within this region in the inbred lines B73, Mo17, CML247, EP1, and PH207 (305). For searches in all inbred lines, the sequences of the flanking markers GTR4M1 and GTR4M5 were BLASTed against these genomes and the genomic area was obtained. The gene models were conserved across the different inbred lines within this region, and in all genomes analysed the high-

confidence gene models were *GRMZM2G107754*, *GRMZM2G333833*, *GRMZM2G035276*, *GRMZM2G035222*, and *GRMZM2G034975* (Table 4.1).

Notably, the gene GRMZM2G035276 is the maize ortholog of *OsSTR2*, encoding a half-size ABCG transporter that is hypothesised to form a transporter complex with OsSTR1 to transport lipids at the arbuscule during the AM symbiosis (165, 166). In order to assess whether any further genes from the *INA*-containing region could have significance in the AM symbiosis, a list of genes predicted to function in the AM symbiosis based on their conservation in AM host species was consulted (154). As this list of conserved potential AM components displays *M. truncatula* genes, the five maize genes were pBLASTed against the *M. truncatula* genome to obtain an orthologous protein-encoding gene. Of the five genes within the *ina*-containing region, only *GRMZM2G035276* (*ZmSTR2*) had an orthologous *M. truncatula* gene (*Medtr5g030910*) that was present on this list of conserved AM symbiosis genes. *Medtr5g030910* encodes MtSTR2, which has been studied through RNA silencing, revealing that its absence causes the formation of stunted *R. irregularis* arbuscules (166).

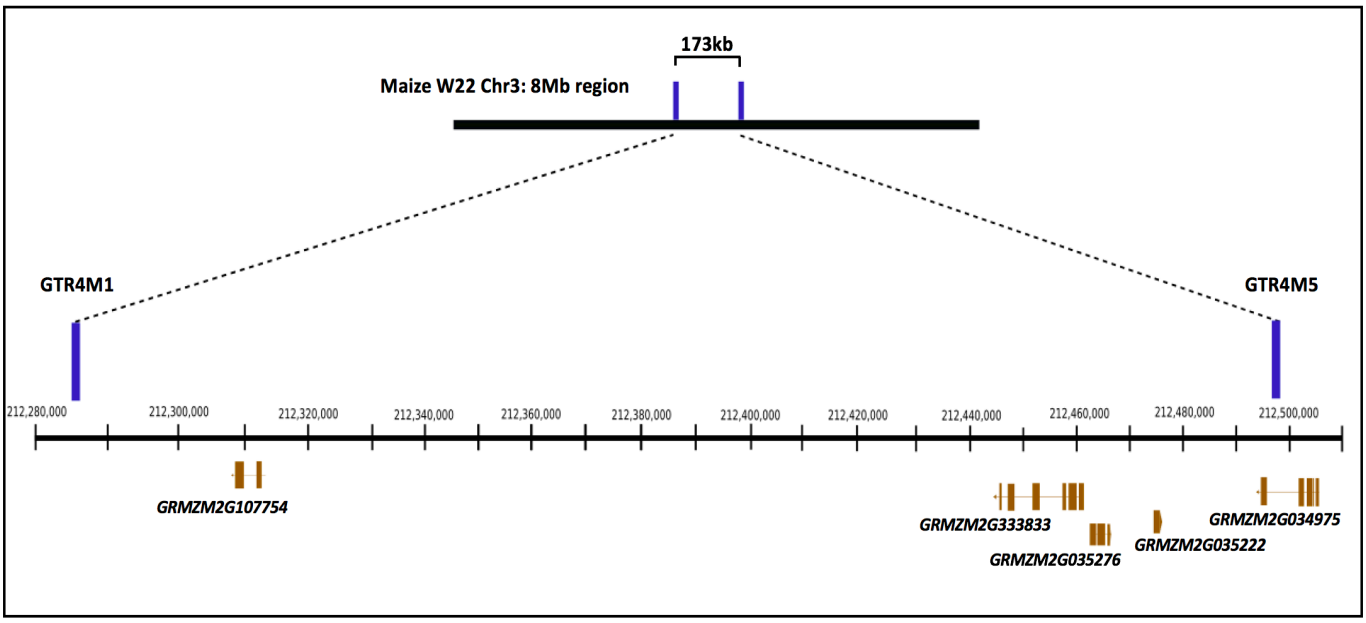

Figure 4.4: Estimated location of the five gene models *GRMZM2G107754*, *GRMZM2G333833*, *GRMZM2G035276*, *GRMZM2G035222*, and *GRMZM2G034975* within the W22 genome. The flanking markers GTR4M1 and GTR4M5 were identified during the fine mapping process. BLAST searches using the sequences of these markers enabled the identification of the five gene models within this marker-flanked region that is predicted to contain the *INA* locus.

Genome assembly	GTR4M1 location	GTR4M5 location	Gene models
B73 Refgen_v4	Chr3:208,146,460	Chr3:208,319,903	*GRMZM2G107754 , GRMZM2G333833, GRMZM2G035276, GRMZM2G035222 , GRMZM2G034975*
W22 v2.0	Chr3:212,285,114	Chr3:212,497,091	*GRMZM2G107754 , GRMZM2G333833, GRMZM2G035276, GRMZM2G035222 , GRMZM2G034975*
Mo17 v1.0	Chr3:212,605,471	Chr3:212,746,194	*GRMZM2G107754 , GRMZM2G333833, GRMZM2G035276, GRMZM2G035222 , GRMZM2G034975*
CML247 v1.0	Chr3:214,890,139	Chr3:215,179,933	*GRMZM2G107754 , GRMZM2G333833, GRMZM2G035276, GRMZM2G035222 , GRMZM2G034975*
EP1 v1.0	Chr3:228,273,887	Chr3:228,450,552	*GRMZM2G107754 , GRMZM2G333833, GRMZM2G035276, GRMZM2G035222 , GRMZM2G034975*
PH207 v1.0	Chr3:205,144,119	Chr3:205,369,916	*GRMZM2G107754 , GRMZM2G333833, GRMZM2G035276, GRMZM2G035222 , GRMZM2G034975*

Table 4.1: Location of SNP markers GTR4M1 and GTR4M5 that flank the *ina* mutation and the gene models located between them in six maize inbred lines. The gene models that lie between the final flanking markers were identified in six maize inbred lines by BLASTing the primers used to genotype these SNPs. The gene models and their order is syntenous between the different maize inbred lines at this location.

4.2.6 Investigating *ZmSTR2* as a candidate gene for *INA*

As *ZmSTR2* emerged from previous analyses as a potential candidate for the gene behind the *ina* phenotype, amplification of this gene in *ina* and WT individuals was carried out using PCR in an attempt to identify a causal mutation. The *ina* mutant was obtained from a maize population containing active *Mu* elements, and thus it was hypothesised that there could be a *Mu*-insertion within this gene in *ina* individuals. As such, the *ZmSTR2* gene was amplified in three fragments in order to assess amplicon length across this gene. For all three fragments, no amplification was possible in HMZ *ina* individuals, despite amplification of these fragments in WT individuals (Figure 4.5A). This was further explored by amplifying one of these *STR2* fragments in individuals from a population segregating for the *ina* phenotype. The *ina* phenotype did indeed co-segregate with the lack of amplification of this *STR2* fragment, and amplification was possible in all WT-phenotyped individuals (Figure 4.5B).

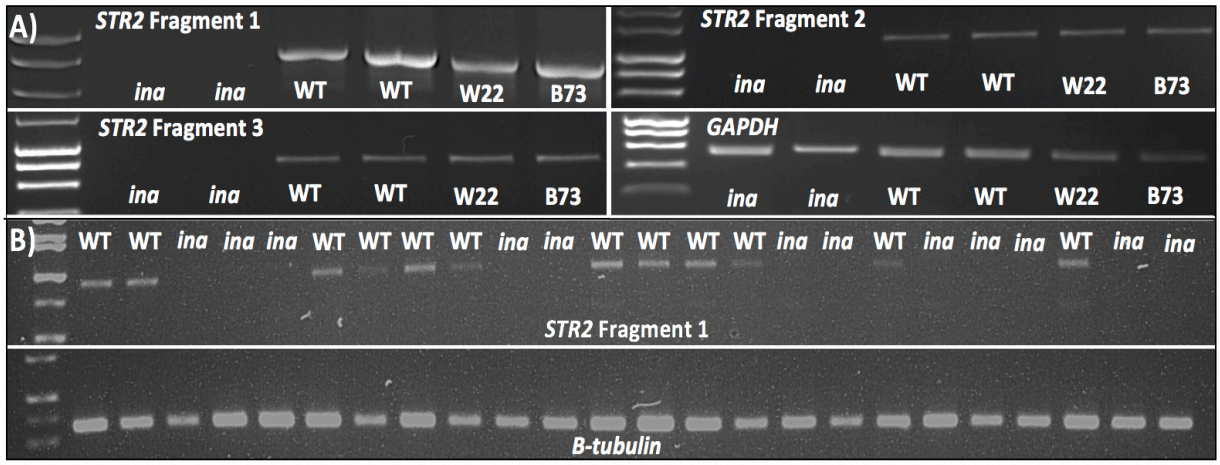

Figure 4.5: Amplification of *STR2* in *ina* and WT individuals. A) Amplification of *STR2* was attempted in *ina,* its related WT genotype, W22, and B73 individuals in 3 fragments, the 878 bp Fragment 1, 1194 bp Fragment 2, and 700 bp Fragment 3. No amplification was observed for any *STR2* fragment in the *ina* individuals tested, though amplification of all fragments was intact in all WT genotypes. **B)** Amplification of *STR2* Fragment 1 in a population segregating for the *ina* mutation. Amplification of this fragment was obtained in all individuals phenotyped as WT, and no amplification was possible in individuals phenotyped as *ina*.

4.2.7 The *ina* phenotype is caused by a deletion spanning multiple genes

The inability to amplify *STR2* in *ina* is not suggestive of an insertional mutant, rather, it is evidence of a deletion spanning the *STR2* gene in *ina* individuals. To define the length of this deletion, primers were designed in the regions around this gene and PCR amplification was used to define the borders of the deletion. During primer design, it was identified that primers designed against the W22 genome annealed best to the genetic background of *ina* and its corresponding WT material, compared to primers designed against the B73 genome. Therefore, all primers used to define the size of the deletion in *ina* are described using genetic locations from the W22 v2.0 genome (Appendix: Table A2).

The genes *GRMZM2G333833*, a chloride channel-encoding gene, *GRMZM2G035276* (*STR2*), and *GRMZM2G035222*, an F-box kelch repeat-encoding gene, were entirely deleted in *ina* individuals, as evidenced by the lack of amplification of these genes (Figure 4.6).

Amplification in *ina* individuals was possible upstream and downstream of the deletion. Upstream, amplification in *ina* individuals was obtained for a 792bp amplicon at Chr3:212,383,365, and, to fully ensure that this area is intact in *ina* individuals, another,

102bp, amplicon was successfully detected at Chr3: 212,384,437. Upstream of this amplicon, the nearest gene model prediction (*GRMZM2G107754*) was located at Chr3:212,307,338 – 212,314,448, which is considerably further upstream of these amplicons intact in *ina.* Just downstream of this amplicon is an area of highly repetitive DNA, and between this repetitive region and the 3' area of *GRMZM2G333833,* the chloride channel-encoding gene, it was not possible to design specific primers. As such, the known boundary of the *ina* deletion could not be narrowed between the chloride channel-encoding gene and the working amplicons upstream of this repetitive region. The closest gene model downstream of the deletion region is *GRMZM2G034975*, and amplification was obtained in the 5' region of this gene, which is fully intact in *ina* individuals. A further primer set was designed that produced a 645bp amplicon in *ina* individuals just upstream of the gene *GRMZM2G034975*, slightly downstream of the F-box kelch repeat-encoding gene, at Chr3:212,490,973. This amplification of intact areas of the *ina* genome around the deletion region has enabled estimation of the size of the deletion at roughly 110 kb.

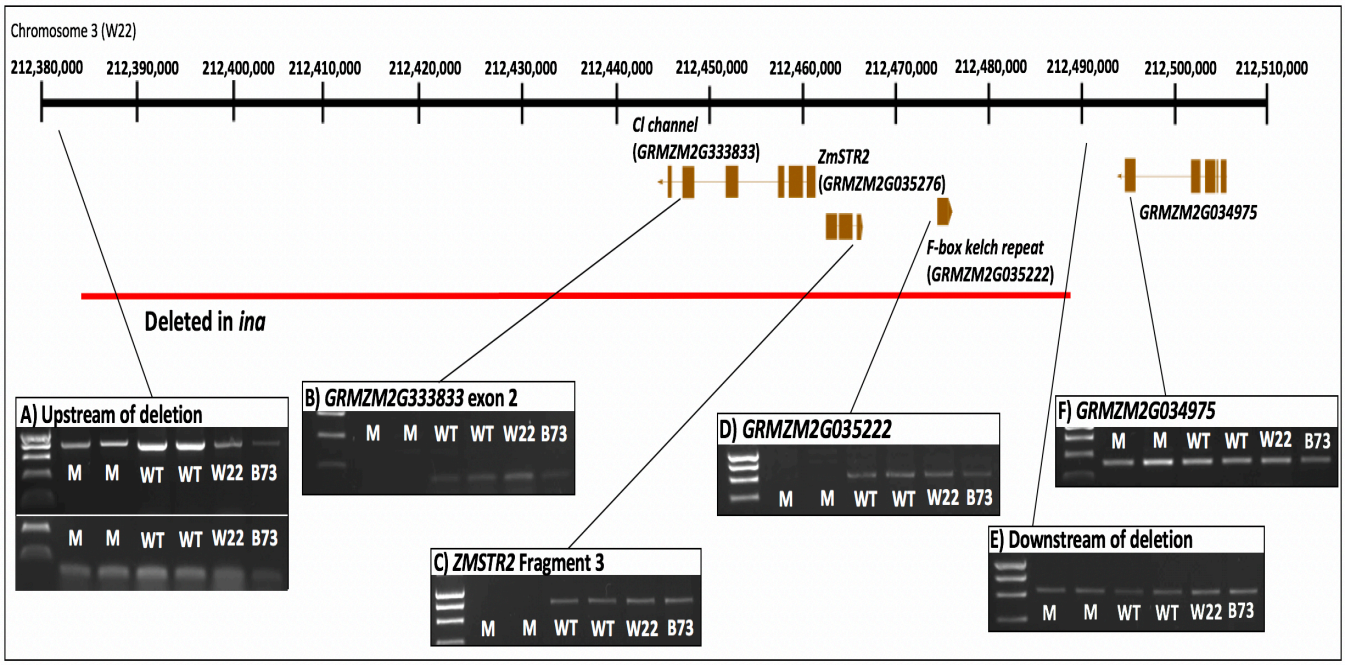

Figure 4.6: Schematic of the area of the maize W22 genome that is deleted in *ina* individuals. No amplification is possible from *ina* samples for any genomic fragments lying within the area indicated in red, in contrast to related WT and control W22 and B73 plants. **A)** Upstream of the identified *ina* deletion, two amplicons, a 792 bp and a 102 bp band, were used to show the 5' deletion boundary, as these bands can be amplified in *ina* samples, illustrating that this area is intact. **B)** No amplification of a 134 bp fragment of *GRMZM2G333833* could be obtained in *ina* individuals, though the fragment appears to be intact in related WT, W22, and B73 individuals. **C)** A 700 bp fragment of *ZmSTR2* that cannot be amplified in *ina* individuals despite clear amplification in related WT, W22, and B73 plants. **D)** A 640 bp of *GRMZM2G035222* is amplifiable from WT, W22, and B73 individuals, though not from *ina* samples. **E)** A boundary downstream of the deletion was identified due to a 645 bp fragment amplifiable in all individuals, including *ina* samples. **F)** The gene *GRMZM2G034975* is intact in all plant genotypes, as shown by the amplification of a 280 bp fragment in all samples.

4.2.8 qRT-PCR analysis of candidate genes

As the three genes *GRMZM2G333833*, *GRMZM2G035276*, and *GRMZM2G035222* are deleted in *ina*, it was hypothesised that there would be no expression of these transcripts in *ina* individuals, and this was confirmed using qRT-PCR analysis *ina* individuals under *R. irregularis* inoculated and non-inoculated conditions (Figure 4.7). Alongside this confirmation, WT individuals were examined under both inoculated and non-inoculated conditions to gather further data on these genes as potential candidates with a role in the AM symbiosis, by identifying whether the presence and colonisation of *R. irregularis* caused the induction of

any of these transcripts in maize (Figure 4.7). This analysis was carried out at a 4wpi time-point and a 9wpi time-point to fully capture any differences in expression. The biological individuals analysed for this experiment were those used for quantification of colonisation in Chapter 3.1.2.1 (Figure 3.1E). At 4wpi, WT individuals supported an average total colonisation of 50%, while *ina* individuals showed no colonisation. At 9wpi, WT individuals had an average total colonisation level of 91%, and *ina* individuals remained completely uncolonised (Figure 3.1E).

Expression of the chloride channel-encoding gene *GRMZM2G333833* was barely detectable in all samples analysed, WT and *ina*, and expression did not increase over time. As WT individuals displayed the same level of *GRMZM2G333833* expression as *ina* individuals, where this gene is deleted, it can be assumed that this gene is not expressed in the tissue and conditions analysed for WT individuals. As has been observed in rice (165), *ZmSTR2* is induced by inoculation with *R. irregularis* in WT individuals, and this is seen at both time-points, though the induction is more pronounced at 9wpi. As is expected, *ina* individuals displayed no expression of *STR2* in either condition. At 4wpi, the F-box kelch repeat-encoding gene *GRMZM2G035222* is expressed at the same level in mycorrhizal and non-inoculated WT individuals, though at 9wpi there is an increase in expression under the mycorrhizal condition. Again, *ina* individuals show no expression of this gene under any condition, supporting the presence of a deletion spanning *GRMZM2G035222* (Figure 4.7).

The expression profiles for these three candidate genes have been described in various maize tissue types. These were consulted to attempt to shed light on the possible functions and expression locations of these genes. All three candidate genes are reported to be expressed in a number of organs, including expression in leaf tissue (Appendix: Figure A4) (306).

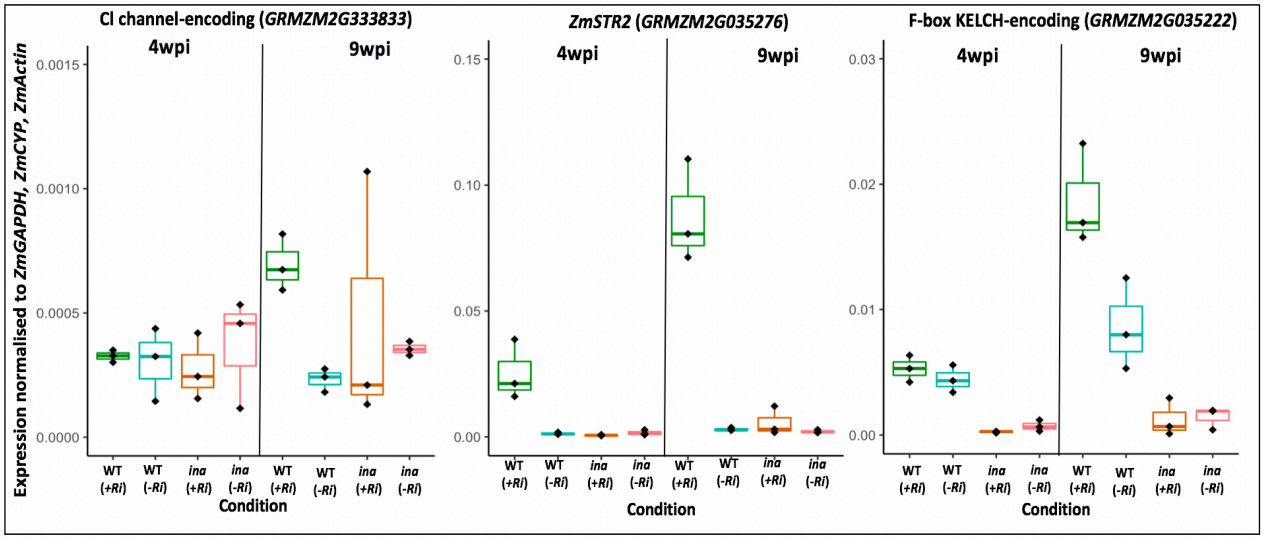

Figure 4.7: qRT-PCR expression analysis of deletion candidate genes in WT and *ina* individuals under mycorrhizal and non-inoculated control conditions at 4wpi and 9wpi. The individuals analysed for expression of candidate genes were three WT mycorrhizal (+*Ri*) and non-inoculated (-*Ri*), and three *ina* inoculated and non-inoculated individuals at 4wpi and 9wpi time-points (Figure 3.1). Expression of candidate genes was normalised to *ZmGAPDH, ZmCYP,* and *ZmActin* for all samples. Biological samples analysed were those used for colonisation quantification in Figure 3.1E – (Average total colonisation: 4wpi WT – 50%, 4wpi *ina* – 0, 9wpi WT – 91%, 9wpi *ina* – 0).

4.2.9 qRT-PCR analysis of candidate genes in a nurse plant system

It is unsurprising to see a lack of induction of *ZmSTR2,* a transcript known to accumulate in mycorrhizal roots, in *ina* individuals, as these plants support no colonisation and are comparable to WT non-inoculated individuals. *R. irregularis* colonisation of *ina* individuals can be enabled by the growth of *ina* plants in a nurse-plant system with WT plants (Chapter 3.1.2.2). This provides an opportunity to observe gene expression of the candidate genes within colonised *ina* root tissue, thus expression of these candidates was assessed under nurse plant systems at 9wpi. For this experiment, the expression of *RiEF1α*, as confirmation of fungal quantity, and the mycorrhizal-specific phosphate transporter *ZmPT6* were also analysed to better understand the functioning of the symbiosis inside colonised *ina* roots.

The biological individuals analysed for this experiment were those displayed for the nurse plant quantification in Chapter 3.1.2.2 (Figure 3.3F). In these individuals, WT plants grown in a monoculture supported 97% average total colonisation, *ina* plants grown with WT nurse

plants supported 69% average total colonisation, and *ina* plants grown in a monoculture displayed no colonisation (Figure 3.3F).

Expression of the chloride channel-encoding gene *GRMZM2G333833* was once again very low under all conditions (Figure 4.8). *STR2* expression likewise followed the same trends seen in the previous expression analysis, with no expression in *ina* individuals with or without the presence of WT nurse plants, an expected result due to the deletion of this gene in the *ina* genome. Despite the fact that this experiment was harvested at 9wpi, there was not a striking induction of the F-box kelch repeat-encoding gene in mycorrhizal WT conditions compared to WT individuals not inoculated with *R. irregularis*.

The phosphate transporter-encoding *PT6* displayed an expected induction in WT individuals (97% total colonisation) inoculated with *R. irregularis* compared to a lack of expression in non-inoculated WT plants (0 total colonisation). Interestingly, there was very low expression of this gene in *ina* individuals grown with a WT nurse plant (Figure 4.8), despite the fact that internal fungal structures are present in these plants (69% total colonisation). A delayed expression of *OsPT11*, the homolog of *ZmPT6*, is observed in *osstr1* mutant individuals, with expression only observed at 7wpi in mutants despite expression at 3wpi in WT plants (165). Despite the late time-point for this experiment, the lack of *ZmPT6* induction in *ina* individuals may therefore be explained not only by the fact that these plants harbour few arbuscules, average 52% compared to 94% arbuscule quantification in inoculated WT monocultured individuals, but also due to a delayed colonisation caused by the need for the presence of a WT nurse plant for fungal penetration of *ina*, causing an even greater delay to *ZmPT6* induction. Expression of the *R. irregularis* elongation factor *RiEF1α* is lower in *ina* individuals where colonisation is enabled by WT nurse plants than in WT inoculated plants grown in a monoculture (Figure 4.8), a result consistent with the low colonisation level observed in these plants (Chapter 3.1.2).

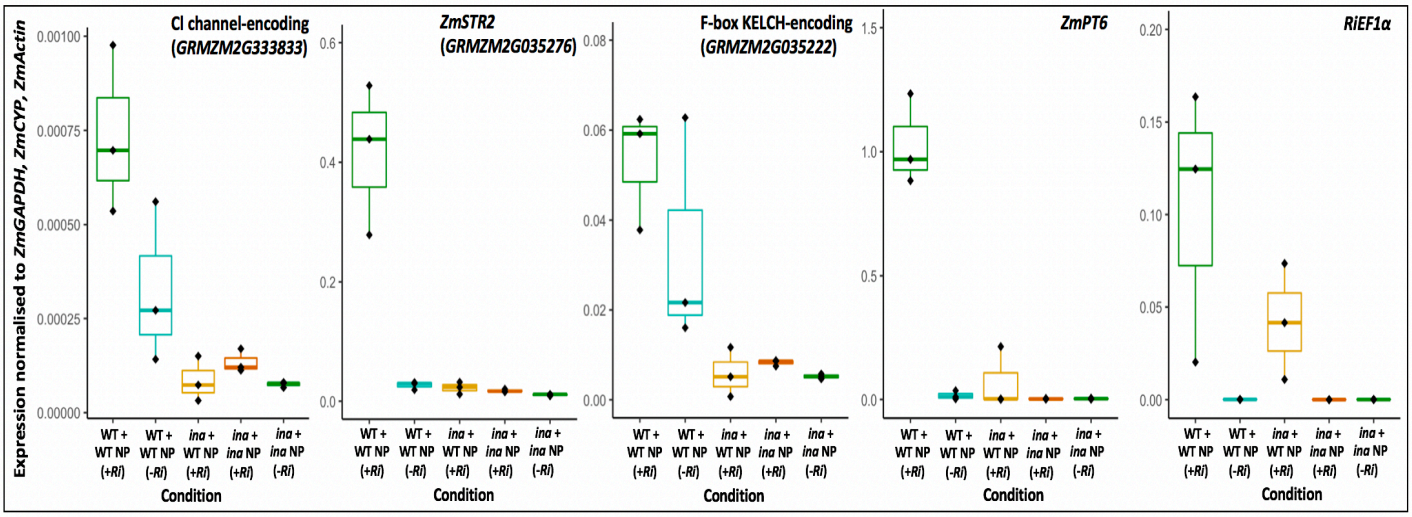

Figure 4.8: qRT-PCR expression analysis of *INA* candidate genes in nurse plant systems. Expression of the chloride channel, STR2, and F-box Kelch protein-encoding genes, phosphate transporter *ZmPT6* and *R. irregularis* elongation factor *RiEF1α* were analysed following 9wpi. Individuals analysed were monocultured WT plants with (+*Ri*) and without (-*Ri*) *R. irregularis* fungal inoculum, *ina* plants grown with WT nurse plants (+*Ri*), and *ina* monocultured plants with (+*Ri*) and without *(-Ri*) fungal inoculum. Expression levels of these genes of interest were normalised to *ZmGAPDH, ZmCYP,* and *ZmActin* for all samples. Biological samples analysed were those used for colonisation quantification in Figure 3.3F – (Average total colonisation: WT monocultured individuals (+*Ri*): 97%, WT monocultured individuals (-*Ri*): 0, *ina* individuals grown with WT NPs: 69%, *ina* monocultured individuals (+*Ri*): 0, *ina* monocultured individuals (-*Ri*): 0).

4.3 Discussion

This positional cloning analysis utilised SNP markers in the maize genome to narrow down the region containing *INA* and subsequently identified a large deletion in *ina* mutant individuals using PCR amplification. It is likely that the *ina* mutant phenotype is therefore caused by a large deletion of roughly 110 kb, and this deletion contains three gene models. Experimental evidence has been gathered on each of these gene models to identify a potential candidate for *INA*. However, although *ZmSTR2* is one of these genes and is an interesting candidate, it has not been possible to identify which of these three genes, if any, is a clear candidate for *INA.*

The original seed population where the *ina* mutation likely arose contained active *Mu* elements (240), and activity from *Mu* elements are known to cause rearrangements and

deletions around the site of their insertion in the host DNA (307). It is thus possible that the action of these transposable elements caused this large deletion identified in *ina.* This mutant phenotype has of yet only been observed in one genetic background, which resulted from crossing W22 and B73 individuals and, though both inbred lines have well-characterised reference genomes (220, 222), it would be advantageous to further backcross the *ina* mutation fully into one or both of these lines to observe the effect of background genotype on the *ina* phenotype. It is also recommended to cross this newly observed mutation into a number of additional diverse inbred lines, as the presence of modulators of mutant phenotype may differ between inbred lines of maize (308).

It has not yet been possible to establish which of the three genes are the cause of the AM symbiotic phenotype. Another possibility is that the cause of the mutant phenotype may be the removal of a regulatory region, rather than the direct removal of one of these gene candidates. However, the mapping and candidate gene analysis has revealed that the known symbiosis gene *STR2* is deleted in *ina* individuals, and that, as with previously described mutants of *str1* (165), this has an effect on the expression level of the symbiosis-induced phosphate transporter *PT6*. This information, taken with the stunted arbuscule phenotype described in Chapter 3 that is characteristic of the *STR* mutants, supports a lack of *STR2* gene activity in *ina* that should be confirmed.

What has yet to be understood is the gene behind the pre-symbiotic phenotype whereby *R. irregularis* is unable to colonise *ina* roots. There is a discrepancy between the phenotype seen here and the described phenotypes of *STR* mutants in other plant species (165, 166). This may be because of a difference in how maize regulates its interactions with AM fungi, as the *STR* mutant phenotypes have not yet been examined in maize. It seems unlikely that *STR2* could cause the observed phenotype, as there is no detectable level of *STR2* transcripts in roots not inoculated with *R. irregularis*, and evidence from Chapter 3 has identified that exudates from WT plants not provided with *R. irregularis* inoculum are still able to complement the *ina* mutant phenotype and enable colonisation in these plants. Due to the nature of this mutation, where multiple genes are deleted in *ina* individuals, it is possible that the pre-symbiotic phenotype is caused by an additional gene. Thus the chloride channel-encoding *GRMZM2G333833* or F-box repeat kelch-encoding *GRMZM2G035222* could be required for pre-symbiotic interactions and initial colonisation by *R. irregularis.* In this scenario, the overall *ina* phenotype is a product of the additive effects of two different deleted genes involved in

distinct aspects of the AM symbiosis; a mutated gene involved in pre-symbiotic signalling, and *ZmSTR2*, causing a stunted arbuscule phenotype when the fungus is enabled entry by external signals from WT nurse plants.

Forward genetics screens have the potential to reveal entirely new components of the AM symbiosis. Positional cloning carried out on the *ina* phenotype identified in a screen for AM mutants has revealed a unique phenotype caused by a large deletion. Further experiments are required to identify which gene underlies the pre-symbiotic phenotype, though this study on the *ina* mutant has revealed a novel mechanism of pre-symbiotic signalling in the AM symbiosis.

CHAPTER 5

General discussion

5.1 The *ina* phenotype is impaired in pre-symbiotic communication

Plant mutants with an AM phenotype that results in severely reduced or the absence of colonisation may be interpreted as harbouring an impairment in pre-symbiotic signalling, resulting in the collapse of communication between plant and fungal partner. This was found to be the case for a number of mutants such as *d14l, cerk1,* and *nope1*, and the roles of these mutants in pre-symbiotic signalling has since been explored (33, 82, 91). The *ina* phenotype falls into the pre-symbiotic category, and its severity is comparable to the complete block in colonisation that is visible in *d14l* mutants, where the fungus does not produce hyphopodia and makes no attempt to penetrate mutant roots (91). In comparison, *cerk1* roots enable the formation of fungal hyphopodia and are capable of hosting low levels of internal colonisation (81), and *nope1* roots can be seen to host hyphopodia, though penetration attempts are aborted (33).

The clear difference in phenotype between *d14l* and *ina* is observable under nurse-plant experimental conditions, where the presence of WT plants is unable to rescue colonisation of *d14l* (91) but complements the pre-symbiotic phenotype of *ina.* This is comparable to the *nope1* phenotype, where the presence of WT nurse-plants provides the required signal for *R. irregularis* to fully colonise *nope1* roots despite the lack of a GlcNAc-like signal from these plants (33).

The use of this nurse-plant experiment enabled the directionality of impairment to be established in *ina* individuals. It is hypothesised that a component required for *R. irregularis* colonisation of maize that is not produced or exuded by *ina* plants is provided by WT nurse-plants, enabling the observed ability of the fungus to enter mutant roots. Interestingly, this signal appears to be produced by rice roots, as growth of *ina* maize plants with WT rice plants also provides *R. irregularis* with sufficient pre-symbiotic signal to penetrate and colonise *ina* roots. This information could mean that the compound missing from *ina* plants is produced

by at least other monocotyledonous plants, and it would be interesting to identify whether a range of diverse plant lineages are also able to complement the *ina* phenotype by acting as WT donors of this compound.

5.2 The *ina* individuals may produce root exudates lacking in a component required for AM fungal colonisation

The hypothesis that *ina* is lacking a required component for AM fungal colonisation is supported by data from root exudate experiments, where WT maize exudates were collected and provided to *ina* mutants, enabling colonisation of *ina* individuals. A number of compounds have been identified with the ability to stimulate AM fungal spores in the form of germination and increased hyphal branching (33, 39, 55, 60). Research into the effect of plant root exudates on AM fungal spores has identified that multiple distinct compounds are likely to act as branching signals, and that these signals show differences in activity based on plant phosphate status and genotype (26, 263).

During the pre-symbiosis, signals generated by the plant may be constitutively produced in a 'one-way' system, or their synthesis may be induced by the proximity of the fungal symbiont, a 'two-way' system, where the signal is produced as a response to the fungal partner's own signals. The existence of constitutive signals from plant to fungus has been shown using exudate experiments, in which plants that had received no exposure to AM fungi were still able to elicit a response in fungal spores (26, 33). Signals such as flavonoids are a staple component of root exudates and likely act as a constitutive signal (309). SLs may act as an example of both of these scenarios, as they are constitutively produced and exuded into the rhizosphere, yet the perception of fungal COs and LCOs increases SL production by the plant, increasing the strength of signal from plant-to-fungus (270). The *NOPE1*-controlled exudation of a GlcNAc-like compound can also be viewed as an example of constitutive signalling due to a basal expression of this transporter in non-inoculated plants, though like *D14L, NOPE1* transcription, and hence signal strength, is induced in the presence of *R. irregularis* (33). Experimentation from this study has shown that WT plants that have not been exposed to *R. irregularis* spores rescue the *ina* phenotype and enable fungal colonisation of these mutant roots. These 'naïve' WT root systems with no exposure to fungal partners still produce this compound that may be collected and used to rescue the *ina* phenotype. This is an important

discovery as it strongly implies that the signal provided to AM fungi that is likely missing from *ina* exudates is constitutively exported into the rhizosphere.

SLs are a core pre-symbiotic component required to prime AM fungi for colonisation (39). Observations of the phenotype of *ina* plants seem to rule out erroneous production or exudation of SLs, as SL biosynthetic pathway mutants are capable of enabling internal colonisation by AM fungi (45, 47), and mutants of this pathway display an above-ground branching phenotype that is not observed in *ina* plants (165). Additionally, SL biosynthetic mutants have been studied for their arbuscule phenotype, and it has been established that, in these mutants, arbuscule formation and lifespan is WT (165, 310). The stunted arbuscule phenotype observed in *ina* individuals would add weight to the evidence against a defect in SL-related processes in these plants. Nonetheless, AM fungal colonisation of SL mutants has not yet been studied in maize to identify whether these plants would still host colonisation. The arbuscule stunting and the strong pre-symbiotic phenotype may be caused by different genes located within the deletion in *ina.* Due to this, it is plausible that one of the three genes located within the deletion identified in *ina* is involved in SL biosynthesis or exudation. It was therefore worth establishing whether rice nurse plants defective in production, and therefore exudation, of SLs, could rescue the *ina* phenotype in the same way that WT maize plants could. As growth of rice SL biosynthesis mutants *d10* and *d27* with *ina* plants did indeed enable *R. irregularis* to colonise *ina* individuals, it is very likely that the compound missing from *ina* exudates is not a SL (Chapter 3). If the *ina* phenotype was caused by a defect in production or exudation of SLs, adding additional nurse plants that were unable to provide SLs for fungal germination and colonisation would be unlikely to complement *ina*.

There is strong evidence against SLs as the missing component from *ina* exudates, and it is also possible to discount other known stimulatory compounds as candidates for the missing signal. Flavonoids are acknowledged to be a non-essential signal for colonisation of plants by AM fungi (58), and *nope1* mutants impaired in exporting a required GlcNAc-like signal still enable the formation of hyphopodia on root surfaces (33). The severe *ina* phenotype would thus suggest that the missing signal is neither of these contenders, though this cannot be entirely ruled out without further evidence. The effect of FAs, known to stimulate AM fungal spores (59, 60), on fungal colonisation has not been studied through the use of plant biosynthetic mutants, and thus it is unknown how a lack of exuded FAs would affect colonisation. Research using fractionated root exudates found that a number of components

of these exudates likely have an effect on AM fungal spores, suggesting that there are several stimulatory compounds that may act as plant-derived signals to AM fungi (26), and it may be the case that *ina* is a previously undescribed activating compound.

There is no reason to believe that the procession of *R. irregularis* into the cortex of *ina* individuals following penetration is impaired. Nurse-plant complemented *ina* individuals are capable of hosting high colonisation, despite a reduction compared to WT levels. The severely low colonisation levels observed in *ina* individuals complemented by addition of WT exudates may be due to the fact that merely adding the required compound to the growth medium is not optimal compared to a sustained signal emanating from a plant root system, causing a reduction in hyphae reaching plant roots and forming hyphopodia. A correlation has previously been identified between number of fungal entry points and colonisation level (57), and perhaps in this exudate complementation experiment *R. irregularis* is forming a small number of hyphopodia for entry due to a low or unsustained concentration of required signal.

5.3 *R. irregularis* spores display distinct transcriptomic responses to *ina* and WT root exudates

Due to the increasing data available on AM fungal genomes and transcriptomes (149, 181), research into compounds that activate AM fungal spores during pre-symbiosis are frequently utilising RNA-Sequencing technologies to gain an insight into the transcriptomic responses of the fungus to the presence of a plant partner or to specific compounds known to stimulate spores. A transcriptomics analysis of *R. irregularis* spores exposed to exudates collected from WT and *nope1* plants was instrumental in demonstrating that the fungal transcriptome displays different responses to plant mycorrhizal mutants (33). Fungal spore responses to the stimulatory compounds GR24 and palmitoleic acid have also been assessed through transcriptomic analyses, and distinct transcriptional responses to these different compounds were observed (60, 63).

The transcriptomics analysis carried out for this thesis echoed results from assessment of *nope1* (33). In both analyses, the incubation of spores with plant root exudates caused the induction of transcripts associated with GO terms linked to metabolic processes when compared to responses observed in spores that were not exposed to exudates. Incubation with WT and *nope1* exudates caused a largely overlapping response in spores when treatment

lasted for 1h, though the transcriptomic response diverged considerably at 24h (33). This observation was echoed in this study using WT, *nope1,* and *ina* exudates, and suggests that perhaps spores initially respond to germination signals from exudates, and that the genotype-specific responses and fine-tuned recognition of a suitable host occurs after more prolonged incubation with exudates, in this case following 24h. Even following 24h of exudate treatment, a considerable overlap of induced transcripts was observed in WT and *ina* exudate-treated spores compared to the 0h response. Among these transcripts were a number of SL-responsive transcripts identified in a study that treated *R. irregularis* spores to GR24 (63). This implies that a basal response to the presence of plant exudates is intact in *ina* exudate-treated spores, and adds further evidence against any hypotheses that SL signalling is impaired in *ina* plants.

Direct comparisons between WT and *ina* exudate-treated spores revealed few transcripts that were differentially expressed between the two treatments at 1h, again reflecting a generic response to the presence of root exudates. Following 24h of treatment, a stronger transcriptional response was observed in spores treated to WT root exudates compared to *ina* exudate-treated spores, and these exclusively WT exudate-responsive transcripts were associated with GO terms for transport, including lipid and cation transport terms. This is notable data when considering the hypothesis that the *ina* phenotype is caused by the absence of a required pre-symbiotic compound, as WT exudate-treated spores may be importing an exudate-borne signal or sustenance. Although this enrichment of GO terms associated with lipid transport in WT exudate-treated spores over those subjected to *ina* exudates is interesting data, it is worth reading these results cautiously. GO term assignment in *R. irregularis* must not be leaned upon too heavily, as it only illuminates the functions of a portion of the total fungal transcripts, and hence only provides a snapshot of information. A large number of transcripts appear to be unique to *R. irregularis* and difficult to assign function to using conventional GO term-assignment programs.

Ultimately it appears that *ina* exudate treatment of spores causes a reduced volume of responsive transcripts compared to WT exudate treatment, perhaps indicating a missing signal required for these spores to fully metabolically and physiologically prepare for colonisation of host plants. Interestingly, despite the severe phenotype of *ina* individuals, treatment of spores with *ina* exudates still causes an increase in metabolic activity, including the induction of transcripts involved in lipid metabolism, consistent with an important role of

storage lipids in fungal spores (140, 278). This data joins previous research into the transcriptomic response of *R. irregularis* to rice *nope1* mutants in highlighting the benefits of understanding the fungal side of AM symbiotic interactions, particularly when it comes to assessing AM mutant phenotypes of this nature (33).

5.4 The *ina* phenotype supports stunted arbuscules

Another well-studied category of AM mutant phenotypes encompasses those that enable entry and movement of AM fungi into the plant roots, but host the formation of abnormal, stunted arbuscules. This category of mutant phenotypes includes the *str* mutants and the phosphate transporter mutants such as *Ospt11/Mtpt4* which are attributed to erroneous nutrient signalling (101, 121, 165). This thesis has described a maize mutant phenotype that displays both a pre-symbiotic defect and a stunted arbuscule phenotype. This is a unique scenario that may add to current knowledge on two stages of the AM symbiosis, not only in maize, but in other model systems used to study this mutualistic relationship.

It is unclear what physiological cause is behind the arbuscule stunting in *ina* plants. Mutants of the phosphate transporters *OsPT11/MtPT4* display a stunted arbuscule phenotype that is due to a hastened arbuscule degeneration (101). It is difficult to dissect this data by studying stunted arbuscules within *ina* due to the necessity to grow *ina* individuals in a nurse-plant experiment in order to achieve internal colonisation, as it is not known when the fungus starts to penetrate *ina* roots with the aid of WT signals.

As well as shedding light on pre-symbiotic phenotypes, nurse-plant experiments have been utilised to understand mutant phenotypes that display defects in the later stages of the symbiosis. Mutants of rice PAM-localised receptor-like kinase, *ark1,* display reduced vesicle formation and reduced root colonisation visible after extended inoculation periods. When *ark1* mutants are grown alongside WT rice plants, vesicles and spore production recover, indicating an involvement of this receptor in fungal fitness (216). The rice mutant *str1* that supports stunted arbuscules and reduced colonisation may be co-cultivated with WT rice plants, and the level of colonisation in these mutant plants is quantitatively increased, though the stunted arbuscules are retained. As the WT nurse plants likely provide nourishment to the fungus through extraradical hyphae, this experiment adds valuable information on the *str1* mutant phenotype, which is likely not only caused by a general lack of fungal fitness (165).

Additionally, mutants of the gene *RAM2,* which is involved in the mycorrhizal-specific lipid export pathway, have been studied in a nurse-plant system. The *ram2* individuals display severely low colonisation, yet, when grown with WT nurse-plants, colonisation levels are significantly improved. These mutants also harbour stunted arbuscules, and, unlike the *str* mutants, growth of *ram2* with WT nurse-plants restores normal arbuscule development, indicating the possible nutritive role of this lipid export pathway, where WT plants are fulfilling the required nutritive function for fungal structures within mutant plants via hyphal connections (170).

Although the *str* mutants have not been studied in maize, the phenotype of *ina* individuals that support colonisation due to their growth with WT nurse-plants does phenocopy that of the *str* mutants observed in rice (165). This is seen in the reduced colonisation levels and stunted arbuscules within *ina* individuals that remain even when the fungus is linked to WT plants through extraradical hyphae in a nurse-plant experimental system. This observation suggests that the perturbation in *ina* plants may be involved in signalling, or is perhaps caused by a lack of localised nutritive provisioning at the arbuscule that cannot be overcome by transport of nutrients from outside of the plant, a hypothesis that has previously been considered for the *str* mutants in rice (165).

5.5 Is *ina* caused by the deletion of one of the three candidate genes located within the deleted region?

Association mapping of *ina* individuals revealed a roughly 110 kb deletion within these mutant plants that encompasses three genes (Chapter 4). Located in the 5' region of the deletion is *GRMZM2G333833,* predicted to encode a chloride channel. Ion channels with a role in the AM symbiosis have previously been described, including the potassium channel DMI1 that interacts with the nucleotide-gated CNGC15 calcium channels (73, 74). These channels are located at the nuclear envelope and facilitate colonisation by enabling the production of calcium spiking responses in response to recognition of pre-symbiotic signals, leading to cellular alterations required to host a fungal symbiont (73). However, these known channels are involved in the perception of pre-symbiotic fungal signals, and *ina* is perturbed in its signalling to the fungus. There is no obvious role for an ion channel in the production or exudation of a signal from plant to fungus, unless initial perception facilitated via ion channels

was perturbed and subsequently so was exudation of a mycorrhizal-induced signal required for fungal colonisation. However, due to evidence from complementation experiments using exudates from WT plants that were not previously exposed to *R. irregularis,* it seems unlikely that the signal missing from *ina* root systems first needs to be induced by the presence of the fungus. Additionally, there is currently no evidence that *ina* experiences erroneous perception of the fungal symbiont, as fungal colonisation of *ina* is possible in the presence of WT nurse-plants.

The second gene within this deleted region, *GRMZM2G035276,* is the homolog of rice ABCG transporter *STR2,* as described previously using a phylogenetic tree produced using the rice *STR* and *STR2* genes (165). These transporters fall within a large protein family, the ABC transporters, that actively transport a wide range of substrates, and the G subfamily are half-sized transporters that oligomerise to form a full, functional transporter (311). In plants, a number of ABC transporters have been characterised and were found to transport a range of substrates such as cell-wall component suberin (167). One transporter described in *P. hybrida*, the full-sized ABC transporter PDR1, is a known exporter of SLs during pre-symbiotic signalling from plants to AM fungi (48). It is therefore not hard to imagine the biological role of an ABCG transporter in exporting a symbiotic signalling compound into the rhizosphere.

The *STR* genes have received recent attention due to the observation that they appear to be specifically required for the AM symbiosis in the most recent common ancestor of all land plants, and have been lost in plant lineages that cannot form a mutualistic relationship with AM fungi (154, 312). As previously discussed, *str* mutants host stunted arbuscules that, in rice, cannot be rescued by the presence of WT nurse-plants. Though this would suggest that a general lack of fungal nutrition could be ruled out, it is still possible that a local signal or nutrient is required at the branching tips of arbuscules (165). If the *STR* transporters were to have a role in pre-symbiotic signalling, perhaps they would be required for local signalling or nourishment to stimulate hyphopodia formation at a stage where the fungal external hyphae were in close proximity to the root.

An interesting aspect of *ZmSTR2* as a candidate for *INA* is the fact that *STR* and *STR2* are widely considered to be strong candidates for the movement of lipids from plant to fungus across the PAM during the lipid export pathway (153). Considering *STR2* as an *INA* candidate for the *ina* pre-symbiotic phenotype would involve a hypothesis that lipid signalling or nourishment is required during the pre-symbiosis. It is not unfeasible that the mycorrhizal-specific lipid

export pathway would play a role in pre-symbiotic interactions, as hyphal branching of *R. irregularis* spores has been successfully induced by branched-chain FAs (60). Indeed, plants are known to exude fatty acids such as palmitic acid from their roots (313), and it has been observed that the parasitic fungal plant pathogen *Golovinomyces cichoracerum* requires host-derived FAs for colonisation of *A. thaliana* (160). In a comparable phenotype to *ina*, *ram2* plants, defective in the mycorrhizal lipid export pathway, have been described with very low colonisation levels and erroneous, infrequent, hyphopodia whose number was increased through the addition of C16 lipids (161, 162). However, this hyphopodia phenotype was not observed in additional studies of the *ram2* phenotype (156). Such low colonisation in *ram2* individuals could be attributed to reduced fungal fitness and proliferation within the root due to a reduced supply of lipids, though it is not implausible to consider that the mycorrhizal-specific lipid export pathway could produce specific lipids for exudation to external hyphae during the pre-symbiotic stage (161). Nonetheless, it is worth noting that, although the genes involved in the lipid export pathway and the regulation of the *STR* genes have not been studied in maize, none of these mutants, such as *ram1*, *ram2, fatb,* and *dis*, have been recorded as essential for fungal hyphal penetration or entry of roots (153, 156, 168).

To date, no experimental evidence has suggested a role for STR or STR2 in pre-symbiotic signalling. The localisation of STR and STR2 also do not support a role of STR2 in the presymbiosis, as an exporter of a signal required for pre-symbiotic interactions would likely localise to the root epidermis in order to export a signalling compound to the rhizosphere. Data from *M. truncatula* observed localisation of STR and STR2 at the PAM surrounding arbuscule branches using a split-YFP system (166, 314). However, this system is limited in only assessing localisation of STR2 in relation to its dimerisation with STR, and it is unknown whether STR2 forms additional partnerships at alternate locations. In rice, root cell types were collected using laser microdissection and assessed for their expression of STR and STR2. Expression was found only in arbusculated cortex cells, and not in cortical cells that did not contain an arbuscule (165). Again, this approach may be limited in fully assessing the localisation of STR and STR2, as only cortical cells were the only root cell types examined. It may therefore be interesting to assess STR2 localisation using alternate methods that may enable its identification without partnership to STR.

The low expression levels of the *STR* genes in non-inoculated plants and their subsequent induction only in colonised tissue in rice would argue against a pre-symbiotic role (165). In

concurrence with this information, overexpression of the *STR* genes in *M. truncatula* roots leads to the accumulation of extracellular lipid polyesters, demonstrating the capacity of the STR proteins to transport these compounds, yet WT and *str* plants that were not inoculated with *R. irregularis* displayed indistinguishable compositions of cutin monomers (160). Data presented in this thesis on the transcription of *STR2* in colonised and uncolonised root tissues of maize also supports an undetectable level of *STR2* transcript in uncolonised tissue, and a strong induction of this transcription in inoculated, colonised maize tissue. This evidence does not align with a role of *STR2* in pre-symbiotic signalling, as the potential signal that is lacking from *ina* exudates appears to be constitutively produced and exuded. It is, however, possible that a small number of exporters could be responsible for sending out a sustained signal and still have an undetectable amount of transcript.

Whether or not *STR2* is the gene behind the pre-symbiotic defect observed in *ina* individuals, it is possible that deletion of *STR2* in these plants is causing the stunted arbuscule defect. As previously mentioned, *ina* phenocopies *str* mutants from rice in that it supports stunted arbuscules that remain even under nurse-plant conditions (165). The homolog of *OsSTR2* is deleted from *ina* plants and no *ZmSTR2* transcript can be detected under mycorrhizal conditions in *ina* individuals, with or without the presence of nurse-plants (Chapter 4). It therefore seems likely that *ina* is defective in the hypothesised role of *STR/STR2* in exporting lipids at the arbuscule interface to the fungal symbiont (153).

It is worth considering the identification of *antiSTR1,* a possible *cis*-natural antisense transcript (NAT) complementary to the *STR1* gene in rice (165). *Cis*-NATs are endogenous RNAs transcribed from the antisense DNA strand of the genomic loci that encodes their sense transcript (315). The discovery of *antiSTR1* brings forth questions regarding the regulation of the *STR* genes. If *STR1* is under regulation by a *cis*-NAT, perhaps *STR2* expression is also regulated by elements that bind somewhere within the deleted region in *ina* plants. However, no *antiSTR2 cis*-NAT was identified in rice, and, as *cis*-NATs target the transcript from the same genomic loci that they are produced from, it is unknown whether the identified *antiSTR1* could have any regulatory effect on *STR2* expression (165). Still, the question of whether the *ina* phenotype is caused by removal of regulatory elements or their binding sites rather than the deleted genes themselves is one worth considering.

Toward the 3' end of the deletion identified within *ina* individuals is *GRMZM2G035222,* a predicted kelch repeat-containing F-box family protein. F-box proteins are a component of

protein degradation mechanisms required for posttranslational regulation via the ubiquitination cascade. Kelch repeat-containing F-box proteins contain a kelch motif, a protein-protein interaction domain responsible for selective degradation of proteins (316). Kelch repeat-containing F-box family proteins have been discovered with roles in the AM and rhizobial symbioses. TOO MUCH LOVE (TML) is one such protein that localises to the nucleus and regulates the number of nodules formed in leguminous species (317). F-box proteins form a component of SCF complexes that mediate protein degradation, a mechanism that regulates cellular processes and signals through alteration of protein levels (85). The rice F-box protein D3 is known to regulate the AM symbiosis by causing the degradation of SUPPRESSOR OF MAX2-1 (SMAX1). SMAX1 acts as a suppressor of AM symbiosis signalling programs, and hence its degradation through the actions of a complex containing D3 results in the activation of AM signalling in the plant (318). Transcriptomics analyses have identified kelch repeat-containing and kelch repeat-containing F-box family transcripts induced under mycorrhizal conditions, thus these proteins may have a strong role in regulating cellular changes required for the AM symbiosis (319-321). It is thus entirely possible that this particular gene, *GRMZM2G035222,* forms part of a pre-symbiotic signalling pathway.

5.6 Future perspectives

The most pressing question raised by this study is the identification of the gene or element causing the *ina* mutant phenotypes. It must be established whether the pre-symbiotic and stunted arbuscule phenotypes observed in *ina* individuals are caused by one gene or two different genes, if indeed any of the three candidate genes are responsible. Alternatively, a non-coding regulatory sequence located within the *ina* deletion may be the culprit. This experiment is ongoing and involves the production of three independent knockout maize lines generated via CRISPR-Cas9 (226). The generation of these knockout lines is being carried out by Corteva Agriscience (IA, US). The phenotyping of these lines through Trypan Blue quantification of colonisation levels would aim to establish whether the knockout of any one of these genes produced a pre-symbiotic phenotype that phenocopies *ina.* It would then be necessary to repeat nurse-plant and exudate complementation experiments in an attempt to decouple the pre-symbiotic and stunted arbuscule phenotypes of *ina,* through examining whether any of these individual lines hosts stunted arbuscules. It would also be beneficial to

study the effect of these novel mutant exudates on *R. irregularis* spores by utilising marker genes identified during this study that display differential expression when exposed to *ina* and WT root exudates.

Understanding the alterations in pre-symbiotic signalling that may take place in *ina* individuals can be assessed from the perspective of the plant. This could be facilitated by a transcriptomics analysis via RNA-Sequencing of *ina* individuals, and of any successfully phenotyped CRISPR-Cas9 knockout lines. Studies of plant pre-symbiotic responses to the presence of an AM fungal partner frequently require treatment of WT and mutant individuals with fungal-derived GSE, analogous to analysing transcript expression of fungal genes through treatment of spores with root exudates. This would produce insight into whether *ina* individuals differ in their initial perception of fungal pre-symbiotic signals, and it would be valuable to include *nope1* mutants in such an analysis, as *ina* and *nope1* are both involved in plant-to-fungus pre-symbiotic signalling (33). Such an analysis could potentially provide information that could place the function of *INA* in context with other known components of pre-symbiotic signalling, such as *d14l* (91). However, this method is often used to study plant mutants with defective pre-symbiotic recognition of AM fungi (91, 322). An analysis of a plant mutant displaying defective communication to the fungal partner would bring challenges. Initial perception does not appear to be perturbed in mutants such as *ina* and *nope1,* and alterations in plant transcriptomic response may occur only due to a knock-on effect caused by insufficiently activated or nourished fungal spores. It may therefore be useful to carry out a transcriptomics analysis of *ina* individuals that have been colonised with the aid of WT nurse-plants, to highlight any differences in transcriptomic signature compared to colonised WT maize plants.

In order to understand whether the requirement for *INA* for pre-symbiotic signalling is conserved among hosts of AM fungi, it would be worth conducting phylogenetic analyses of the gene in question, and perhaps exploring mutant phenotypes in other plant systems. In addition, studying plant AM phenotypes with multiple species and genera of AM fungi is informative in understanding the role of the gene in question (33, 165). For example, the effect of flavonoids on fungal spore germination and hyphal growth differs between genera of AM fungi (53), and the observed *str* phenotype in rice was found to be more severe when mutants were inoculated with *G. rosea* compared to inoculation with *R. irregularis* (165).

5.7 Final conclusions

Phenotypic characterisation and genetic analyses of plant mycorrhizal mutants have revealed a great deal about the molecular machinery required for plants to attract and host AM fungi (101, 165). The identification of the *d14l* mutant opened up a new signalling pathway for further study (91), studies into the *nope1* mutant identified a novel signal required by AM fungi for colonisation of host roots (33), and recent research into plant genes required for a mycorrhizal-specific lipid export pathway has surged forward the understanding of AM symbiotic nutrition (153, 156, 157). This study set out to identify the causal gene behind a novel mycorrhizal mutant in maize.

This thesis describes the successful identification of a deleted region cosegregating with the *ina* mutant phenotype, achieved through positional cloning. This study has resulted in the identification of three candidate genes located within a deletion in *ina* plants, including a known component of the AM symbiosis, *STR2.* Despite the requirement for further research into this mutant phenotype and the generation of independent knockout lines, this study has provided a strong understanding of the *ina* phenotype and has taken steps toward characterising the symbiotic function that may be missing from these plants. Due to experimentation carried out for this thesis, it is understood that *INA* functions in pre-symbiotic interactions where it is likely required for plant-to-fungus signalling. This was highlighted by a transcriptomics analysis of *R. irregularis* spores that produce differing responses to WT and *ina* root exudates, suggesting the absence of a required pre-symbiotic signal from *ina* exudates. In addition to the characterisation of the *ina* pre-symbiotic phenotype, through the aid of nurse-plant experiments, a stunted arbuscule phenotype was also identified, adding to the complexity of this phenotype. It is clear that *ina* is a unique mycorrhizal mutant, and, due to its multifaceted phenotype, further research into this mutant that builds upon the discoveries highlighted here may provide a deeper understanding of the molecular underpinnings of the AM symbiosis.

APPENDIX

Table A1: Hoagland's Solution components

Solution	Chemical	Concentration (g)	mL of stock in 1L	
			Full Hoagland's	½ Hoagland's
A 20x stock (g/L)	KNO_3	10	50	25
	$Ca(NO_3)_2.4H_2O$	2.36		
	$MgSO_4.7H_2O$	9.86		
B 100x stock (g/L)	KH_2PO_4	1.36	10	-
	KCl	6.7		
B 100x stock (g/L)	KH_2PO_4	0.68	-	5
	KCl	6.9		
C 20x stock (g/L)	Fe-citrate	0.5	10	5
D 1000x stock (g/100mL)	$MnSO_4.H_2O$	0.137	1	0.5
	$ZnSO_4.7H_2O$	0.02		
	$CuSO_4.5H_2O$	0.008		
E 1000x stock (g/100mL)	$Na_2B_4O_7.10H_2O$	0.2	1	0.5
	$(NH_4)_6Mo_7O_{24}.4H_2O$	0.01		

Table A2: Maize genotyping primers

Gene	Gene ID	Sequence
ZmNOPE1	*GRMZM2G176737*	**F:** 5'-CCT CAT CTG CTT CTG CTG-3' **R:** 5'-CGA GCA TGA ATG CCA TGA AG-3'
Zmnope1	*GRMZM2G176737*	**F:** 5'-ATC TTC CAG TTG GCG AAG AG-3' **R:** 5'-GTT CGA AAT CGA TCG GGA TA-3'
ZmSTR2-fragment 1	*GRMZM2G035276*	**F:** 5'-AAA CTA AGA TGG GCC CTG GA-3' **R:** 5'-GAT GAG CGC TTG ATG AGG CT-3'
ZmSTR2-fragment 2	*GRMZM2G035276*	**F:** 5'-ACC ATG TTC ACC AAG CCC AA-3' **R:** 5'- ACC AGT TCC TAT CAT CAG GGG-3'
ZmSTR2-fragment 3	*GRMZM2G035276*	**F:** 5'-TCT TCT ACC GCG TCC TCT TCT A-3' **R:** 5'-TAG ATA GAG TCA TAG AGG CAG GCT T-3'
Upstream of deletion 1	-	**F:** 5'-CCT CGA GGC TAT GGA TCG TG-3' **R:** 5'-TGG GTC CTT CTA ACC TCC GT-3'
Upstream of deletion 2	-	**F:** 5'- TAG GGA GAG TGA TGC CTG GT-3' **R:** 5'- GCT TGT CGT CGT CTT GGA TT-3'
Chloride channel exon	*GRMZM2G333833*	**F:** 5'-TCT TCT ACC GCG TCC TCT TCT A-3' **R:** 5'-TAG ATA GAG TCA TAG AGG CAG GCT T-3'
Kelch F-box	*GRMZM2G035222*	**F:** 5'-ACT ATC CTT CAA GCA CCG CC-3' **R:** 5'-AGG TGC TCT CAC CCT TGT AGA-3'
Downstream of deletion 1	-	**F:** 5'-TAA AGC GGT CTG TTC GCT ACA-3' **R:** 5'-AAA TGC GCT GTG CCT CAG A-3'
Downstream of deletion 2	*GRMZM2G034975*	**F:** 5'-AGT CTG GAG ACC TTT GCA GC-3' **R:** 5'-AGC ATT TAG CTG GAC CTT GAA GA-3'

Figure A1: Genotyping of maize material segregating for *nope1* (Primers: Table A2)

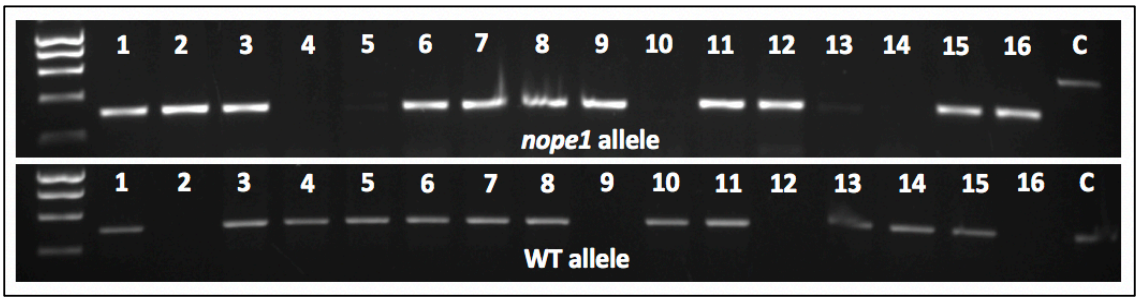

Table A3: Maize qRT-PCR primers

Gene	Gene ID	Sequence
ZmGAPDH	*GRMZM2G046804*	**F:** 5'-CTT CGG CAT TGT TGA GGG TTT G -3' **R:** 5'-TCC TTG GCT GAG GGT CCG TC-3'
ZmCyclophilin	*GRMZM2G326111*	**F:** 5'-CTG AGT GGT GGT CTT AGT-3' **R:** 5'-AAC ACG ATT CAA GCA GAG-3'
Zmβ-Actin	*GRMZM2G126010*	**F:** 5'-AAG TAC CCG ATT GAG CAT GG-3' **R:** 5'-CGG AGC TCG TTG TAG AAG GT-3'
ZmAM3	*GRMZM2G135244*	**F:** 5'-ATC TGT CGT TGC GTT CCT CT-3' **R:** 5'-GCA TCT ATC ACT GCG GGA AT-3'
ZmPT6	*GRMZM5G881088*	**F:** 5'-GAT CCA GCT CAT CGG TTT CT-3' **R:** 5'-GAG CGT GGT GTG TTT GTT CT-3'
ZmARK1	*GRMZM5G849471*	**F:** 5'-TAG CAA GCG AAA GAC CA-3' **R:** 5'-GTT GAA CTC GCA GAG GGT GA-3'
ZmPT14	*GRMZM2G139639*	**F:** 5'-GAC TCC AAG ATT CTC CCG CT-3' **R:** 5'-TCT TCC AAA TTC ATG AGC ACA AA-3'
-	*GRMZM2G333833*	**F:** 5'-AAG CTC ACA GAG GGT GCA AT-3' **R:** 5'-TTT ACA CTT GCC TGC TTG GC-3'
ZmSTR2	*GRMZM2G035276*	**F:** 5'-CAA GTG GTG GAT GGT GCT CT-3' **R:** 5'-TCG TAC ATC CAG GCC CTA CA-3'
-	*GRMZM2G035222*	**F:** 5'- ATA GCG AGG ACC GCT CTT TC-3' **R:** 5'- AAA TTC CTT GCG GGG AGA CC-3'

Figure A2: qRT-PCR Program

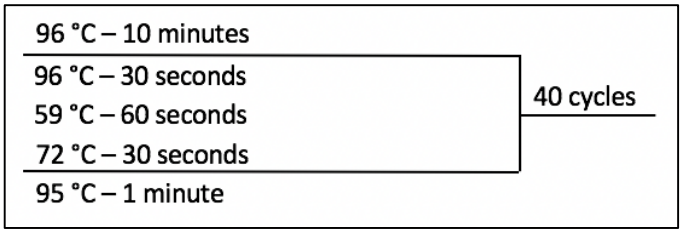

Figure A3: KASP PCR Program

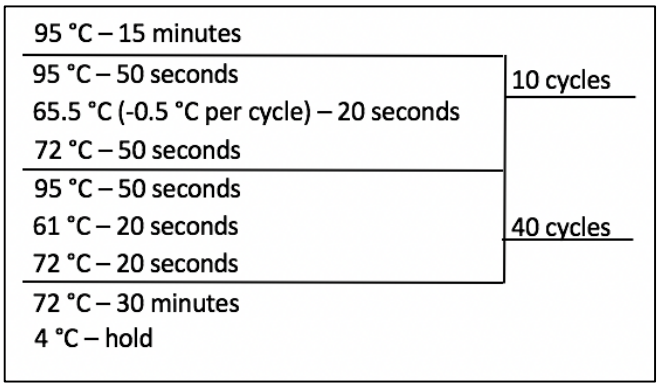

Table A4: M Media components

Solution	Chemical	Concentration (g)	mL of stock in 1L
A 100x stock (g/L)	$MgSO_4x7H_2O$	73.1	10
	KNO_3	8	
	KCl	6.5	
	KH_2PO_4	0.48	
B 100x stock (g/L)	$Ca(NO_3)2x4H_2O$	28.8	10
C 1000x stock (g/100mL)	$MnCl_2x4H_2O$	0.6	1
	$ZnSO_4x7H_2O$	0.26	
	H_3BO_3	0.15	
	$CuSO_4x5H_2O$	0.013	
D 1000x stock (g/100mL)	$Na_2MoO_4x2H_2O$	0.24	1
E (1000x stock)	KI	0.075	1
F 1000x stock (g/100mL)	Glycine	0.3	1
	Thiamine hydrochloride	0.01	
	Peroxide hydrochloride	0.01	
	Nicotinic acid	0.05	
	Myo-inositol	5.0	
G 100x stock (g/L)	Na Fe-EDTA	0.8	10

Table A5: *R. irregularis* qRT-PCR primers

Gene	Transcript ID	Sequence
RiGAPDH	1687567	**F:** 5'-GTC GCG TGG TAC GAT AAC GA-3' **R:** 5'-GTT ATT GCC TAT GCT GCG CC-3'
RiEF1α	1699167	**F:** 5'-GCT ATT TTG ATC ATT GCC GCC-3' **R:** 5'-TCA TTA AAA CGT TCT TCC GAC C-3'
Riα-tubulin	1648057	**F:** 5'-CAT TGG TCA CAT ACG CTC CAG-3' **R:** 5'-CGG CCA CAG TAA GTT GTT CGT-3'
-	1590502	**F:** 5'-GGC ACT CAA GGC CAA AGG AT-3' **R:** 5'-TGT TGC GGG AGT ATT AGG GG-3'
-	1616147	**F:** 5'-CAT GGA ACA CGT CCC CAG AA-3' **R:** 5'-ATT CAT TGG ACG CGG AGG TG-3'
-	1575284	**F:** 5'-AAC CAA TAC GGT CGT GCT CA-3' **R:** 5'-TTT AGG TTC CCC CTT TCC GC-3'

Figure A4: Expression of the three candidate genes *GRMZM2G333833, GRMZM2G035276,* and *GRMZM2G035222* in 79 maize organs. Figure obtained from MaizeGDB (305), produced using data from Stelpflug et al. (306).

REFERENCES

1. Müller DB, Vogel C, Bai Y, Vorholt JA. The Plant Microbiota: Systems-Level Insights and Perspectives. Annual Review of Genetics. 2016;50(1):211-34.
2. Berendsen RL, Pieterse CMJ, Bakker PAHM. The rhizosphere microbiome and plant health. Trends in Plant Science. 2012;17(8):478-86.
3. Gams W. Biodiversity of soil-inhabiting fungi. Biodiversity and Conservation. 2007;16(1):69-72.
4. Spatafora JW, Chang Y, Benny GL, Lazarus K, Smith ME, Berbee ML, et al. A phylum-level phylogenetic classification of zygomycete fungi based on genome-scale data. Mycologia. 2016;108(5):1028-46.
5. Pirozynski KA, Malloch DW. The origin of land plants: A matter of mycotrophism. Biosystems. 1975;6(3):153-64.
6. Remy W, Taylor TN, Hass H, Kerp H. Four hundred-million-year-old vesicular arbuscular mycorrhizae. Proceedings of the National Academy of Sciences. 1994;91(25):11841-3.
7. Lutzoni F, Nowak MD, Alfaro ME, Reeb V, Miadlikowska J, Krug M, et al. Contemporaneous radiations of fungi and plants linked to symbiosis. Nature Communications. 2018;9(1):5451.
8. Heckman DS, Geiser DM, Eidell BR, Stauffer RL, Kardos NL, Hedges SB. Molecular Evidence for the Early Colonization of Land by Fungi and Plants. Science. 2001;293(5532):1129-33.
9. Wang B, Yeun LH, Xue J-Y, Liu Y, Ané J-M, Qiu Y-L. Presence of three mycorrhizal genes in the common ancestor of land plants suggests a key role of mycorrhizas in the colonization of land by plants. New Phytologist. 2010;186(2):514-25.
10. Bidartondo M, Rimington W, Pressel S, Duckett J, Field K, Read D. Ancient plants with ancient fungi: liverworts associate with early-diverging arbuscular mycorrhizal fungi. 2018.
11. Martin FM, Uroz S, Barker DG. Ancestral alliances: Plant mutualistic symbioses with fungi and bacteria. Science. 2017;356(6340).
12. Smith SE, Read D. Introduction. In: Smith SE, Read D, editors. Mycorrhizal Symbiosis (Third Edition). London: Academic Press; 2008. p. 1-9.
13. Hodge A, Helgason T, Fitter AH. Nutritional ecology of arbuscular mycorrhizal fungi. Fungal Ecology. 2010;3(4):267-73.
14. Read D. The ties that bind. Nature. 1997;388(6642):517-8.
15. Giovannetti M, Azzolini D, Citernesi AS. Anastomosis Formation and Nuclear and Protoplasmic Exchange in Arbuscular Mycorrhizal Fungi. Applied and Environmental Microbiology. 1999;65(12):5571-5.
16. Friese CF, Allen MF. The Spread of VA Mycorrhizal Fungal Hyphae in the Soil: Inoculum Types and External Hyphal Architecture. Mycologia. 1991;83(4):409-18.
17. Giovannetti M, Fortuna P, Citernesi AS, Morini S, Nuti MP. The occurrence of anastomosis formation and nuclear exchange in intact arbuscular mycorrhizal networks. New Phytologist. 2001;151(3):717-24.
18. Sanders FE, Tinker PB. Mechanism of Absorption of Phosphate from Soil by Endogone Mycorrhizas. Nature. 1971;233(5317):278-9.

19. Bender SF, Conen F, Van der Heijden MGA. Mycorrhizal effects on nutrient cycling, nutrient leaching and N2O production in experimental grassland. Soil Biology and Biochemistry. 2015;80:283-92.
20. Nottingham AT, Turner BL, Winter K, van der Heijden MGA, Tanner EVJ. Arbuscular mycorrhizal mycelial respiration in a moist tropical forest. New Phytologist. 2010;186(4):957-67.
21. Johnson D, Leake JR, Ostle N, Ineson P, Read DJ. In situ13CO2 pulse-labelling of upland grassland demonstrates a rapid pathway of carbon flux from arbuscular mycorrhizal mycelia to the soil. New Phytologist. 2002;153(2):327-34.
22. Siddiqui ZA, Futai K. Mycorrhizae: sustainable agriculture and forestry: Springer; 2008.
23. Cano C, Dickson S, González-Guerrero M, Bago A. In vitro Cultures Open New Prospects for Basic Research in Arbuscular Mycorrhizas. In: Varma A, editor. Mycorrhiza: State of the Art, Genetics and Molecular Biology, Eco-Function, Biotechnology, Eco-Physiology, Structure and Systematics. Berlin, Heidelberg: Springer Berlin Heidelberg; 2008. p. 627-54.
24. Nadal M, Paszkowski U. Polyphony in the rhizosphere: presymbiotic communication in arbuscular mycorrhizal symbiosis. Current Opinion in Plant Biology. 2013;16(4):473-9.
25. Choi J, Summers W, Paszkowski U. Mechanisms Underlying Establishment of Arbuscular Mycorrhizal Symbioses. Annual Review of Phytopathology. 2018;56(1):135-60.
26. Nagahashi G, Douds DD. Partial separation of root exudate components and their effects upon the growth of germinated spores of AM fungi. Mycological Research. 2000;104(12):1453-64.
27. Giovannetti M, Sbrana C, Citernesi AS, Avio L. Analysis of factors involved in fungal recognition responses to host-derived signals by arbuscular mycorrhizal fungi. New Phytologist. 1996;133(1):65-71.
28. Buee M, Rossignol M, Jauneau A, Ranjeva R, Bécard G. The Pre-Symbiotic Growth of Arbuscular Mycorrhizal Fungi Is Induced by a Branching Factor Partially Purified from Plant Root Exudates. Molecular Plant-Microbe Interactions®. 2000;13(6):693-8.
29. Besserer A, Bécard G, Jauneau A, Roux C, Séjalon-Delmas N. GR24, a Synthetic Analog of Strigolactones, Stimulates the Mitosis and Growth of the Arbuscular Mycorrhizal Fungus Gigaspora rosea by Boosting Its Energy Metabolism. Plant Physiology. 2008;148(1):402-13.
30. Gaspar M, Pollero R, Cabello M. Triacylglycerol consumption during spore germination of vesicular-arbuscular mycorrhizal fungi. Journal of the American Oil Chemists' Society. 1994;71(4):449-52.
31. Olsson PA, Johansen A. Lipid and fatty acid composition of hyphae and spores of arbuscular mycorrhizal fungi at different growth stages. Mycological Research. 2000;104(4):429-34.
32. Tamasloukht MB, Waschke A, Franken P. Root exudate-stimulated RNA accumulation in the arbuscular mycorrhizal fungus Gigaspora rosea. Soil Biology and Biochemistry. 2007;39(7):1824-7.
33. Nadal M, Sawers R, Naseem S, Bassin B, Kulicke C, Sharman A, et al. An N-acetylglucosamine transporter required for arbuscular mycorrhizal symbioses in rice and maize. Nature Plants. 2017;3(6):17073.
34. Nagahashi G, Douds D. Separated components of root exudate and cytosol stimulate different morphologically identifiable types of branching responses by arbuscular mycorrhizal fungi. Mycological Research. 2007;111(4):487-92.

35. Umehara M, Hanada A, Yoshida S, Akiyama K, Arite T, Takeda-Kamiya N, et al. Inhibition of shoot branching by new terpenoid plant hormones. Nature. 2008;455(7210):195-200.
36. Cook C, Whichard LP, Turner B, Wall ME, Egley GH. Germination of witchweed (Striga lutea Lour.): isolation and properties of a potent stimulant. Science. 1966;154(3753):1189-90.
37. Bouwmeester HJ, Matusova R, Zhongkui S, Beale MH. Secondary metabolite signalling in host–parasitic plant interactions. Current Opinion in Plant Biology. 2003;6(4):358-64.
38. Akiyama K, Matsuzaki K-i, Hayashi H. Plant sesquiterpenes induce hyphal branching in arbuscular mycorrhizal fungi. Nature. 2005;435(7043):824-7.
39. Besserer A, Puech-Pagès V, Kiefer P, Gomez-Roldan V, Jauneau A, Roy S, et al. Strigolactones Stimulate Arbuscular Mycorrhizal Fungi by Activating Mitochondria. PLOS Biology. 2006;4(7):e226.
40. Alder A, Jamil M, Marzorati M, Bruno M, Vermathen M, Bigler P, et al. The Path from β-Carotene to Carlactone, a Strigolactone-Like Plant Hormone. Science. 2012;335(6074):1348-51.
41. Zhang Y, Van Dijk AD, Scaffidi A, Flematti GR, Hofmann M, Charnikhova T, et al. Rice cytochrome P450 MAX1 homologs catalyze distinct steps in strigolactone biosynthesis. Nature chemical biology. 2014;10(12):1028.
42. Abe S, Sado A, Tanaka K, Kisugi T, Asami K, Ota S, et al. Carlactone is converted to carlactonoic acid by MAX1 in Arabidopsis and its methyl ester can directly interact with AtD14 in vitro. Proceedings of the National Academy of Sciences. 2014;111(50):18084-9.
43. Mori N, Nishiuma K, Sugiyama T, Hayashi H, Akiyama K. Carlactone-type strigolactones and their synthetic analogues as inducers of hyphal branching in arbuscular mycorrhizal fungi. Phytochemistry. 2016;130:90-8.
44. Westwood JH. Characterization of the Orobanche–Arabidopsis system for studying parasite–host interactions. Weed Science. 2017;48(6):742-8.
45. Koltai H, LekKala SP, Bhattacharya C, Mayzlish-Gati E, Resnick N, Wininger S, et al. A tomato strigolactone-impaired mutant displays aberrant shoot morphology and plant interactions. Journal of Experimental Botany. 2010;61(6):1739-49.
46. Gomez-Roldan V, Fermas S, Brewer PB, Puech-Pagès V, Dun EA, Pillot J-P, et al. Strigolactone inhibition of shoot branching. Nature. 2008;455(7210):189-94.
47. Kobae Y, Kameoka H, Sugimura Y, Saito K, Ohtomo R, Fujiwara T, et al. Strigolactone Biosynthesis Genes of Rice are Required for the Punctual Entry of Arbuscular Mycorrhizal Fungi into the Roots. Plant and Cell Physiology. 2018;59(3):544-53.
48. Kretzschmar T, Kohlen W, Sasse J, Borghi L, Schlegel M, Bachelier JB, et al. A petunia ABC protein controls strigolactone-dependent symbiotic signalling and branching. Nature. 2012;483(7389):341-4.
49. Simonetti N, Strippoli V, Cassone A. Yeast-mycelial conversion induced by N-acetyl-D-glucosamine in Candida albicans. Nature. 1974;250(5464):344-6.
50. Konopka JB. N-acetylglucosamine functions in cell signaling. Scientifica. 2012;2012.
51. Alvarez FJ, Konopka JB. Identification of an N-Acetylglucosamine Transporter That Mediates Hyphal Induction in Candida albicans. Molecular Biology of the Cell. 2007;18(3):965-75.
52. Boulanger A, Zischek C, Lautier M, Jamet S, Rival P, Carrère S, et al. The plant pathogen Xanthomonas campestris pv. campestris exploits N-acetylglucosamine during infection. MBio. 2014;5(5):e01527-14.

53. Scervino JM, Ponce MA, Erra-Bassells R, Vierheilig H, Ocampo JA, Godeas A. Flavonoids exhibit fungal species and genus specific effects on the presymbiotic growth of Gigaspora and Glomus. Mycological Research. 2005;109(7):789-94.
54. Bécard G, Douds DD, Pfeffer PE. Extensive In Vitro Hyphal Growth of Vesicular-Arbuscular Mycorrhizal Fungi in the Presence of CO2 and Flavonols. Applied and environmental microbiology. 1992;58(3):821-5.
55. Tsai SM, Phillips DA. Flavonoids released naturally from alfalfa promote development of symbiotic glomus spores in vitro. Applied and environmental microbiology. 1991;57(5):1485-8.
56. Larose G, Chênevert R, Moutoglis P, Gagné S, Piché Y, Vierheilig H. Flavonoid levels in roots of Medicago sativa are modulated by the developmental stage of the symbiosis and the root colonizing arbuscular mycorrhizal fungus. Journal of Plant Physiology. 2002;159(12):1329-39.
57. Scervino JM, Ponce MA, Erra-Bassells R, Bompadre J, Vierheilig H, Ocampo JA, et al. The effect of flavones and flavonols on colonization of tomato plants by arbuscular mycorrhizal fungi of the genera Gigaspora and Glomus. Canadian journal of microbiology. 2007;53(6):702-9.
58. Becard G, Taylor LP, Douds DD, Pfeffer PE, Doner LW. Flavonoids are not necessary plant signal compounds in arbuscular mycorrhizal symbioses. MPMI-Molecular Plant Microbe Interactions. 1995;8(2):252-8.
59. Nagahashi G, Douds DD. The effects of hydroxy fatty acids on the hyphal branching of germinated spores of AM fungi. Fungal Biology. 2011;115(4):351-8.
60. Kameoka H, Tsutsui I, Saito K, Kikuchi Y, Handa Y, Ezawa T, et al. Stimulation of asymbiotic sporulation in arbuscular mycorrhizal fungi by fatty acids. Nature Microbiology. 2019;4(10):1654-60.
61. Genre A, Chabaud M, Balzergue C, Puech-Pagès V, Novero M, Rey T, et al. Short-chain chitin oligomers from arbuscular mycorrhizal fungi trigger nuclear Ca2+ spiking in Medicago truncatula roots and their production is enhanced by strigolactone. New Phytologist. 2013;198(1):190-202.
62. Maillet F, Poinsot V, André O, Puech-Pagès V, Haouy A, Gueunier M, et al. Fungal lipochitooligosaccharide symbiotic signals in arbuscular mycorrhiza. Nature. 2011;469(7328):58-63.
63. Tsuzuki S, Handa Y, Takeda N, Kawaguchi M. Strigolactone-Induced Putative Secreted Protein 1 Is Required for the Establishment of Symbiosis by the Arbuscular Mycorrhizal Fungus Rhizophagus irregularis. Molecular Plant-Microbe Interactions®. 2016;29(4):277-86.
64. Newman M-A, Sundelin T, Nielsen J, Erbs G. MAMP (microbe-associated molecular pattern) triggered immunity in plants. Frontiers in Plant Science. 2013;4(139).
65. Boller T, Felix G. A renaissance of elicitors: perception of microbe-associated molecular patterns and danger signals by pattern-recognition receptors. Annual review of plant biology. 2009;60:379-406.
66. Gow NAR, Latge J-P, Munro CA. The Fungal Cell Wall: Structure, Biosynthesis, and Function. Microbiology Spectrum. 2017;5(3).
67. Liu T, Liu Z, Song C, Hu Y, Han Z, She J, et al. Chitin-induced dimerization activates a plant immune receptor. Science. 2012;336(6085):1160-4.
68. Couto D, Zipfel C. Regulation of pattern recognition receptor signalling in plants. Nature Reviews Immunology. 2016;16(9):537-52.

69. Griesmann M, Chang Y, Liu X, Song Y, Haberer G, Crook MB, et al. Phylogenomics reveals multiple losses of nitrogen-fixing root nodule symbiosis. Science. 2018;361(6398):eaat1743.
70. Gobbato E. Recent developments in arbuscular mycorrhizal signaling. Current Opinion in Plant Biology. 2015;26:1-7.
71. Stracke S, Kistner C, Yoshida S, Mulder L, Sato S, Kaneko T, et al. A plant receptor-like kinase required for both bacterial and fungal symbiosis. Nature. 2002;417(6892):959-62.
72. Czaja LF, Hogekamp C, Lamm P, Maillet F, Martinez EA, Samain E, et al. Transcriptional responses toward diffusible signals from symbiotic microbes reveal MtNFP-and MtDMI3-dependent reprogramming of host gene expression by arbuscular mycorrhizal fungal lipochitooligosaccharides. Plant Physiology. 2012;159(4):1671-85.
73. Charpentier M, Sun J, Martins TV, Radhakrishnan GV, Findlay K, Soumpourou E, et al. Nuclear-localized cyclic nucleotide–gated channels mediate symbiotic calcium oscillations. Science. 2016;352(6289):1102-5.
74. Charpentier M, Bredemeier R, Wanner G, Takeda N, Schleiff E, Parniske M. Lotus japonicus CASTOR and POLLUX Are Ion Channels Essential for Perinuclear Calcium Spiking in Legume Root Endosymbiosis. The Plant Cell. 2008;20(12):3467-79.
75. Mitra RM, Gleason CA, Edwards A, Hadfield J, Downie JA, Oldroyd GED, et al. A Ca2+calmodulin-dependent protein kinase required for symbiotic nodule development: Gene identification by transcript-based cloning. Proceedings of the National Academy of Sciences of the United States of America. 2004;101(13):4701-5.
76. Messinese E, Mun J-H, Yeun LH, Jayaraman D, Rougé P, Barre A, et al. A Novel Nuclear Protein Interacts With the Symbiotic DMI3 Calcium- and Calmodulin-Dependent Protein Kinase of Medicago truncatula. Molecular Plant-Microbe Interactions®. 2007;20(8):912-21.
77. Yano K, Yoshida S, Müller J, Singh S, Banba M, Vickers K, et al. CYCLOPS, a mediator of symbiotic intracellular accommodation. Proceedings of the National Academy of Sciences. 2008;105(51):20540-5.
78. Genre A, Chabaud M, Faccio A, Barker DG, Bonfante P. Prepenetration Apparatus Assembly Precedes and Predicts the Colonization Patterns of Arbuscular Mycorrhizal Fungi within the Root Cortex of Both Medicago truncatula and Daucus carota. The Plant Cell. 2008;20(5):1407-20.
79. Oldroyd GE, Murray JD, Poole PS, Downie JA. The rules of engagement in the legume-rhizobial symbiosis. Annual review of genetics. 2011;45:119-44.
80. Parniske M. Intracellular accommodation of microbes by plants: a common developmental program for symbiosis and disease? Current Opinion in Plant Biology. 2000;3(4):320-8.
81. Zhang X, Dong W, Sun J, Feng F, Deng Y, He Z, et al. The receptor kinase CERK1 has dual functions in symbiosis and immunity signalling. The Plant Journal. 2015;81(2):258-67.
82. Miyata K, Kozaki T, Kouzai Y, Ozawa K, Ishii K, Asamizu E, et al. The bifunctional plant receptor, OsCERK1, regulates both chitin-triggered immunity and arbuscular mycorrhizal symbiosis in rice. Plant and Cell Physiology. 2014;55(11):1864-72.
83. Carotenuto G, Chabaud M, Miyata K, Capozzi M, Takeda N, Kaku H, et al. The rice LysM receptor-like kinase Os CERK 1 is required for the perception of short-chain chitin oligomers in arbuscular mycorrhizal signaling. New Phytologist. 2017;214(4):1440-6.
84. Kaku H, Nishizawa Y, Ishii-Minami N, Akimoto-Tomiyama C, Dohmae N, Takio K, et al. Plant cells recognize chitin fragments for defense signaling through a plasma membrane receptor. Proceedings of the National Academy of Sciences. 2006;103(29):11086-91.

85. Somers DE, Fujiwara S. Thinking outside the F-box: novel ligands for novel receptors. Trends in plant science. 2009;14(4):206-13.
86. Nakamura H, Xue Y-L, Miyakawa T, Hou F, Qin H-M, Fukui K, et al. Molecular mechanism of strigolactone perception by DWARF14. Nature Communications. 2013;4(1):2613.
87. Stirnberg P, van De Sande K, Leyser HO. MAX1 and MAX2 control shoot lateral branching in Arabidopsis. Development. 2002;129(5):1131-41.
88. Ishikawa S, Maekawa M, Arite T, Onishi K, Takamure I, Kyozuka J. Suppression of Tiller Bud Activity in Tillering Dwarf Mutants of Rice. Plant and Cell Physiology. 2005;46(1):79-86.
89. Toh S, Holbrook-Smith D, Stokes Michael E, Tsuchiya Y, McCourt P. Detection of Parasitic Plant Suicide Germination Compounds Using a High-Throughput Arabidopsis HTL/KAI2 Strigolactone Perception System. Chemistry & Biology. 2014;21(8):988-98.
90. Waters MT, Nelson DC, Scaffidi A, Flematti GR, Sun YK, Dixon KW, et al. Specialisation within the DWARF14 protein family confers distinct responses to karrikins and strigolactones in Arabidopsis. Development. 2012;139(7):1285-95.
91. Gutjahr C, Gobbato E, Choi J, Riemann M, Johnston MG, Summers W, et al. Rice perception of symbiotic arbuscular mycorrhizal fungi requires the karrikin receptor complex. Science. 2015;350(6267):1521-4.
92. Conn CE, Nelson DC. Evidence that KARRIKIN-INSENSITIVE2 (KAI2) Receptors may Perceive an Unknown Signal that is not Karrikin or Strigolactone. Frontiers in Plant Science. 2016;6(1219).
93. Flematti GR, Waters MT, Scaffidi A, Merritt DJ, Ghisalberti EL, Dixon KW, et al. Karrikin and Cyanohydrin Smoke Signals Provide Clues to New Endogenous Plant Signaling Compounds. Molecular Plant. 2013;6(1):29-37.
94. Giovanetti M, Sbrana C, Avio L, Citernesi AS, Logi C. Differential hyphal morphogenesis in arbuscular mycorrhizal fungi during pre-infection stages. New Phytologist. 1993;125(3):587-93.
95. Parniske M. Arbuscular mycorrhiza: the mother of plant root endosymbioses. Nature Reviews Microbiology. 2008;6(10):763-75.
96. Genre A, Chabaud M, Timmers T, Bonfante P, Barker DG. Arbuscular Mycorrhizal Fungi Elicit a Novel Intracellular Apparatus in Medicago truncatula Root Epidermal Cells before Infection. The Plant Cell. 2005;17(12):3489-99.
97. Dickson S, Smith FA, Smith SE. Structural differences in arbuscular mycorrhizal symbioses: more than 100 years after Gallaud, where next? Mycorrhiza. 2007;17(5):375-93.
98. Hong JJ, Park Y-S, Bravo A, Bhattarai KK, Daniels DA, Harrison MJ. Diversity of morphology and function in arbuscular mycorrhizal symbioses in Brachypodium distachyon. Planta. 2012;236(3):851-65.
99. Pumplin N, Harrison MJ. Live-Cell Imaging Reveals Periarbuscular Membrane Domains and Organelle Location in Medicago truncatula Roots during Arbuscular Mycorrhizal Symbiosis. Plant Physiology. 2009;151(2):809-19.
100. Toth R, Miller RM. Dynamics of arbuscule development and degeneration in a Zea mays mycorrhiza. American Journal of Botany. 1984;71(4):449-60.
101. Harrison MJ, Dewbre GR, Liu J. A Phosphate Transporter from Medicago truncatula Involved in the Acquisition of Phosphate Released by Arbuscular Mycorrhizal Fungi. The Plant Cell. 2002;14(10):2413-29.

102. Pumplin N, Zhang X, Noar RD, Harrison MJ. Polar localization of a symbiosis-specific phosphate transporter is mediated by a transient reorientation of secretion. Proceedings of the National Academy of Sciences. 2012;109(11):E665-E72.
103. Harrison MJ. Molecular and cellular aspects of the arbuscular mycorrhizal symbiosis. Annual review of plant biology. 1999;50(1):361-89.
104. Alexander T, Toth R, Meier R, Weber HC. Dynamics of arbuscule development and degeneration in onion, bean, and tomato with reference to vesicular–arbuscular mycorrhizae in grasses. Canadian Journal of Botany. 1989;67(8):2505-13.
105. Kobae Y, Hata S. Dynamics of Periarbuscular Membranes Visualized with a Fluorescent Phosphate Transporter in Arbuscular Mycorrhizal Roots of Rice. Plant and Cell Physiology. 2010;51(3):341-53.
106. Floss DS, Gomez SK, Park H-J, MacLean AM, Müller LM, Bhattarai KK, et al. A Transcriptional Program for Arbuscule Degeneration during AM Symbiosis Is Regulated by MYB1. Current Biology. 2017;27(8):1206-12.
107. Roth R, Paszkowski U. Plant carbon nourishment of arbuscular mycorrhizal fungi. Current Opinion in Plant Biology. 2017;39:50-6.
108. Beilby JP, Kidby DK. Biochemistry of ungerminated and germinated spores of the vesicular-arbuscular mycorrhizal fungus, Glomus caledonius: changes in neutral and polar lipids. Journal of Lipid Research. 1980;21(6):739-50.
109. Marleau J, Dalpé Y, St-Arnaud M, Hijri M. Spore development and nuclear inheritance in arbuscular mycorrhizal fungi. BMC Evolutionary Biology. 2011;11(1):51.
110. Jakobsen I, Abbott LK, Robson AD. External hyphae of vesicular-arbuscular mycorrhizal fungi associated with Trifolium subterraneum L. New Phytologist. 1992;120(3):371-80.
111. Sawers RJH, Svane SF, Quan C, Grønlund M, Wozniak B, Gebreselassie M-N, et al. Phosphorus acquisition efficiency in arbuscular mycorrhizal maize is correlated with the abundance of root-external hyphae and the accumulation of transcripts encoding PHT1 phosphate transporters. New Phytologist. 2017;214(2):632-43.
112. Martin F. Molecular mycorrhizal symbiosis: John Wiley & Sons; 2016.
113. Kikuchi Y, Hijikata N, Yokoyama K, Ohtomo R, Handa Y, Kawaguchi M, et al. Polyphosphate accumulation is driven by transcriptome alterations that lead to near-synchronous and near-equivalent uptake of inorganic cations in an arbuscular mycorrhizal fungus. New Phytologist. 2014;204(3):638-49.
114. Hothorn M, Neumann H, Lenherr ED, Wehner M, Rybin V, Hassa PO, et al. Catalytic Core of a Membrane-Associated Eukaryotic Polyphosphate Polymerase. Science. 2009;324(5926):513-6.
115. Hijikata N, Murase M, Tani C, Ohtomo R, Osaki M, Ezawa T. Polyphosphate has a central role in the rapid and massive accumulation of phosphorus in extraradical mycelium of an arbuscular mycorrhizal fungus. New Phytologist. 2010;186(2):285-9.
116. Kikuchi Y, Hijikata N, Ohtomo R, Handa Y, Kawaguchi M, Saito K, et al. Aquaporin-mediated long-distance polyphosphate translocation directed towards the host in arbuscular mycorrhizal symbiosis: application of virus-induced gene silencing. New Phytologist. 2016;211(4):1202-8.
117. Kojima T, Saito M. Possible involvement of hyphal phosphatase in phosphate efflux from intraradical hyphae isolated from mycorrhizal roots colonized by Gigaspora margarita. Mycological research. 2004;108(6):610-5.
118. Ohtomo R, Saito M. Polyphosphate dynamics in mycorrhizal roots during colonization of an arbuscular mycorrhizal fungus. New Phytologist. 2005;167(2):571-8.

119. Ezawa T, Saito K. How do arbuscular mycorrhizal fungi handle phosphate? New insight into fine-tuning of phosphate metabolism. New Phytologist. 2018;220(4):1116-21.
120. Rausch C, Bucher M. Molecular mechanisms of phosphate transport in plants. Planta. 2002;216(1):23-37.
121. Paszkowski U, Kroken S, Roux C, Briggs SP. Rice phosphate transporters include an evolutionarily divergent gene specifically activated in arbuscular mycorrhizal symbiosis. Proceedings of the National Academy of Sciences. 2002;99(20):13324-9.
122. Javot H, Penmetsa RV, Terzaghi N, Cook DR, Harrison MJ. A Medicago truncatula phosphate transporter indispensable for the arbuscular mycorrhizal symbiosis. Proceedings of the National Academy of Sciences. 2007;104(5):1720-5.
123. Yang S-Y, Grønlund M, Jakobsen I, Grotemeyer MS, Rentsch D, Miyao A, et al. Nonredundant Regulation of Rice Arbuscular Mycorrhizal Symbiosis by Two Members of the PHOSPHATE TRANSPORTER1 Gene Family. The Plant Cell. 2012;24(10):4236-51.
124. Govindarajulu M, Pfeffer PE, Jin H, Abubaker J, Douds DD, Allen JW, et al. Nitrogen transfer in the arbuscular mycorrhizal symbiosis. Nature. 2005;435(7043):819-23.
125. Cruz C, Egsgaard H, Trujillo C, Ambus P, Requena N, Martins-Loução MA, et al. Enzymatic Evidence for the Key Role of Arginine in Nitrogen Translocation by Arbuscular Mycorrhizal Fungi. Plant Physiology. 2007;144(2):782-92.
126. Kobae Y, Tamura Y, Takai S, Banba M, Hata S. Localized Expression of Arbuscular Mycorrhiza-Inducible Ammonium Transporters in Soybean. Plant and Cell Physiology. 2010;51(9):1411-5.
127. Koegel S, Ait Lahmidi N, Arnould C, Chatagnier O, Walder F, Ineichen K, et al. The family of ammonium transporters (AMT) in Sorghum bicolor: two AMT members are induced locally, but not systemically in roots colonized by arbuscular mycorrhizal fungi. New Phytologist. 2013;198(3):853-65.
128. Breuillin-Sessoms F, Floss DS, Gomez SK, Pumplin N, Ding Y, Levesque-Tremblay V, et al. Suppression of Arbuscule Degeneration in Medicago truncatula phosphate transporter4 Mutants Is Dependent on the Ammonium Transporter 2 Family Protein AMT2;3. The Plant Cell. 2015;27(4):1352-66.
129. Javot H, Penmetsa RV, Breuillin F, Bhattarai KK, Noar RD, Gomez SK, et al. Medicago truncatula mtpt4 mutants reveal a role for nitrogen in the regulation of arbuscule degeneration in arbuscular mycorrhizal symbiosis. The Plant Journal. 2011;68(6):954-65.
130. Jakobsen I, Rosendahl L. Carbon flow into soil and external hyphae from roots of mycorrhizal cucumber plants. New Phytologist. 1990;115(1):77-83.
131. Solaiman MZ, Saito M. Use of sugars by intraradical hyphae of arbuscular mycorrhizal fungi revealed by radiorespirometry. The New Phytologist. 1997;136(3):533-8.
132. Pfeffer PE, Douds DD, Bécard G, Shachar-Hill Y. Carbon Uptake and the Metabolism and Transport of Lipids in an Arbuscular Mycorrhiza. Plant Physiology. 1999;120(2):587-98.
133. Douds DD, Pfeffer PE, Shachar-Hill Y. Carbon partitioning, cost, and metabolism of arbuscular mycorrhizas. Arbuscular mycorrhizas: physiology and function: Springer; 2000. p. 107-29.
134. Helber N, Wippel K, Sauer N, Schaarschmidt S, Hause B, Requena N. A Versatile Monosaccharide Transporter That Operates in the Arbuscular Mycorrhizal Fungus Glomus sp Is Crucial for the Symbiotic Relationship with Plants. The Plant Cell. 2011;23(10):3812-23.
135. Ait Lahmidi N, Courty P-E, Brulé D, Chatagnier O, Arnould C, Doidy J, et al. Sugar exchanges in arbuscular mycorrhiza: RiMST5 and RiMST6, two novel Rhizophagus irregularis

monosaccharide transporters, are involved in both sugar uptake from the soil and from the plant partner. Plant Physiology and Biochemistry. 2016;107:354-63.
136. Bago B, Pfeffer PE, Shachar-Hill Y. Carbon Metabolism and Transport in Arbuscular Mycorrhizas. Plant Physiology. 2000;124(3):949-58.
137. Schaarschmidt S, Hause B. Apoplastic invertases. Plant Signaling & Behavior. 2008;3(5):317-9.
138. Manck-Götzenberger J, Requena N. Arbuscular mycorrhiza symbiosis induces a major transcriptional reprogramming of the potato SWEET sugar transporter family. Frontiers in plant science. 2016;7:487.
139. Bago B, Pfeffer PE, Abubaker J, Jun J, Allen JW, Brouillette J, et al. Carbon export from arbuscular mycorrhizal roots involves the translocation of carbohydrate as well as lipid. Plant physiology. 2003;131(3):1496-507.
140. Bago B, Zipfel W, Williams RM, Jun J, Arreola R, Lammers PJ, et al. Translocation and Utilization of Fungal Storage Lipid in the Arbuscular Mycorrhizal Symbiosis. Plant Physiology. 2002;128(1):108-24.
141. Trépanier M, Bécard G, Moutoglis P, Willemot C, Gagné S, Avis TJ, et al. Dependence of arbuscular-mycorrhizal fungi on their plant host for palmitic acid synthesis. Appl Environ Microbiol. 2005;71(9):5341-7.
142. Madan R, Pankhurst C, Hawke B, Smith S. Use of fatty acids for identification of AM fungi and estimation of the biomass of AM spores in soil. Soil Biology and Biochemistry. 2002;34(1):125-8.
143. Wewer V, Brands M, Dörmann P. Fatty acid synthesis and lipid metabolism in the obligate biotrophic fungus Rhizophagus irregularis during mycorrhization of Lotus japonicus. The Plant Journal. 2014;79(3):398-412.
144. Jenni S, Leibundgut M, Boehringer D, Frick C, Mikolásek B, Ban N. Structure of Fungal Fatty Acid Synthase and Implications for Iterative Substrate Shuttling. Science. 2007;316(5822):254-61.
145. Reich M, xf, bel C, Kohler A, Bu, xe, et al. Fatty Acid Metabolism in the Ectomycorrhizal Fungus Laccaria bicolor. The New Phytologist. 2009;182(4):950-64.
146. Smith S, Witkowski A, Joshi AK. Structural and functional organization of the animal fatty acid synthase. Progress in Lipid Research. 2003;42(4):289-317.
147. Teichmann B, Linne U, Hewald S, Marahiel MA, Bölker M. A biosynthetic gene cluster for a secreted cellobiose lipid with antifungal activity from Ustilago maydis. Molecular Microbiology. 2007;66(2):525-33.
148. Tang N, San Clemente H, Roy S, Bécard G, Zhao B, Roux C. A survey of the gene repertoire of Gigaspora rosea unravels conserved features among Glomeromycota for obligate biotrophy. Frontiers in microbiology. 2016;7:233.
149. Tisserant E, Malbreil M, Kuo A, Kohler A, Symeonidi A, Balestrini R, et al. Genome of an arbuscular mycorrhizal fungus provides insight into the oldest plant symbiosis. Proceedings of the National Academy of Sciences. 2013;110(50):20117-22.
150. Trépanier M, Bécard G, Moutoglis P, Willemot C, Gagné S, Avis TJ, et al. Dependence of Arbuscular-Mycorrhizal Fungi on Their Plant Host for Palmitic Acid Synthesis. Applied and Environmental Microbiology. 2005;71(9):5341-7.
151. Li-Beisson Y, Shorrosh B, Beisson F, Andersson MX, Arondel V, Bates PD, et al. Acyl-lipid metabolism. Arabidopsis Book. 2013;11:e0161-e.

152. Groth M, Kosuta S, Gutjahr C, Haage K, Hardel SL, Schaub M, et al. Two Lotus japonicus symbiosis mutants impaired at distinct steps of arbuscule development. The Plant Journal. 2013;75(1):117-29.
153. Keymer A, Pimprikar P, Wewer V, Huber C, Brands M, Bucerius SL, et al. Lipid transfer from plants to arbuscular mycorrhiza fungi. bioRxiv. 2017:143883.
154. Bravo A, York T, Pumplin N, Mueller LA, Harrison MJ. Genes conserved for arbuscular mycorrhizal symbiosis identified through phylogenomics. Nature Plants. 2016;2(2):15208.
155. Jones A, Davies HM, Voelker TA. Palmitoyl-acyl carrier protein (ACP) thioesterase and the evolutionary origin of plant acyl-ACP thioesterases. The Plant Cell. 1995;7(3):359-71.
156. Bravo A, Brands M, Wewer V, Dörmann P, Harrison MJ. Arbuscular mycorrhiza-specific enzymes FatM and RAM2 fine-tune lipid biosynthesis to promote development of arbuscular mycorrhiza. New Phytologist. 2017;214(4):1631-45.
157. Brands M, Wewer V, Keymer A, Gutjahr C, Dörmann P. The Lotus japonicus acyl-acyl carrier protein thioesterase FatM is required for mycorrhiza formation and lipid accumulation of Rhizophagus irregularis. The Plant Journal. 2018;95(2):219-32.
158. Dormann P, Voelker TA, Ohlrogge JB. Cloning and expression in Escherichia coli of a novel thioesterase from Arabidopsis thaliana specific for long-chain acyl-acyl carrier proteins. Archives of Biochemistry and Biophysics. 1995;316(1):612-8.
159. Gobbato E, Marsh John F, Vernié T, Wang E, Maillet F, Kim J, et al. A GRAS-Type Transcription Factor with a Specific Function in Mycorrhizal Signaling. Current Biology. 2012;22(23):2236-41.
160. Jiang Y, Wang W, Xie Q, Liu N, Liu L, Wang D, et al. Plants transfer lipids to sustain colonization by mutualistic mycorrhizal and parasitic fungi. Science. 2017;356(6343):1172-5.
161. Wang E, Schornack S, Marsh John F, Gobbato E, Schwessinger B, Eastmond P, et al. A Common Signaling Process that Promotes Mycorrhizal and Oomycete Colonization of Plants. Current Biology. 2012;22(23):2242-6.
162. Gobbato E, Wang E, Higgins G, Bano SA, Henry C, Schultze M, et al. RAM1 and RAM2 function and expression during arbuscular mycorrhizal symbiosis and Aphanomyces euteiches colonization. Plant signaling & behavior. 2013;8(10):e26049.
163. Yang W, Simpson JP, Li-Beisson Y, Beisson F, Pollard M, Ohlrogge JB. A Land-Plant-Specific Glycerol-3-Phosphate Acyltransferase Family in Arabidopsis: Substrate Specificity, sn2 Preference, and Evolution. Plant Physiology. 2012;160(2):638-52.
164. Schreiber L. Transport barriers made of cutin, suberin and associated waxes. Trends in plant science. 2010;15(10):546-53.
165. Gutjahr C, Radovanovic D, Geoffroy J, Zhang Q, Siegler H, Chiapello M, et al. The half-size ABC transporters STR1 and STR2 are indispensable for mycorrhizal arbuscule formation in rice. The Plant Journal. 2012;69(5):906-20.
166. Zhang Q, Blaylock LA, Harrison MJ. Two Medicago truncatula half-ABC transporters are essential for arbuscule development in arbuscular mycorrhizal symbiosis. The Plant Cell. 2010;22(5):1483-97.
167. Yadav V, Molina I, Ranathunge K, Castillo IQ, Rothstein SJ, Reed JW. ABCG Transporters Are Required for Suberin and Pollen Wall Extracellular Barriers in Arabidopsis. The Plant Cell. 2014;26(9):3569-88.
168. Park H-J, Floss DS, Levesque-Tremblay V, Bravo A, Harrison MJ. Hyphal Branching during Arbuscule Development Requires Reduced Arbuscular Mycorrhiza1. Plant Physiology. 2015;169(4):2774-88.

169. Pimprikar P, Carbonnel S, Paries M, Katzer K, Klingl V, Bohmer Monica J, et al. A CCaMK-CYCLOPS-DELLA Complex Activates Transcription of RAM1 to Regulate Arbuscule Branching. Current Biology. 2016;26(8):987-98.
170. Luginbuehl LH, Menard GN, Kurup S, Van Erp H, Radhakrishnan GV, Breakspear A, et al. Fatty acids in arbuscular mycorrhizal fungi are synthesized by the host plant. Science. 2017;356(6343):1175-8.
171. Rey T, Bonhomme M, Chatterjee A, Gavrin A, Toulotte J, Yang W, et al. The Medicago truncatula GRAS protein RAD1 supports arbuscular mycorrhiza symbiosis and Phytophthora palmivora susceptibility. Journal of Experimental Botany. 2017;68(21-22):5871-81.
172. Xue L, Cui H, Buer B, Vijayakumar V, Delaux P-M, Junkermann S, et al. Network of GRAS Transcription Factors Involved in the Control of Arbuscule Development in Lotus japonicus. Plant Physiology. 2015;167(3):854-71.
173. Boon E, Halary S, Bapteste E, Hijri M. Studying Genome Heterogeneity within the Arbuscular Mycorrhizal Fungal Cytoplasm. Genome Biology and Evolution. 2015;7(2):505-21.
174. Lin K, Limpens E, Zhang Z, Ivanov S, Saunders DGO, Mu D, et al. Single Nucleus Genome Sequencing Reveals High Similarity among Nuclei of an Endomycorrhizal Fungus. PLOS Genetics. 2014;10(1):e1004078.
175. Ropars J, Corradi N. Homokaryotic vs heterokaryotic mycelium in arbuscular mycorrhizal fungi: different techniques, different results? New Phytologist. 2015;208(3):638-41.
176. Rosendahl S, Taylor JW. Development of multiple genetic markers for studies of genetic variation in arbuscular mycorrhizal fungi using AFLP™. Molecular Ecology. 1997;6(9):821-9.
177. Vandenkoornhuyse P, Leyval C, Bonnin I. High genetic diversity in arbuscular mycorrhizal fungi: evidence for recombination events. Heredity. 2001;87(2):243-53.
178. den Bakker HC, VanKuren NW, Morton JB, Pawlowska TE. Clonality and Recombination in the Life History of an Asexual Arbuscular Mycorrhizal Fungus. Molecular Biology and Evolution. 2010;27(11):2474-86.
179. Halary S, Malik S-B, Lildhar L, Slamovits CH, Hijri M, Corradi N. Conserved Meiotic Machinery in Glomus spp., a Putatively Ancient Asexual Fungal Lineage. Genome Biology and Evolution. 2011;3:950-8.
180. Mohanta TK, Bae H. The diversity of fungal genome. Biological Procedures Online. 2015;17(1):8.
181. Maeda T, Kobayashi Y, Kameoka H, Okuma N, Takeda N, Yamaguchi K, et al. Evidence of non-tandemly repeated rDNAs and their intragenomic heterogeneity in Rhizophagus irregularis. Communications Biology. 2018;1(1):87.
182. Chen ECH, Morin E, Beaudet D, Noel J, Yildirir G, Ndikumana S, et al. High intraspecific genome diversity in the model arbuscular mycorrhizal symbiont Rhizophagus irregularis. New Phytologist. 2018;220(4):1161-71.
183. Kobayashi Y, Maeda T, Yamaguchi K, Kameoka H, Tanaka S, Ezawa T, et al. The genome of Rhizophagus clarus HR1 reveals a common genetic basis for auxotrophy among arbuscular mycorrhizal fungi. BMC genomics. 2018;19(1):465.
184. Morin E, Miyauchi S, San Clemente H, Chen ECH, Pelin A, de la Providencia I, et al. Comparative genomics of Rhizophagus irregularis, R. cerebriforme, R. diaphanus and Gigaspora rosea highlights specific genetic features in Glomeromycotina. New Phytologist. 2019;222(3):1584-98.

185. Sun X, Chen W, Ivanov S, MacLean AM, Wight H, Ramaraj T, et al. Genome and evolution of the arbuscular mycorrhizal fungus Diversispora epigaea (formerly Glomus versiforme) and its bacterial endosymbionts. New Phytologist. 2019;221(3):1556-73.
186. Tisserant E, Kohler A, Dozolme-Seddas P, Balestrini R, Benabdellah K, Colard A, et al. The transcriptome of the arbuscular mycorrhizal fungus Glomus intraradices (DAOM 197198) reveals functional tradeoffs in an obligate symbiont. New Phytologist. 2012;193(3):755-69.
187. Salvioli A, Ghignone S, Novero M, Navazio L, Venice F, Bagnaresi P, et al. Symbiosis with an endobacterium increases the fitness of a mycorrhizal fungus, raising its bioenergetic potential. The ISME Journal. 2016;10(1):130-44.
188. Sugimura Y, Saito K. Transcriptional profiling of arbuscular mycorrhizal roots exposed to high levels of phosphate reveals the repression of cell cycle-related genes and secreted protein genes in Rhizophagus irregularis. Mycorrhiza. 2017;27(2):139-46.
189. Handa Y, Nishide H, Takeda N, Suzuki Y, Kawaguchi M, Saito K. RNA-seq Transcriptional Profiling of an Arbuscular Mycorrhiza Provides Insights into Regulated and Coordinated Gene Expression in Lotus japonicus and Rhizophagus irregularis. Plant and Cell Physiology. 2015;56(8):1490-511.
190. Presti LL, Lanver D, Schweizer G, Tanaka S, Liang L, Tollot M, et al. Fungal Effectors and Plant Susceptibility. Annual Review of Plant Biology. 2015;66(1):513-45.
191. Kamel L, Tang N, Malbreil M, San Clemente H, Le Marquer M, Roux C, et al. The Comparison of Expressed Candidate Secreted Proteins from Two Arbuscular Mycorrhizal Fungi Unravels Common and Specific Molecular Tools to Invade Different Host Plants. Frontiers in plant science. 2017;8:124-.
192. Prasad Singh P, Srivastava D, Jaiswar A, Adholeya A. Effector proteins of Rhizophagus proliferus: conserved protein domains may play a role in host-specific interaction with different plant species. Brazilian Journal of Microbiology. 2019;50(3):593-601.
193. Sędzielewska Toro K, Brachmann A. The effector candidate repertoire of the arbuscular mycorrhizal fungus Rhizophagus clarus. BMC Genomics. 2016;17(1):101.
194. Zeng T, Holmer R, Hontelez J, te Lintel-Hekkert B, Marufu L, de Zeeuw T, et al. Host- and stage-dependent secretome of the arbuscular mycorrhizal fungus Rhizophagus irregularis. The Plant Journal. 2018;94(3):411-25.
195. Kloppholz S, Kuhn H, Requena N. A Secreted Fungal Effector of Glomus intraradices Promotes Symbiotic Biotrophy. Current Biology. 2011;21(14):1204-9.
196. Zeng T, Holmer R, Hontelez J, te Lintel-Hekkert B, Marufu L, de Zeeuw T, et al. Host- and stage-dependent secretome of the arbuscular mycorrhizal fungus Rhizophagus irregularis. The Plant Journal. 2018;94(3):411-25.
197. Schmitz AM, Pawlowska TE, Harrison MJ. A short LysM protein with high molecular diversity from an arbuscular mycorrhizal fungus, Rhizophagus irregularis. Mycoscience. 2019;60(1):63-70.
198. Voß S, Betz R, Heidt S, Corradi N, Requena N. RiCRN1, a Crinkler Effector From the Arbuscular Mycorrhizal Fungus Rhizophagus irregularis, Functions in Arbuscule Development. Frontiers in Microbiology. 2018;9(2068).
199. Seddas PMA, Arnould C, Tollot M, Arias CM, Gianinazzi-Pearson V. Spatial monitoring of gene activity in extraradical and intraradical developmental stages of arbuscular mycorrhizal fungi by direct fluorescent in situ RT-PCR. Fungal Genetics and Biology. 2008;45(8):1155-65.
200. Maldonado-Mendoza IE, Dewbre GR, Harrison MJ. A Phosphate Transporter Gene from the Extra-Radical Mycelium of an Arbuscular Mycorrhizal Fungus Glomus intraradices Is

Regulated in Response to Phosphate in the Environment. Molecular Plant-Microbe Interactions®. 2001;14(10):1140-8.
201. López-Pedrosa A, González-Guerrero M, Valderas A, Azcón-Aguilar C, Ferrol N. GintAMT1 encodes a functional high-affinity ammonium transporter that is expressed in the extraradical mycelium of Glomus intraradices. Fungal Genetics and Biology. 2006;43(2):102-10.
202. Pérez-Tienda J, Testillano PS, Balestrini R, Fiorilli V, Azcón-Aguilar C, Ferrol N. GintAMT2, a new member of the ammonium transporter family in the arbuscular mycorrhizal fungus Glomus intraradices. Fungal Genetics and Biology. 2011;48(11):1044-55.
203. Ahringer J. Reverse genetics. WormBook: The Online Review of C elegans Biology [Internet]: WormBook; 2006.
204. Forbes PJ, Millam S, Hooker JE, Harrier LA. Transformation of the arbuscular mycorrhiza Gigaspora rosea by particle bombardment. Mycological Research. 1998;102(4):497-501.
205. Harrier LA, Millam S. Biolistic transformation of arbuscular mycorrhizal fungi. Molecular Biotechnology. 2001;18(1):25-33.
206. Helber N, Requena N. Expression of the fluorescence markers DsRed and GFP fused to a nuclear localization signal in the arbuscular mycorrhizal fungus Glomus intraradices. New Phytologist. 2008;177(2):537-48.
207. Sun Z, Song J, Xin Xa, Xie X, Zhao B. Arbuscular Mycorrhizal Fungal 14-3-3 Proteins Are Involved in Arbuscule Formation and Responses to Abiotic Stresses During AM Symbiosis. Frontiers in Microbiology. 2018;9(91).
208. Tian C, Kasiborski B, Koul R, Lammers PJ, Bücking H, Shachar-Hill Y. Regulation of the Nitrogen Transfer Pathway in the Arbuscular Mycorrhizal Symbiosis: Gene Characterization and the Coordination of Expression with Nitrogen Flux. Plant Physiology. 2010;153(3):1175-87.
209. Wong Sak Hoi J, Dumas B. Ste12 and Ste12-Like Proteins, Fungal Transcription Factors Regulating Development and Pathogenicity. Eukaryotic Cell. 2010;9(4):480-5.
210. Horbach R, Navarro-Quesada AR, Knogge W, Deising HB. When and how to kill a plant cell: Infection strategies of plant pathogenic fungi. Journal of Plant Physiology. 2011;168(1):51-62.
211. Tollot M, Wong Sak Hoi J, Van Tuinen D, Arnould C, Chatagnier O, Dumas B, et al. An STE12 gene identified in the mycorrhizal fungus Glomus intraradices restores infectivity of a hemibiotrophic plant pathogen. New Phytologist. 2009;181(3):693-707.
212. Fiorilli V, Belmondo S, Khouja HR, Abbà S, Faccio A, Daghino S, et al. RiPEIP1, a gene from the arbuscular mycorrhizal fungus Rhizophagus irregularis, is preferentially expressed in planta and may be involved in root colonization. Mycorrhiza. 2016;26(6):609-21.
213. Recorbet G, Rogniaux H, Gianinazzi-Pearson V, DumasGaudot E. Fungal proteins in the extra-radical phase of arbuscular mycorrhiza: a shotgun proteomic picture. New Phytologist. 2009;181(2):248-60.
214. Vannini C, Carpentieri A, Salvioli A, Novero M, Marsoni M, Testa L, et al. An interdomain network: the endobacterium of a mycorrhizal fungus promotes antioxidative responses in both fungal and plant hosts. New Phytologist. 2016;211(1):265-75.
215. Murphy CL, Youssef NH, Hartson S, Elshahed MS. The extraradical proteins of Rhizophagus irregularis: A shotgun proteomics approach. Fungal Biology. 2020;124(2):91-101.

216. Roth R, Chiapello M, Montero H, Gehrig P, Grossmann J, O'Holleran K, et al. A rice Serine/Threonine receptor-like kinase regulates arbuscular mycorrhizal symbiosis at the peri-arbuscular membrane. Nature Communications. 2018;9(1):4677.
217. Dowswell C. Maize in the third world: CRC Press; 2019.
218. Rodriguez A, Sanders IR. The role of community and population ecology in applying mycorrhizal fungi for improved food security. The ISME journal. 2015;9(5):1053-61.
219. Igiehon NO, Babalola OO. Biofertilizers and sustainable agriculture: exploring arbuscular mycorrhizal fungi. Applied Microbiology and Biotechnology. 2017;101(12):4871-81.
220. Jiao Y, Peluso P, Shi J, Liang T, Stitzer MC, Wang B, et al. Improved maize reference genome with single-molecule technologies. Nature. 2017;546(7659):524-7.
221. Schnable PS, Ware D, Fulton RS, Stein JC, Wei F, Pasternak S, et al. The B73 Maize Genome: Complexity, Diversity, and Dynamics. Science. 2009;326(5956):1112-5.
222. Springer NM, Anderson SN, Andorf CM, Ahern KR, Bai F, Barad O, et al. The maize W22 genome provides a foundation for functional genomics and transposon biology. Nature Genetics. 2018;50(9):1282-8.
223. Yang N, Liu J, Gao Q, Gui S, Chen L, Yang L, et al. Genome assembly of a tropical maize inbred line provides insights into structural variation and crop improvement. Nature Genetics. 2019;51(6):1052-9.
224. Sun S, Zhou Y, Chen J, Shi J, Zhao H, Zhao H, et al. Extensive intraspecific gene order and gene structural variations between Mo17 and other maize genomes. Nature Genetics. 2018;50(9):1289-95.
225. Chilcoat D, Liu Z-B, Sander J. Chapter Two - Use of CRISPR/Cas9 for Crop Improvement in Maize and Soybean. In: Weeks DP, Yang B, editors. Progress in Molecular Biology and Translational Science. 149: Academic Press; 2017. p. 27-46.
226. Svitashev S, Schwartz C, Lenderts B, Young JK, Mark Cigan A. Genome editing in maize directed by CRISPR–Cas9 ribonucleoprotein complexes. Nature Communications. 2016;7(1):13274.
227. Nagy R, Vasconcelos M, Zhao S, McElver J, Bruce W, Amrhein N, et al. Differential regulation of five Pht1 phosphate transporters from maize (Zea mays L.). Plant Biology. 2006;8(02):186-97.
228. Glassop D, Smith SE, Smith FW. Cereal phosphate transporters associated with the mycorrhizal pathway of phosphate uptake into roots. Planta. 2005;222(4):688-98.
229. Liu F, Xu Y, Han G, Wang W, Li X, Cheng B. Identification and Functional Characterization of a Maize Phosphate Transporter Induced by Mycorrhiza Formation. Plant and Cell Physiology. 2018;59(8):1683-94.
230. Kaeppler SM, Parke JL, Mueller SM, Senior L, Stuber C, Tracy WF. Variation among Maize Inbred Lines and Detection of Quantitative Trait Loci for Growth at Low Phosphorus and Responsiveness to Arbuscular Mycorrhizal Fungi Work supported by USDA-Hatch, University of Wisconsin University-Industry Relations, and Cargill Fertilizer. Crop Science. 2000;40(2):358-64.
231. Quiroga G, Erice G, Aroca R, Zamarreño ÁM, García-Mina JM, Ruiz-Lozano JM. Radial water transport in arbuscular mycorrhizal maize plants under drought stress conditions is affected by indole-acetic acid (IAA) application. Journal of Plant Physiology. 2020;246-247:153115.
232. Ramírez-Flores MR, Bello-Bello E, Rellán-Álvarez R, Sawers RJH, Olalde-Portugal V. Inoculation with the mycorrhizal fungus Rhizophagus irregularis modulates the relationship

between root growth and nutrient content in maize (Zea mays ssp. mays L.). Plant Direct. 2019;3(12):e00192.
233. Ramírez-Flores MR, Rellán-Álvarez R, Wozniak B, Gebreselassie M-N, Jakobsen I, Olalde-Portugal V, et al. Co-ordinated Changes in the Accumulation of Metal Ions in Maize (Zea mays ssp. mays L.) in Response to Inoculation with the Arbuscular Mycorrhizal Fungus Funneliformis mosseae. Plant and Cell Physiology. 2017;58(10):1689-99.
234. Gaut BS, Doebley JF. DNA sequence evidence for the segmental allotetraploid origin of maize. Proceedings of the National Academy of Sciences. 1997;94(13):6809-14.
235. Schnable JC, Springer NM, Freeling M. Differentiation of the maize subgenomes by genome dominance and both ancient and ongoing gene loss. Proceedings of the National Academy of Sciences. 2011;108(10):4069-74.
236. Chandler VL, Hardeman KJ. The Mu Elements of Zea mays. In: Scandalios JG, Wright TRF, editors. Advances in Genetics. 30: Academic Press; 1992. p. 77-122.
237. Robertson DS. Characterization of a mutator system in maize. Mutation Research/Fundamental and Molecular Mechanisms of Mutagenesis. 1978;51(1):21-8.
238. Alleman M, Freeling M. The Mu transposable elements of maize: evidence for transposition and copy number regulation during development. Genetics. 1986;112(1):107.
239. Lisch D. Regulation of the Mutator System of Transposons in Maize. In: Peterson T, editor. Plant Transposable Elements: Methods and Protocols. Totowa, NJ: Humana Press; 2013. p. 123-42.
240. Paszkowski U, Jakovleva L, Boller T. Maize mutants affected at distinct stages of the arbuscular mycorrhizal symbiosis. The Plant Journal. 2006;47(2):165-73.
241. Klingner A, Bothe H, Wray V, Marner F-J. Identification of a yellow pigment formed in maize roots upon mycorrhizal colonization. Phytochemistry. 1995;38(1):53-5.
242. Walter MH, Floß DS, Hans J, Fester T, Strack D. Apocarotenoid biosynthesis in arbuscular mycorrhizal roots: Contributions from methylerythritol phosphate pathway isogenes and tools for its manipulation. Phytochemistry. 2007;68(1):130-8.
243. Fester T, Hause B, Schmidt D, Halfmann K, Schmidt J, Wray V, et al. Occurrence and Localization of Apocarotenoids in Arbuscular Mycorrhizal Plant Roots. Plant and Cell Physiology. 2002;43(3):256-65.
244. Slotkin RK, Freeling M, Lisch D. Mu killer Causes the Heritable Inactivation of the Mutator Family of Transposable Elements in Zea mays. Genetics. 2003;165(2):781-97.
245. Vollbrecht E, Duvick J, Schares JP, Ahern KR, Deewatthanawong P, Xu L, et al. Genome-Wide Distribution of Transposed Dissociation Elements in Maize. The Plant Cell. 2010;22(6):1667-85.
246. Arite T, Iwata H, Ohshima K, Maekawa M, Nakajima M, Kojima M, et al. DWARF10, an RMS1/MAX4/DAD1 ortholog, controls lateral bud outgrowth in rice. The Plant Journal. 2007;51(6):1019-29.
247. Lin H, Wang R, Qian Q, Yan M, Meng X, Fu Z, et al. DWARF27, an Iron-Containing Protein Required for the Biosynthesis of Strigolactones, Regulates Rice Tiller Bud Outgrowth. The Plant Cell. 2009;21(5):1512-25.
248. Wickham H. ggplot2. Wiley Interdisciplinary Reviews: Computational Statistics. 2011;3(2):180-5.
249. Ganal MW, Durstewitz G, Polley A, Bérard A, Buckler ES, Charcosset A, et al. A Large Maize (Zea mays L.) SNP Genotyping Array: Development and Germplasm Genotyping, and Genetic Mapping to Compare with the B73 Reference Genome. PLOS ONE. 2011;6(12):e28334.

250. Ewels P, Magnusson M, Lundin S, Käller M. MultiQC: summarize analysis results for multiple tools and samples in a single report. Bioinformatics. 2016;32(19):3047-8.
251. Patro R, Duggal G, Love MI, Irizarry RA, Kingsford C. Salmon provides fast and bias-aware quantification of transcript expression. Nature methods. 2017;14(4):417.
252. Love MI, Huber W, Anders S. Moderated estimation of fold change and dispersion for RNA-seq data with DESeq2. Genome Biology. 2014;15(12):550.
253. Conesa A, Götz S, García-Gómez JM, Terol J, Talón M, Robles M. Blast2GO: a universal tool for annotation, visualization and analysis in functional genomics research. Bioinformatics. 2005;21(18):3674-6.
254. MacLean AM, Bravo A, Harrison MJ. Plant Signaling and Metabolic Pathways Enabling Arbuscular Mycorrhizal Symbiosis. The Plant Cell. 2017;29(10):2319-35.
255. Montero H, Choi J, Paszkowski U. Arbuscular mycorrhizal phenotyping: the dos and don'ts. New Phytologist. 2019;221(3):1182-6.
256. Miyata K, Kozaki T, Kouzai Y, Ozawa K, Ishii K, Asamizu E, et al. The Bifunctional Plant Receptor, OsCERK1, Regulates Both Chitin-Triggered Immunity and Arbuscular Mycorrhizal Symbiosis in Rice. Plant and Cell Physiology. 2014;55(11):1864-72.
257. Giovannetti M. Structure, extent and functional significance of belowground arbuscular mycorrhizal networks. Mycorrhiza: Springer; 2008. p. 59-72.
258. David-Schwartz R, Badani H, Smadar W, Levy AA, Galili G, Kapulnik Y. Identification of a novel genetically controlled step in mycorrhizal colonization: plant resistance to infection by fungal spores but not extra-radical hyphae. The Plant Journal. 2001;27(6):561-9.
259. Lakshmanan V. Chapter Three - Root Microbiome Assemblage is Modulated by Plant Host Factors. In: Bais H, Sherrier J, editors. Advances in Botanical Research. 75: Academic Press; 2015. p. 57-79.
260. Glenn MG, Chew FS, Williams PH. Hyphal penetration of Brassica (Cruciferae) roots by a vesicular-arbuscular mycorrhizal fungal. New Phytologist. 1985;99(3):463-72.
261. Nagahashi G, Douds DD. Rapid and sensitive bioassay to study signals between root exudates and arbuscular mycorrhizal fungi**. Biotechnology Techniques. 1999;13(12):893-7.
262. Nagahashi G, Douds DD. Partial separation of root exudate components and their effects upon the growth of germinated spores of AM fungi* *Mention of a brand name or company name does not constitute an endorsement by the US Department of Agriculture. Mycological Research. 2000;104(12):1453-64.
263. Ellouze W, Hamel C, Cruz AF, Ishii T, Gan Y, Bouzid S, et al. Phytochemicals and spore germination: At the root of AMF host preference? Applied Soil Ecology. 2012;60:98-104.
264. Tamasloukht MB, Séjalon-Delmas N, Kluever A, Jauneau A, Roux C, Bécard G, et al. Root Factors Induce Mitochondrial-Related Gene Expression and Fungal Respiration during the Developmental Switch from Asymbiosis to Presymbiosis in the Arbuscular Mycorrhizal FungusGigaspora rosea. Plant physiology. 2003;131(3):1468-78.
265. Sun S, Wang J, Zhu L, Liao D, Gu M, Ren L, et al. An active factor from tomato root exudates plays an important role in efficient establishment of mycorrhizal symbiosis. PLoS ONE. 2012;7(8).
266. Gutjahr C, Banba M, Croset V, An K, Miyao A, An G, et al. Arbuscular Mycorrhiza–Specific Signaling in Rice Transcends the Common Symbiosis Signaling Pathway. The Plant Cell. 2008;20(11):2989-3005.
267. Pérez-Tienda J, Corrêa A, Azcón-Aguilar C, Ferrol N. Transcriptional regulation of host NH4+ transporters and GS/GOGAT pathway in arbuscular mycorrhizal rice roots. Plant Physiology and Biochemistry. 2014;75:1-8.

268. Sun J, Miller JB, Granqvist E, Wiley-Kalil A, Gobbato E, Maillet F, et al. Activation of Symbiosis Signaling by Arbuscular Mycorrhizal Fungi in Legumes and Rice. The Plant Cell. 2015;27(3):823-38.
269. Tanaka K, Cho S-H, Lee H, Pham AQ, Batek JM, Cui S, et al. Effect of lipo-chitooligosaccharide on early growth of C4 grass seedlings. Journal of Experimental Botany. 2015;66(19):5727-38.
270. Giovannetti M, Mari A, Novero M, Bonfante P. Early Lotus japonicus root transcriptomic responses to symbiotic and pathogenic fungal exudates. Frontiers in Plant Science. 2015;6(480).
271. Bücking H, Abubaker J, Govindarajulu M, Tala M, Pfeffer PE, Nagahashi G, et al. Root exudates stimulate the uptake and metabolism of organic carbon in germinating spores of Glomus intraradices. New Phytologist. 2008;180(3):684-95.
272. Ropars J, Toro KS, Noel J, Pelin A, Charron P, Farinelli L, et al. Evidence for the sexual origin of heterokaryosis in arbuscular mycorrhizal fungi. Nature Microbiology. 2016;1(6):16033.
273. Tang N, San Clemente H, Roy S, Bécard G, Zhao B, Roux C. A Survey of the Gene Repertoire of Gigaspora rosea Unravels Conserved Features among Glomeromycota for Obligate Biotrophy. Frontiers in Microbiology. 2016;7(233).
274. Reedy JL, Floyd AM, Heitman J. Mechanistic Plasticity of Sexual Reproduction and Meiosis in the Candida Pathogenic Species Complex. Current Biology. 2009;19(11):891-9.
275. Gilmore SA, Naseem S, Konopka JB, Sil A. N-acetylglucosamine (GlcNAc) triggers a rapid, temperature-responsive morphogenetic program in thermally dimorphic fungi. PLoS genetics. 2013;9(9):e1003799-e.
276. Inohara N, Nuñez G. ML – a conserved domain involved in innate immunity and lipid metabolism. Trends in Biochemical Sciences. 2002;27(5):219-21.
277. Štros M, Launholt D, Grasser KD. The HMG-box: a versatile protein domain occurring in a wide variety of DNA-binding proteins. Cellular and Molecular Life Sciences. 2007;64(19):2590.
278. Kameoka H, Maeda T, Okuma N, Kawaguchi M. Structure-Specific Regulation of Nutrient Transport and Metabolism in Arbuscular Mycorrhizal Fungi. Plant and Cell Physiology. 2019;60(10):2272-81.
279. Sidoux-Walter F, Pettersson N, Hohmann S. The Saccharomyces cerevisiae aquaporin Aqy1 is involved in sporulation. Proceedings of the National Academy of Sciences. 2004;101(50):17422-7.
280. Krajinski F, Courty P-E, Sieh D, Franken P, Zhang H, Bucher M, et al. The H+-ATPase HA1 of Medicago truncatula Is Essential for Phosphate Transport and Plant Growth during Arbuscular Mycorrhizal Symbiosis. The Plant Cell. 2014;26(4):1808-17.
281. Guan JC, Koch KE, Suzuki M, Wu S, Latshaw S, Petruff T, et al. Diverse Roles of Strigolactone Signaling in Maize Architecture and the Uncoupling of a Branching-Specific Subnetwork. Plant Physiology. 2012;160(3):1303-17.
282. Catty P, de Kerchove d'Exaerde A, Goffeau A. The complete inventory of the yeast Saccharomyces cerevisiae P-type transport ATPases. FEBS Letters. 1997;409(3):325-32.
283. Ayling SM, Smith SE, Smith FA. Transmembrane electric potential difference of germ tubes of arbuscular mycorrhizal fungi responds to external stimuli. New Phytologist. 2000;147(3):631-9.
284. Ramos AC, Façanha AR, Feijó JA. Proton (H+) flux signature for the presymbiotic development of the arbuscular mycorrhizal fungi. New Phytologist. 2008;178(1):177-88.

285. Requena N, Breuninger M, Franken P, Ocón A. Symbiotic Status, Phosphate, and Sucrose Regulate the Expression of Two Plasma Membrane H+-ATPase Genes from the Mycorrhizal Fungus Glomus mosseae. Plant Physiology. 2003;132(3):1540-9.
286. Harrison MJ, Buuren MLv. A phosphate transporter from the mycorrhizal fungus Glomus versiforme. Nature. 1995;378(6557):626-9.
287. Okorokova-Façanha AL, Okorokov LA, Ekwall K. An inventory of the P-type ATPases in the fission yeast Schizosaccharomyces pombe. Current Genetics. 2003;43(4):273-80.
288. Boch A, Trampczynska A, Simm C, Taudte N, Krämer U, Clemens S. Loss of Zhf and the tightly regulated zinc-uptake system SpZrt1 in Schizosaccharomyces pombe reveals the delicacy of cellular zinc balance. FEMS Yeast Research. 2008;8(6):883-96.
289. Črešnar B, Petrič Š. Cytochrome P450 enzymes in the fungal kingdom. Biochimica et Biophysica Acta (BBA) - Proteins and Proteomics. 2011;1814(1):29-35.
290. Hannemann F, Bichet A, Ewen KM, Bernhardt R. Cytochrome P450 systems—biological variations of electron transport chains. Biochimica et Biophysica Acta (BBA)-General Subjects. 2007;1770(3):330-44.
291. Senoo K, Solaiman MZ, Kawaguchi M, Imaizumi-Anraku H, Akao S, Tanaka A, et al. Isolation of two different phenotypes of mycorrhizal mutants in the model legume plant Lotus japonicus after EMS-treatment. Plant and Cell Physiology. 2000;41(6):726-32.
292. Duc G, Trouvelot A, Gianinazzi-Pearson V, Gianinazzi S. First report of non-mycorrhizal plant mutants (Myc−) obtained in pea (Pisum sativum L.) and fababean (Vicia faba L.). Plant Science. 1989;60(2):215-22.
293. Sagan M, Morandi D, Tarenghi E, Duc G. Selection of nodulation and mycorrhizal mutants in the model plant Medicago truncatula (Gaertn.) after γ-ray mutagenesis. Plant Science. 1995;111(1):63-71.
294. Rich MK, Schorderet M, Bapaume L, Falquet L, Morel P, Vandenbussche M, et al. The Petunia GRAS Transcription Factor ATA/RAM1 Regulates Symbiotic Gene Expression and Fungal Morphogenesis in Arbuscular Mycorrhiza. Plant Physiology. 2015;168(3):788-97.
295. Lukowitz W, Gillmor CS, Scheible W-R. Positional Cloning in Arabidopsis. Why It Feels Good to Have a Genome Initiative Working for You. Plant Physiology. 2000;123(3):795-806.
296. Rodgers-Melnick E, Vera DL, Bass HW, Buckler ES. Open chromatin reveals the functional maize genome. Proceedings of the National Academy of Sciences. 2016;113(22):E3177-E84.
297. Fu H, Zheng Z, Dooner HK. Recombination rates between adjacent genic and retrotransposon regions in maize vary by 2 orders of magnitude. Proceedings of the National Academy of Sciences. 2002;99(2):1082-7.
298. Gallavotti A, Whipple CJ. Positional cloning in maize (Zea mays subsp. mays, Poaceae). Applications in Plant Sciences. 2015;3(1):1400092.
299. Pflieger S, Lefebvre V, Causse M. The candidate gene approach in plant genetics: a review. Molecular Breeding. 2001;7(4):275-91.
300. Berger J, Suzuki T, Senti K-A, Stubbs J, Schaffner G, Dickson BJ. Genetic mapping with SNP markers in Drosophila. Nature Genetics. 2001;29(4):475-81.
301. Tenaillon MI, Sawkins MC, Long AD, Gaut RL, Doebley JF, Gaut BS. Patterns of DNA sequence polymorphism along chromosome 1 of maize Zea mays ssp. mays). Proceedings of the National Academy of Sciences. 2001;98(16):9161-6.
302. Xu C, Ren Y, Jian Y, Guo Z, Zhang Y, Xie C, et al. Development of a maize 55 K SNP array with improved genome coverage for molecular breeding. Mol Breed. 2017;37(3):20-.

303. Gallavotti A, Barazesh S, Malcomber S, Hall D, Jackson D, Schmidt RJ, et al. sparse inflorescence1 encodes a monocot-specific YUCCA-like gene required for vegetative and reproductive development in maize. Proceedings of the National Academy of Sciences. 2008;105(39):15196-201.
304. Zuo W, Chao Q, Zhang N, Ye J, Tan G, Li B, et al. A maize wall-associated kinase confers quantitative resistance to head smut. Nature Genetics. 2015;47(2):151-7.
305. Portwood JL, II, Woodhouse MR, Cannon EK, Gardiner JM, Harper LC, Schaeffer ML, et al. MaizeGDB 2018: the maize multi-genome genetics and genomics database. Nucleic Acids Research. 2018;47(D1):D1146-D54.
306. Stelpflug SC, Sekhon RS, Vaillancourt B, Hirsch CN, Buell CR, de Leon N, et al. An Expanded Maize Gene Expression Atlas based on RNA Sequencing and its Use to Explore Root Development. The Plant Genome. 2016;9(1):plantgenome2015.04.0025.
307. Taylor LP, Walbot V. A deletion adjacent to the maize transposable element Mu-1 accompanies loss of Adh1 expression. The EMBO Journal. 1985;4(4):869-76.
308. Chintamanani S, Hulbert SH, Johal GS, Balint-Kurti PJ. Identification of a maize locus that modulates the hypersensitive defense response, using mutant-assisted gene identification and characterization. Genetics. 2010;184(3):813-25.
309. Phillips DA. Flavonoids: plant signals to soil microbes. Phenolic metabolism in plants: Springer; 1992. p. 201-31.
310. Liu W, Kohlen W, Lillo A, Op den Camp R, Ivanov S, Hartog M, et al. Strigolactone Biosynthesis in Medicago truncatula and Rice Requires the Symbiotic GRAS-Type Transcription Factors NSP1 and NSP2. The Plant Cell. 2011;23(10):3853-65.
311. Velamakanni S, Wei SL, Janvilisri T, van Veen HW. ABCG transporters: structure, substrate specificities and physiological roles. Journal of Bioenergetics and Biomembranes. 2007;39(5):465-71.
312. Radhakrishnan GV, Keller J, Rich MK, Vernié T, Mbadinga Mbadinga DL, Vigneron N, et al. An ancestral signalling pathway is conserved in intracellular symbioses-forming plant lineages. Nature Plants. 2020;6(3):280-9.
313. BADRI DV, VIVANCO JM. Regulation and function of root exudates. Plant, Cell & Environment. 2009;32(6):666-81.
314. Zhang X, Pumplin N, Ivanov S, Harrison Maria J. EXO70I Is Required for Development of a Sub-domain of the Periarbuscular Membrane during Arbuscular Mycorrhizal Symbiosis. Current Biology. 2015;25(16):2189-95.
315. Wang X-J, Gaasterland T, Chua N-H. Genome-wide prediction and identification of cis-natural antisense transcripts in Arabidopsis thaliana. Genome Biology. 2005;6(4):R30.
316. Schumann N, Navarro-Quezada A, Ullrich K, Kuhl C, Quint M. Molecular Evolution and Selection Patterns of Plant F-Box Proteins with C-Terminal Kelch Repeats. Plant Physiology. 2011;155(2):835-50.
317. Magori S, Oka-Kira E, Shibata S, Umehara Y, Kouchi H, Hase Y, et al. TOO MUCH LOVE, a Root Regulator Associated with the Long-Distance Control of Nodulation in Lotus japonicus. Molecular Plant-Microbe Interactions®. 2009;22(3):259-68.
318. Choi J, Lee T, Cho J, Servante EK, Pucker B, Summers W, et al. The negative regulator SMAX1 controls mycorrhizal symbiosis and strigolactone biosynthesis in rice. Nature Communications. 2020;11(1):2114.
319. Gaude N, Bortfeld S, Duensing N, Lohse M, Krajinski F. Arbuscule-containing and non-colonized cortical cells of mycorrhizal roots undergo extensive and specific reprogramming during arbuscular mycorrhizal development. The Plant Journal. 2012;69(3):510-28.

320. Pawlowski ML, Vuong TD, Valliyodan B, Nguyen HT, Hartman GL. Whole-genome resequencing identifies quantitative trait loci associated with mycorrhizal colonization of soybean. Theoretical and Applied Genetics. 2020;133(2):409-17.
321. Sakamoto K, Ogiwara N, Kaji T, Sugimoto Y, Ueno M, Sonoda M, et al. Transcriptome analysis of soybean (Glycine max) root genes differentially expressed in rhizobial, arbuscular mycorrhizal, and dual symbiosis. Journal of Plant Research. 2019;132(4):541-68.
322. Chiu CH, Choi J, Paszkowski U. Independent signalling cues underpin arbuscular mycorrhizal symbiosis and large lateral root induction in rice. New Phytologist. 2018;217(2):552-7.